Analysis of the interaction of Hsp90 with the extracellular matrix protein fibronectin (FN)

A thesis submitted in the fulfillment of the requirements for the degree of

Master of Science

of

Rhodes University

by

Morgan Campbell Hunter

December 2013

ABSTRACT

Mounting evidence suggests that Hsp90 is present and functionally active in the extracellular space. The biological function of extracellular Hsp90 (eHsp90) remains relatively uncharacterized compared to that of intracellular Hsp90. eHsp90 has been shown to interact with a finite number of extracellular proteins, however, despite the identification of eHsp90 interacting proteins, the function of eHsp90 in these complexes is unknown. Several reports suggest a role for eHsp90α in cell migration and invasion. Reported targets for eHsp90 stimulated cell migration include MMPs, LRP-1, tyrosine kinase receptors and possible others unidentified. Limited studies report a role for eHsp90β.

Recently, Hsp90α and Hsp90β were isolated in a complex containing fibronectin (FN) on the surface of MDA-MB-231 breast cancer cells. Herein, we report direct binding of Hsp90α and Hsp90β to FN using a solid phase binding assay and surface plasmon resonance (SPR) spectroscopy. SPR spectroscopy showed that Hsp90β bound the 70 kDa amino-terminal fragment of FN (FN70), but that binding of FN to Hsp90β was not limited to FN70. Confocal microscopy showed regions of colocalization of Hsp90 with extracellular FN matrix fibrils in Hs578T breast cancer cell lines. Treatment of Hs578T breast cancer cells with novobiocin (an Hsp90 inhibitor) and an LRP-1 blocking antibody resulted in a loss of FN matrix and FN endocytosis (novobiocin treated). Addition of exogenous Hsp90β was able to recover such effect after both treatments. FN was shown to colocalize with intracellular LRP-1 in novobiocin treated Hs578T cells. Immunoprecipitation of an LRP-1 containing complex showed the presence of Hsp90 and 70 and 120+ kDa FN fragments. Treatment of Hs578T cells with novobiocin increased the level of FN120+ bound in LRP-1 immunoprecipitate. Exogenous Hsp90β decreased the level of low and high molecular weight FN fragments in a complex with LRP-1, despite the fact that higher levels of lower molecular weight FN fragments were detected in this cell lysate compared to the other treatments.

We report FN as a novel interacting protein of eHsp90. Taken together, we provide evidence for a direct role of eHsp90β in FN matrix remodeling. We suggest that Hsp90 plays a direct role in FN matrix dynamics through interaction with FN and LRP-1. The identification of FN as a novel interacting protein of eHsp90 suggests a role for Hsp90 in FN matrix remodeling, which is important for a number of fundamental cellular processes including cell migration and metastasis.

DECLARATION

I declare that this thesis is my own, unaided work. It is being submitted for the degree of Master of Science of Rhodes University. It has not been submitted before for any degree or examination at any other university.

_____

Morgan Campbell Hunter

December 2013

Grahamstown

TABLE OF CONTENTS

LIST OF FIGURES

LIST OF TABLES

LIST OF ABBREVIATIONS AND SHORT HAND NOTATIONS

17-AAG	17-N-allylamino-17-demethoxygeldanamycin
Akt	Protein Kinase B
Amp	Ampicillin
ANOVA	Analysis Of Variance
ATCC	American Type Culture Collection
ATP	Adenosine Triphosphate
ATPase	Adenosine 5´-Triphosphatase
BAG-1	Bcl-2-associated anthanogene 1
BSA	Bovine Serum Albumin
Cdc37	Cell Division Cycle 37
ColE1	Colicin E1
CRC	Colorectal Cancer
CS1	Connecting Segment 1
CSSI	Cell Stress Society International
CXCR4	C-X-C Chemokine Receptor 4
DMEM	Dulbecco's Modified Eagle Medium
DNA	Deoxyribonucleic Acid
DOC	Sodium deoxycholate
DP	Denatured Protein
DTSSP	3,3'-Dithiobis(sulfosuccinimidyl propionate)
ECL	Enhanced Chemiluminescence
ECM	Extracellular Matrix
EDAC	1-ethyl-3-(3-dimethylaminopropyl)carbodiimide
EDTA	Ethylenediaminetetraacetic Acid
EEVD	Glutamate-glutamate-valine-aspartate motif
EGCG	Epigallocatechin gallate
EGF	Endothelial Growth Factor
EGFR	Epidermal Growth Factor Receptor
EGTA	Ethyleneglycol-bis(beta-aminoethylether)N'N'N'N-tetraacetic Acid
ELISA	Enzyme-Linked Immunosorbent Assay
EphA2	Ephrin type-A receptor 2
ER	Endoplasmic Reticulum

Erbb2	Erythroblastic leukemia viral oncogene homolog 2
Erk	Extracellular signal-regulated kinase
Etop	Etoposide
FACS	Fluorescence Activated Cell Sorting
FCS	Foetal Calf Serum
FITC	Fluorescein isothiocyanate
FN	Fibronectin
FN70	70 kDa N-terminal fragment of fibronectin
GCUNC45	General Cell UNC45
GDF-5	Growth Differentiation Factor 5
GHKL	(Gyrase, Hsp90, Histidine Kinase, MutL)
Grp94	Glucose-regulated protein 94
GSH	Gluthathione
GST	Glutathione-S-Transferase
HCl	Hydrochloric acid
HEPES	2-[4-(2-hydroxyethyl)piperazin-1-yl]ethanesulfonic acid
Her-2	Human Epidermal growth factor Receptor 2
hERG	Human Ether a-go-go
HIP	HSC70-interacting Protein
HIS	Histidine
Hop	Hsp90/Hsp70 Organising Protein
HRP	Horseradish Peroxidase
HSE	Heat Shock Element
HSF-1	Heat Shock Factor 1
Hsps	Heat Shock Proteins
IB	Immunoblot
IBDV	Infectious Bursal Disease Virus
IL-8	Interleukin 8
IP	Immunoprecipitation
IPTG	Isopropyl β-D-1-thiogalactopyranoside
K_d	Dissociation constant
kDa	Kilodalton
KSHV	Kaposi's Sarcoma-associated Herpesvirus
LAL	*Limulus* Amebocyte Lysate

LAMP-1	Lysosomal-Associated Membrane Protein-1
LAP	Latency-Associated Peptide
LDL	Low-Density Lipoprotein
LPS	Lipopolysaccharide
LRP-1	Low density lipoprotein receptor-related protein 1
LRPab	LRP-1 blocking antibody
LSM	Laser Scanning Microscope
LTBP-1	Latent Transforming growth factor beta Binding Protein 1
MAPK	Mitogen Activated Protein Kinase
MHC	Major Histocompatability Complex
Mek	Meiosis-specific serine/threonine Kinase
MMP	Matrix Metalloproteinase
MSF	Migration-Stimulating Factor
NF-κB	Nuclear Factor Kappa-light-chain-enhancer of activated B cells)
NHS	*N*-hydroxysulfosuccinimide
NTA	Nitrilotriacetic Acid
OG	Oregon Green
p23	The protein encoded by the PTGES3 gene
PBS	Phosphate Buffered Saline
PDM	Product Differences of the Mean
PE	Phycoerythrin
PHSRN	Proline-histidine-serine-arginine-asparagine peptide
PI3K	Phosphatidylinositol 3-kinase
PMSF	phenylmethylsulfonyl fluoride
RAP1	Ras-proximate-1
RGD	Arginine-glycine-aspartic acid peptide
RIPA	Radioimmunoprecipitation Assay buffer
RU	Response Units
SDS	Sodium-Dodecyl-Sulphate
SDS-PAGE	Sodium-Dodecyl-Sulphate Polyacrylamide Gel Electrophoresis
SPR	Surface Plasmon Resonance
Src	Sarcoma Tyrosine Kinase
Stat3	Signal Transducer and activator of transcription 3
TBS	Tris-buffered Saline

TBST	Tris-buffered Saline with Tween-20
TCF12	Transcription Factor 12
TGFβ	Transforming Growth Factor beta
TLR-4	Toll-like Receptor 4
TMB	Tetramethylbenzidine
TMR	Tetra-methyl Rhodamine
tPA	Tissue Plasminogen Activator
TPR	Tetratricopeptide Repeat
TRAP1	TNF Receptor Associated Protein 1
UK	United Kingdom
uPa	Urinary Plasminogen Activator
uPAR	Urinary Plasminogen Activator Receptor
USA	United States of America
UV	Ultra-violet
VEGF	Vascular Endothelial Growth Factor
YT	Yeast Tryptone

LIST OF SYMBOLS

α	Alpha
β	Beta
oC	Degree Celsius
M	Molar
mM	Millimolar
nM	Nanomolar
µg	Micrograms
µl	Microlitres
L	Litres
g	Grams
mg	Milligrams
kDa	Kilodaltons
min	Minutes
mol	Mole
ml	Millilitre(s)
%	Percent or g/100 ml
x *g*	Relative centrifugal force to gravity

ACKNOWLEDGMENTS

To my supervisor, Dr Adrienne Edkins: Thank you most kindly for all your guidance, expertise and support throughout the duration of my Masters Research project. It was awesome to be supported by a passionate and thought-provoking supervisor. I look forward to being a part of your team in the upcoming year.

To my funders, Rhodes University and DAAD-NRF: This work is solely thanks to your financial funding and support. I would not have been able to fulfill my goals without your financial assistance. Thank you.

To the BioBRU team: Nothing compares. Thank you for all the support, assistance and good times along the way. This thesis would not have come together even half as well if it wasn't for our fantastic work environment. On that note, thank you for putting up with all my nonsense.

To my family: You are the most important thing to me in this world. Thanks to the Lord almighty for his continual support and guidance in my life. Thanks mom and dad for all your assisted funding and support and for always listening to my science thoughts. Thanks to my brother (Gus Bus) and sister (Ezzy) for just being as you are. Thanks to all my extended family as well. Most importantly, I dedicate this thesis to my gran, my nana. Hopefully one day this work contributes to the discovery of preventative agents of metastatic cancers. I will always love you.

To my friends and girlfriend: To those who are close to me all the time, Thank you Thank you Thank you. I truly appreciate you all in my life. To my friends who have been through the system with me (Adam, Lara, Claire, Dustin, Lance, Stacey and others), what a journey we have had. I truly thank you for everything over the past six years. Step by step we have done it together; I look forward to Grad to celebrate OUR achievements. I look forward to friendships that last forever. Shout out to the digsies over these past two years as well, Jayo, Nick and Sam. Good times. To my stunning girlfriend, your name (Tarryn Melissa Horne) is now forever in the library archives. Thank you for being there through the stressful times. I appreciate you.

To all others I haven't mentioned: THANK YOU

CHAPTER 1: LITERATURE REVIEW

1.1 MOLECULAR CHAPERONES

The synthesis of proteins by cellular ribosomes results in the production of unfolded proteins containing multiple solvent-exposed hydrophobic groups (Hendrick & Hartl 1995; Hartl & Hayer-Hartl 2002). These solvent-exposed hydrophobic groups may result in the formation of intramolecular and intermolecular aggregates (Hendrick & Hartl 1995; Chaudhury et al. 2006; Hartl & Hayer-Hartl 2002). Molecular chaperones are cellular proteins that prevent or reverse such interactions and associations and functionally assist in the folding of a newly synthesized protein, or unfolding of a misfolded or denatured protein, into its correct tertiary structure (Hendrick & Hartl 1995; Hartl & Hayer-Hartl 2002). Many molecular chaperones are ATPases and use the free energy of ATP to functionally assist in correct protein folding (Chaudhury et al. 2006; Didenko et al. 2012).

1.2 HEAT SHOCK PROTEINS

Heat Shock Proteins (Hsps) form the largest family of molecular chaperones, assisting in protein folding and cellular homeostasis (Fulda et al. 2010; Vabulas et al. 2010). Hsps were originally discovered when chromosomal puffs developed in the salivary glands of *Drosophila melanogaster* cells in response to heat shock (Tissières et al. 1974; Ritossa 1962). Hsps were thus termed as such as they are overexpressed in cells during cell stress conditions, particularly heat shock (Chiosis et al. 2003). Stressed conditions can occur during elevated temperatures, nutrient deprivation, malignancy, non-physiological pH, hypoxia, ischemia, hyperoxia, anoxia, exposure to UV light and chemicals, nicotine, emotional and mechanical stress or injury, viral agents, carcinogens or other stresses (Chaudhury et al. 2006; Khalil et al. 2011). Stressed conditions within a cell result in protein damage and an accumulation of misfolded and denatured proteins (Chaudhury et al. 2006). In order to counteract this, Hsps are overexpressed in an attempt to assist in the folding of newly translated polypeptides and refolding of denatured proteins (Chaudhury et al. 2006; Fulda et al. 2010). Hsps have been shown to play a pivotal role in the cell cycle and apoptosis and thus the heat shock response is an adaptive response by the cell to maintain cellular homeostasis under stress (Khalil et al. 2011; Sreedhar et al. 2004). A stress factor results in the activation of signaling pathways that trigger the inducible heat shock response through the activation of selective transcription factors (Sarto et al. 2000; Morimoto et al. 1992). Dependent on the nature of the stress, different members of the heat shock transcription factors (HSFs) will be activated (Whitley et al. 1999; Morimoto et al. 1992; Khalil et al. 2011). HSF-1 has been reported as the main

regulator of short term induction of Hsps. In the normal resting state HSF-1 is maintained in a monomeric form through interaction with heat shock protein 90 (Hsp90) and co-chaperones (Shamovsky & Nudler 2008; Fulda et al. 2010). During cell stress, an accumulation of unfolded proteins compete for Hsp90 binding (Fulda et al. 2010). HSF-1 is released from Hsp90 stimulating the transition of HSF-1 from its monomer to its homotrimer (Fulda et al. 2010). Trimeric HSF-1 translocates to the nucleus and binds to upstream heat shock elements (HSE) in the promoters of target Hsps, stimulating overexpression of Hsps (Fulda et al. 2010). The produced Hsps bind denatured proteins and assist in their correct folding (Shamovsky & Nudler 2008; Fulda et al. 2010). The mechanism of Hsp activation and denatured protein repair can be seen in Figure 1.

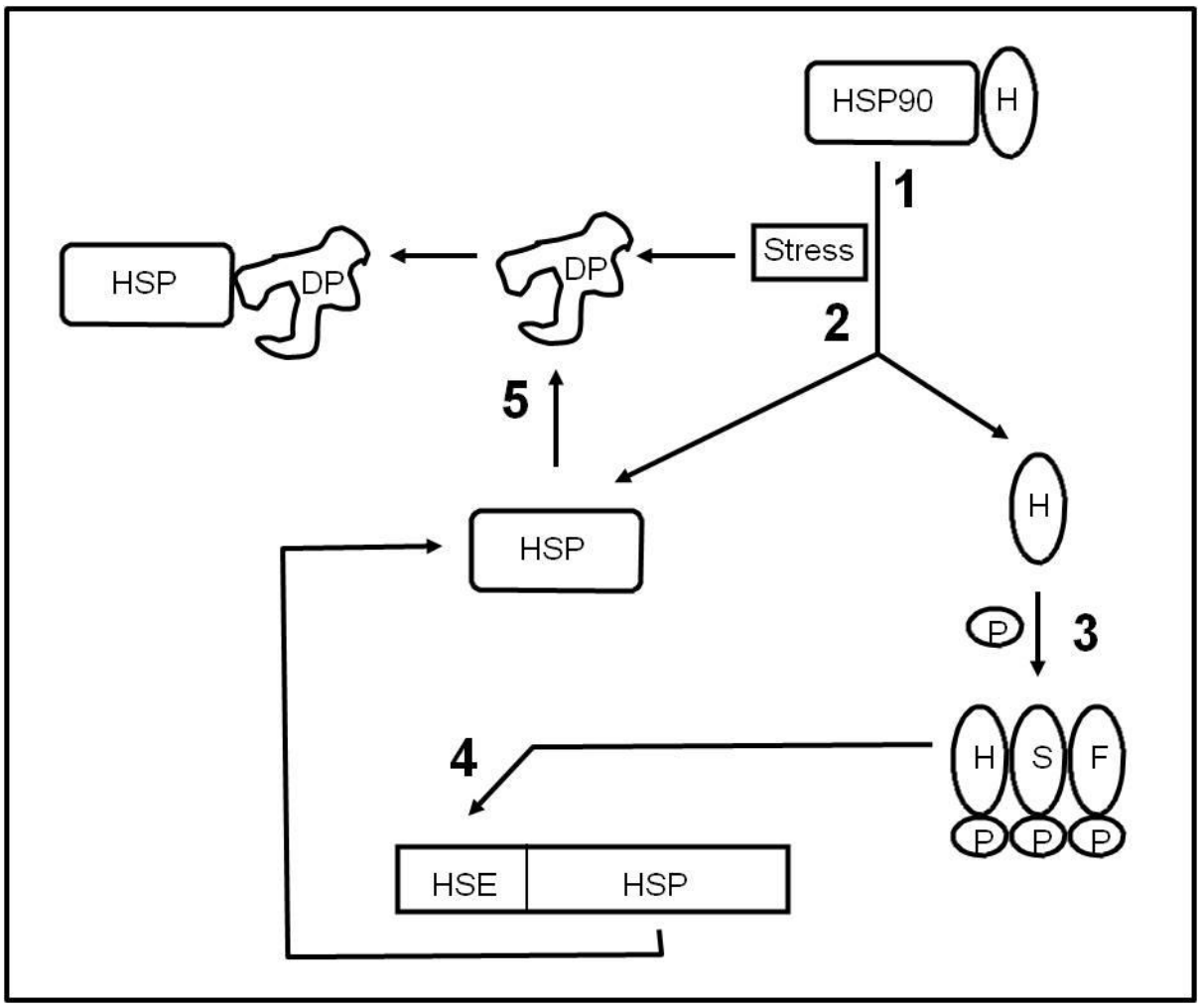

Figure 1: legend over page

Figure 1: Heat shock protein activation and denatured protein repair

(1) During resting cell state HSFs exist as a complex with Hsp90 and are inactive. (2) Cell stress conditions result in the formation of denatured proteins (DP) that trigger the dissociation of the Hsp90-HSF complex. (3) HSF is activated through phosphorylation resulting in the formation of an active HSF trimer. (4) The active HSF trimer binds to an upstream HSE on the promoter site that regulates the transcription of stress inducible Hsps, thus initiating increased production of Hsps. (5) The produced Hsps bind denatured proteins and assist in their correct folding. Over-expression of the Hsps in non-stress conditions result in the binding of Hsps to the trans-activation domain of HSF thus preventing further production of Hsps.

Hsps exist as a set of highly conserved proteins (Khalil et al. 2011; Hartl & Hayer-Hartl 2002). Mammalian Hsps are categorized into six families based on their molecular weight: Hsp100, Hsp90, Hsp70, Hsp60, Hsp40 and the small Hsps ranging in size from 15 to 30 kDa (Khalil et al. 2011; Redlak & Miller 2011). The high molecular weight Hsps are generally dependent on the energy supplied through the hydrolysis of ATP to perform their function whilst the small Hsps can act independently of ATP (Didelot et al. 2007). Each HSP family is composed of members that are expressed in different sub-cellular compartments and in either constitutive or inducible forms (Schmitt et al. 2007). Individual heat shock protein families play several important roles in homeostasis of a cell. Broadly, Hsp100s act in quality control of intracellular protein levels through interactions with other chaperones and proteases (Maurizi & Xia 2004). Hsp70s participate in *de novo* ATPase driven protein folding, refolding of misfolded or denatured proteins, protein membrane translocation and controlled activity of regulatory proteins (Hartl & Hayer-Hartl 2002; Mayer & Bukau 2005). Hsp60s mediate correct protein folding and prevent aggregation of mitochondrial proteins (Khalil et al. 2011; Hendrick & Hartl 1995). Hsp40s act as co-chaperones of Hsp70 chaperone activity by increasing the rate of ATP turnover (Khalil et al. 2011; Mayer & Bukau 2005). Folding of substrate proteins involves not only the Hsp70-Hsp40 system, but also the transfer of a substrate from this system to the Hsp90 family, in combination with co-chaperones such as Cdc37 and p23, for terminal folding (Mayer & Bukau 2005).

1.3 HEAT SHOCK PROTEIN 90 (Hsp90)

Hsp90 is one of the most abundant and ubiquitously expressed chaperone proteins (Garnier et al. 2002; Li & Buchner 2013). During non-stress conditions, Hsp90 comprises as much as 1-2 % of total cellular protein (Bagatell & Whitesell 2004; Didenko et al. 2012). Hsp90 plays a fundamental role in cell signaling, proliferation and survival of the cell (Donnelly & Blagg 2008; Li & Buchner 2013). Hsp expression profiles differ in tumor cells in comparison to their normal cell counterparts (Ferrarini et al. 1992; Bagatell & Whitesell 2004; Sarto et al.

2000). Hsp90 expression is reported to be constitutive in cancer cells, at levels 2- to 10- fold higher than normal cells (Ferrarini et al. 1992). Elevated expression of Hsp70 and Hsp90 has been associated with poor prognosis in breast cancer (Pick et al. 2007; Zagouri et al. 2012). It is well established that Hsp90 plays a fundamental role in facilitating malignant transformation (Donnelly & Blagg 2008; Bagatell & Whitesell 2004). The chaperone activity of Hsp90 plays a vital role in the stability, refolding and maturation of key oncogenic proteins expressed in tumor cells (Donnelly & Blagg 2008; Holzbeierlein et al. 2010). Hsps are required for carcinogenesis in the pathways used for cells to escape tumor suppression, promote progression, acquire resistance to treatment and facilitate metastasis (Zagouri et al. 2012).

1.3.1 Structure

Hsp90 has an approximate molecular weight of 90 kDa and commonly exists as a homodimer comprised of three highly conserved structural domains: a 25 kDa N-terminal domain with an ATP-binding site and ATP-hydrolysis capability; a 35 kDa middle domain with a high affinity for selective co-chaperones and client proteins; and a 12 kDa C-terminal dimerization domain (Donnelly & Blagg 2008; Didenko et al. 2012). The middle and N-terminal domains are linked by a highly charged linker (Donnelly & Blagg 2008; Li & Buchner 2013). Four human isoforms of Hsp90 have been identified (Johnson 2012; Li & Buchner 2013). The cytosolic isoforms are the inducible Hsp90α and the constitutively active Hsp90β (Li & Buchner 2013). Other Hsp90 isoforms include the endoplasmic reticulum localized Grp94 and mitochondrial localized Hsp75/TRAP1 (Johnson 2012; Li & Buchner 2013). Grammatikakis and colleagues report a fifth member of the Hsp90 family, Hsp90N (Grammatikakis et al. 2002). Hsp90N lacks the N-terminal nucleotide binding domain present in Hsp90α and Hsp90β but shares the same N-terminal hydrophilic region (residues 31-100), the middle client binding domain and the C-terminal dimerization domain (Lee et al. 2011; Grammatikakis et al. 2002). Debate on the existence of Hsp90N is ongoing. It is thought this newly discovered Hsp90N is primarily membrane associated due to a unique hydrophobic N-terminal domain (Whitesell & Lindquist 2005; Lee et al. 2011; Grammatikakis et al. 2002). The N-terminal region of Hsp90N is replaced with a 30-residue long hydrophobic motif thought to be membrane associated (Lee et al. 2011). Lee and co-workers report that an identified transmembrane helix of 19 amino acids (residues 12-30) is present within the N-terminal hydrophobic motif of Hsp90N (Lee et al. 2011). Zurawska and colleagues suggested Hsp90N to be an accidental product of a fortuitous chromosomal

translocation in a single cell line (Zurawska et al. 2008). The schematic structures of the Hsp90 isoforms and structure of Hsp90 in a closed conformation are shown in Figure 2.

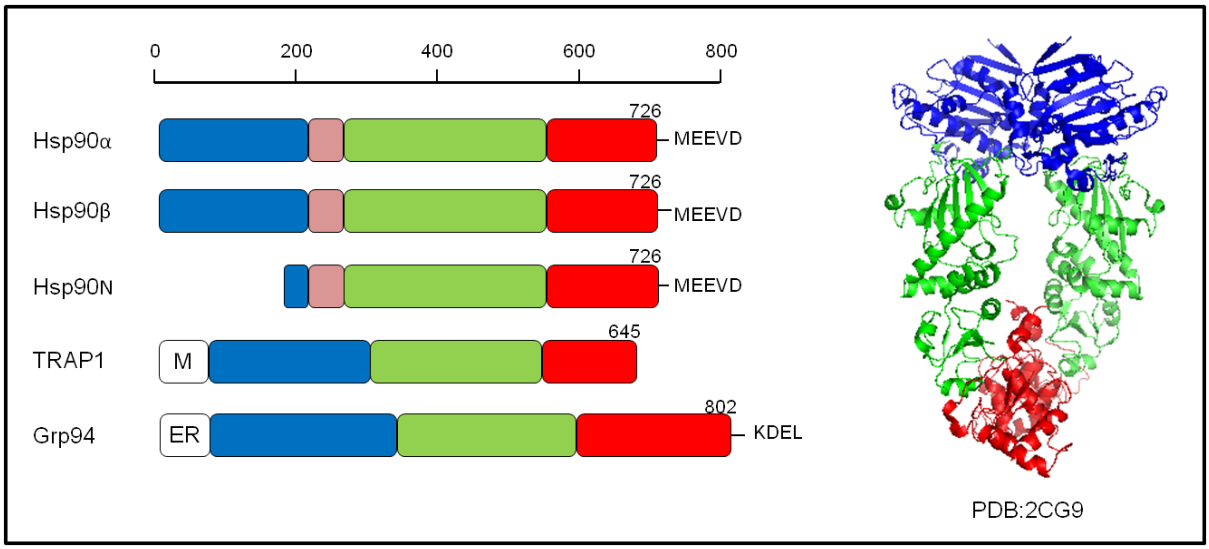

Figure 2: Structure of five isoforms of Hsp90

The structure of Hsp90 isoforms composed of an ATP binding N-terminal domain (blue), highly charged linker region (pink), middle domain (green) and C-terminal dimerization domain (red). Mitochondrial (M) and endoplasmic reticulum (ER) signal sequences are shown for TRAP1 and Grp94 respectively. Scale bar shows the amino acid length of each domain with respect to each isomer. Numbers at the end of the C-terminal domain show the length of each isomer. Conserved C-terminal amino acid sequences are shown. Hsp90α and Hsp90β share high sequence identity (86 %) whereas Grp94, TRAP1 and the newly discovered Hsp90N differ significantly.

The N-terminal domain of Hsp90 is approximately 210 amino acids in length (25 kDa) and contains an unusual ATP-binding pocket, known as the Bergerat fold, as well as a co-chaperone binding motif (Donnelly & Blagg 2008; Whitesell & Lindquist 2005; Lee et al. 2011). The Bergerat fold structural motif belongs to the GHKL superfamily (DNA gyrase B, histidine kinase and MutL), all of which bind ATP in a bent conformation (Whitesell & Lindquist 2005; Chaudhury et al. 2006; Dutta & Inouye 2000). The Bergerat fold exists as an α/β sandwich consisting of four-stranded mixed β-sheets and three α-helices, including an ATP-lid (Dutta & Inouye 2000). Linking the N-terminal and middle domains of Hsp90 is a flexible, highly charged linker sequence (Whitesell & Lindquist 2005; Li & Buchner 2013). The middle domain of Hsp90 is approximately 350 amino acids in length (35 kDa), is highly charged, and site-directed mutagenesis has shown it to play a key role in binding co-chaperones and client proteins (Donnelly & Blagg 2008; Didenko et al. 2012). The middle domain also binds the γ-phosphate of ATP molecules that are bound in the N-terminal pocket

indicating the important role that the middle domain plays in modulating ATP hydrolysis (Whitesell & Lindquist 2005).

A second flexible, highly charged linker sequence links the middle domain to the C-terminal domain of Hsp90 (Whitesell & Lindquist 2005). The C-terminal domain of Hsp90 shows independent chaperone activity as well as mediating dimerization of the chaperone (Allan et al. 2006). The crystal structure of MC-Hsp90, an N-terminal truncated Hsp90, shows that in the absence of the N-terminal ATPase domain, the C-terminal domain structure contains an amphipathic loop, curved α-helix, a three-stranded β-sheet, a three-helix coil and an extended disordered arm (Lee et al. 2011). The hydrophobic helix H2 is proposed to provide a binding surface for substrates while helices 3-5 (H3-H5) interface with the corresponding helices of the opposite monomer to facilitate dimer formation (Allan et al. 2006). Amino acids 640-694 are implicated in dimerization of Hsp90 (Allan et al. 2006). C-terminal dimerization of Hsp90 is essential for efficient ATP-hydrolysis by the N-terminal domains (Grammatikakis et al. 2002). The C-terminal of Hsp90 contains an EEVD motif that is essential for interaction with co-chaperones possessing a tetratricopeptide (TPR) repeat (Chen et al. 1998; Carrello 1999; Wang et al. 2009). Upstream of the EEVD motif lies an α-helical region that includes a hydrophobic microdomain that contributes to the interaction of Hsp90 with the immunophilin co-chaperones (Allan et al. 2006). Allen and colleagues suggest that the C-terminal hydrophobic microdomain of Hsp90 may have a stabilizing effect on the interaction of Hsp90 with co-chaperones, with the potential to impose additional specificities of the interaction of Hsp90 with its TPR-containing co-chaperones (Allan et al. 2006). This is supported by the fact that deletion of the hydrophobic sequence (residues 661 – 677) impacts Hsp90 dimerization, substrate binding and interaction with TPR-containing co-chaperones (Allan et al. 2006). The microdomain is also said to be a nucleotide binding pocket that binds inhibitors novobiocin, cisplatin and epigallocatechin-3-gallate (EGCG) but that also binds ATP (Donnelly & Blagg 2008; Allan et al. 2006; Marcu et al. 2000). The hydrophobic microdomain is encompassed within the dimerization domain of Hsp90 suggesting bound co-chaperones mask the nucleotide binding pocket (Allan et al. 2006). The hydrophobic microdomain of Hsp90 is identified by Allan and co-workers as residues 653 – 681, a region that encompasses the binding site of novobiocin (residues 660 – 681) (Allan et al. 2006).

Csermely and co-workers showed that the C-terminal hydrophobic microdomain only becomes available for binding after the N-terminal site has been bound by ATP (Csermely et al. 1998). It was also shown that while the N-terminal ATP-binding site is specific for

adenine nucleotides, the C-terminal binding site is less specific, binding both purines and pyrimidines (Soti et al. 2003). Large conformational rearrangements occur during the ATP cycle of the Hsp90 dimer (Ratzke et al. 2010). The dimer itself consists of two chains with dimerization interfaces at both the N- and C-terminal domains (Ratzke et al. 2010). Ratzke reports that contrary to previous reported assumptions, fast opening and closing kinetics of the C-terminal domain occurs and that the occupancy of the C-terminal open conformation is modulated by nucleotides bound to the N-terminal domain (Ratzke et al. 2010). This suggests a long distance form of communication between the termini. The shift to a more open conformation of the C-terminal is linked to the destabilization of the C-terminal dimerization complex upon ATP binding (Ratzke et al. 2010). Communication between the termini was also observed by Allan and co-workers who show that the binding of novobiocin to the C-terminal domain of Hsp90, precluded interaction of Hsp90 with the p50 co-chaperone, a protein that targets the N-terminal domain of Hsp90 (Allan et al. 2006). Other authors show that a point mutation within the C-terminal domain at position 597 effects ATPase activity of the N-terminal, suggesting communication between the domains (Retzlaff et al. 2009). This communication and co-ordination between the domains was surprising considering the long flexible linker region that links the middle and N-terminal domain (Ratzke et al. 2010). The microdomain ATP-binding site has been shown to resemble a Rossman fold (Garnier et al. 2002). Unlike the N-terminal ATP-binding site of Hsp90, the C-terminal ATP-binding microdomain does not exhibit ATPase activity but does play a key role in trapping the nucleotide during the ATPase cycle, resulting in a conformational change of the homodimer (Garnier et al. 2002). Results from Garnier and colleagues also show that when a nucleotide is bound to the N-terminus, the molecule exhibits a strong negative effect on the binding of nucleotides to the C-terminus (Garnier et al. 2002). This result was confirmed by a truncated C-terminus Hsp90 having a much greater affinity for ATP than the full length Hsp90 chaperone (Garnier et al. 2002).

The crystal structure of an N-terminal truncated Hsp90 (MC-Hsp90) shows MC-Hsp90 to exist as a dimer, tetramer and hexamer in solution (Lee et al. 2011). The protein subunits of MC-Hsp90 were arranged as a parallel homodimer with a left-handed helical twist (Lee et al. 2011). The open state of MC-Hsp90 was observed through the formation of a “Twisted V” shape as each protomer extended from its C-terminal helix coil at the central axis of the dimer (Lee et al. 2011). Residues W320 and R346 of MC-Hsp90 were shown to play a critical role in hexamer oligomerization (Lee et al. 2011). Oligomeric forms of MC-Hsp90 are induced by

divalent cations, such as magnesium or calcium, or in the presence of non-ionic detergents (Lee et al. 2011). The self-oligomerization of Hsp90 is inhibited by the presence of ATP and geldanamycin (Lee et al. 2011). This suggests that occupation of the N-terminal ATP binding pocket by either ATP, or inhibitory compounds like geldanamycin, prevent oligomerization induced by the heat response. Oligomerization of Hsp90 induced by divalent cations also resulted in instantaneous loss of molecular chaperone function (Lee et al. 2011). The functional roles of Hsp90 oligomers in chaperone function are not yet fully understood (Lee et al. 2011). The self-oligomerization of Hsp90 is thought to play a crucial role in cell protection through the ability of oligomers to bind substrates and prevent irreversible aggregation (Lee et al. 2011).

1.3.2 Interaction with client proteins, co-chaperones and antigenic peptides

Hsp90 modulates the stability and transport of a diverse set of cellular proteins critical for cell survival. These cellular proteins, known as "client proteins," have critical roles in signal transduction, cellular trafficking, chromatin remodeling, cell growth, differentiation and reproduction (Zuehlke & Johnson 2011). Client proteins of intracellular Hsp90 are defined by two criteria, firstly that they should be capable of direct association with the chaperone, and secondly it should be dependent on the interaction with Hsp90 for stability or conformational regulation (Theodoraki & Caplam 2013; Citri et al. 2006; Zuehlke & Johnson 2011; Echtenkamp & Freeman 2012). The interaction of Hsp90 with client proteins is thought to be characterized by low-affinity binding and repeated cycles of association and release (Smith 1998; Citri et al. 2006). Client proteins bind transiently and non-covalently to Hsp90 (Khalil et al. 2011; Li & Buchner 2013; Taipale et al. 2012). Under most conditions, Hsp90 maintains client proteins in a folded conformation poised to respond to an activation signal (Zuehlke & Johnson 2011). The role of Hsp90 in the maintenance of stability and conformational regulation of client proteins is reflected by increased degradation of clients upon pharmacological inhibition (Citri et al. 2006).

Hsp90 facilitates the folding and maturation of more than 300 client proteins (Lee et al. 2011). A comprehensive regularly updated list of Hsp90 client proteins can be found on the Picard website (http://www.picard.ch/downloads/Hsp90interactors.pdf). The principles governing chaperone-client protein interaction are not fully understood (Echtenkamp & Freeman 2012). Hsp90 client proteins encompass a broad range of proteins (transcription factors, kinases, steroid hormone receptors and others) with unrelated amino acid sequence,

quaternary structure and cellular function (Taipale et al. 2010). Taipale and colleagues express that although Hsp90 chaperones a wide range of structurally unrelated client proteins, there must be specific structural features that are recognized by Hsp90 (Taipale et al. 2012). Moreover, some proteins of the same family robustly interact with Hsp90 whilst closely related homologs do so less strongly (Xu et al. 1999), or not at all (Xu et al. 2005). This suggests that despite conservation of protein fold, there must be specific sequence or structural features that define the interaction of Hsp90 with client proteins (Taipale et al. 2012). Several reports suggest the αC helix β4 strand in the N-lobe of the kinase domain as the recognition site for the interaction of Hsp90 with protein kinases (Citri et al. 2006; Xu et al. 2005; Prince & Matts 2004). Citri and colleagues suggest that the interaction of Hsp90 with client kinases is based upon surface features rather than contiguous amino acid sequence (Citri et al. 2006). They further suggest, along with others, that Hsp90 interacts with features that are common to unstable proteins with a higher level of specificity gained through mediation with co-chaperones (Citri et al. 2006; Taipale et al. 2012; Caplan et al. 2007).

Hsp90 does not function alone in its stabilization and transport of client proteins, but rather recruits the help of co-chaperones for binding and release of substrate proteins (Khalil et al. 2011; Li & Buchner 2013). Hsp90 forms a multichaperone complex with other chaperones, co-chaperones and client proteins that work synergistically in the folding, re-folding, maturation, transport, activation and inactivation of proteins involved in vital cellular processes (Pearl & Prodromou 2001). More than 20 co-chaperones have been identified (Li & Buchner 2013). Some of these co-chaperones include Hsc70 interacting protein (Hip), Hsp70-Hsp90 organizing protein (Hop), Bcl-2-associated anthanogene (BAG-1), DnaJC7 and p23 (Khalil et al. 2011). Co-chaperones regulate the ATPase activity of Hsp90 or direct specific client protein interactions (Zuehlke & Johnson 2011). Co-chaperones of Hsp90 play a crucial role in the quality control process that leads to degradation of misfolded Hsp90 client proteins (Zuehlke & Johnson 2011). Co-chaperones regulate the function of Hsp90 in different ways dependent to some degree on the presence of a specific client protein (Li & Buchner 2013). Taipale and colleagues suggest that co-chaperones assist in the recognition of specific types of folds in a client protein, whilst thermal and conformational stability determine the extent of the interaction (Taipale et al. 2012). Most recently, Echtenkamp and colleagues suggest that co-chaperones contribute to client regulation both separately and in conjunction with Hsp90 (Echtenkamp & Freeman 2012). Despite these suggestions, the role

of co-chaperones in Hsp90 client protein recognition is not well understood (Taipale et al. 2012).

Hsp90 has previously been shown to interact with antigenic peptides necessary for immunological processes such as antigen presentation by major histocompatibility complex (MHC) (Li et al. 2002). Two roles have been suggested for HSPs in their interaction with peptides as an HSP-peptide complex: the chaperoning of peptides in their journey to MHC molecules by HSPs of the cytosol and endoplasmic reticulum; and presentation of peptides on the cell surface or in the extracellular space that are taken up by antigen-presenting cells (APCs) and re-presented by MHC molecules of APCs (Li et al. 2002). Several studies suggest a role for Hsp90 in antigen presentation to APCs (Li et al. 2011; Csermely et al. 1998; Tsutsumi & Neckers 2007). Binder et al., showed that treatment with deoxyspergualin, an Hsp90 binding drug, prevented MHC class I presentation of endogenously produced antigenic peptides (Binder et al. 2001).

1.3.3 Pharmacological inhibition

Hsp90 inhibitors result in the destabilization and degradation of Hsp90 client proteins (Tsutsumi & Neckers 2007). The binding of N-terminal inhibitors to Hsp90 prevents the binding of client proteins in a protected complex and thus allows for ubiquitination of the client protein followed by proteosomal degradation (Holzbeierlein et al. 2010). The overexpression of Hsp90 and increased affinity for ATP, coupled with increased ATPase activity in active cancer cells provides the possibility of inhibitors of Hsp90 having cancer cell selectivity (Holzbeierlein et al. 2010; Kamal et al. 2003; Neckers & Lee 2003). The chaperone function of Hsp90 is dependent on the Bergerat fold on the N-terminal domain to bind and hydrolyze ATP and thus the majority of Hsp90 inhibition studies have identified analogues of ATP that bind the N-terminal ATP-binding site (Young et al. 1998). Known inhibitors of the N-terminus of Hsp90 include geldanamycin and its synthetic derivatives 17-(Allylamino)-17-demethoxygeldanamycin (17-AAG), and 17-(Dimethylaminoethylamino)-17-demethoxygeldanamycin (17-DMAG), radicicol and pochonin (Amolins & Blagg 2009). Initial experiments revealed that binding of geldanamycin and radicicol to Hsp90 resulted in the degradation of the client protein v-src (Holzbeierlein et al. 2010). Although IC_{50} values are reported against various cancer cell lines, the poor solubility of geldanamycin and hepatotoxicity in animal studies has hampered its progress as an anti-cancer agent (Amolins & Blagg 2009). The development of the geldanamycin analogues 17-AAG and 17-DMAG

improved the associated toxicity, and chemical synthesis was significantly improved (Holzbeierlein et al. 2010). The analogues 17-AAG and 17-DMAG still however struggle with issues such as poor solubility, hepatotoxicity and the development of resistance (Holzbeierlein et al. 2010). Radicicol as an anti-cancer agent also shows little prospect as it lacks activity *in vivo* due to its rapid conversion into inactive metabolites (Chaudhury et al. 2006; Holzbeierlein et al. 2010). This, together with the difficult chemical synthesis, means that the development of radicicol as an anti-cancer compound has hampered (Holzbeierlein et al. 2010). The resistance of cells to Hsp90 inhibitors targeted to the N-terminal primarily arises from the initiating heat shock response (Holzbeierlein et al. 2010). Upon binding of an N-terminal inhibitor to the Hsp90 N-terminal domain, HSF-1 (the mediator of the heat shock response) is released from the heteroprotein complex and activates the heat shock response. The induced heat shock response results in the overproduction of Hsp27 and Hsp70, both which are anti-apoptotic factors and thus compensate for the role played by Hsp90 within the cell (Holzbeierlein et al. 2010).

The binding of inhibitors to the Hsp90 C-terminal microdomain is not well understood. EGCG, the active ingredient in green tea, has been shown to bind the C-terminus of Hsp90 but does not prevent Hsp90 from forming complexes with co-chaperones and client proteins (Donnelly & Blagg 2008). Studies have revealed that novobiocin competes with ATP for binding of the C-terminal hydrophobic ATP-binding microdomain and that the binding of novobiocin to the C-terminal displaces inhibitors bound to the N-terminus (Donnelly & Blagg 2008). Novobiocin has been shown to have a differential ability to interfere with the binding of TPR motif containing co-chaperones and client proteins (Allan et al. 2006).

1.4 EXTRACELLULAR HSP90 (eHsp90)

Hsp90α and Hsp90β have been shown to reside both in the cytosol (Sreedhar et al. 2004) and the extracellular space (Becker et al. 2004; Eustace & Jay 2004; Tsutsumi & Neckers 2007). The means by which eHsp90α and eHsp90β localize to the extracellular space is yet fully determined. Hsp90 lacks any signal sequences at its N-terminus and can therefore not be secreted via the canonical E.R/Golgi transport pathway (Chieh-Fang Cheng et al. 2008a). Evidence points towards the secretion of Hsp90α from invasive cancer cells via exosomes (McCready et al. 2010), suggesting that eHsp90 is derived from one of the intracellular isoforms and not from a separate gene. eHsp90 has been detected on the cell surface of numerous cells (Eustace & Jay 2004; Tsutsumi, Beebe, et al. 2009; C.-F. Cheng et al. 2008;

Sidera et al. 2008), as well as in the extracellular space (Li et al. 2007; Liao et al. 2000; Wang et al. 2009), suggesting eHsp90 resides both as a pool of membrane associated eHsp90 as well as a pool of soluble eHsp90. Whether soluble eHsp90 is derived from the proteolytic cleavage of membrane associated eHsp90 is unknown. Grp94 has also been shown to reside extracellularly despite its ER retention signal (Basu et al. 2001). Crossman and colleagues suggest Grp94 functions as a cross-presentation antigen (Crossman & Nicchitta 2007; Suto & Srivastava 1995), however limited studies expand upon the role of Grp94 in the extracellular space.

There is current discussion around the distinct localization of eHsp90α and eHsp90β isoforms and most studies do not distinguish between membrane associated and soluble eHsp90α and eHsp90β isoforms. Few reports show secretion of both soluble Hsp90α and Hsp90β into the extracellular space (Hegmans et al. 2004). Others show the presence of Hsp90α on the surface of cancer cells coupled with the secretion of soluble Hsp90α, and not Hsp90β, into the extracellular space (Eustace et al. 2004; Li et al. 2007; Liao et al. 2000). Interestingly, the secretion of a truncated form of Hsp90α, lacking the EEVD motif, has also been reported (Wang et al. 2009). The presence of eHsp90 is not specific to malignant cell types. Immunostaining of live cerebellar cells has shown Hsp90α and Hsp90β isoforms localized on the cell surface of neural cells (Sidera et al. 2004). Hsp90β has been identified on the cell surface of cultured oligodendrocytes (Cid et al. 2004) whilst Hsp90α was detected in the conditioned medium of human dermal fibroblasts (Li et al. 2007). This evidence points towards an important functional role for eHsp90 for both normal physiology and diseased state (Eustace & Jay 2004).

eHsp90 has been shown to interact with a finite number of extracellular proteins (Eustace & Jay 2004). Some of the reported eHsp90 interacting proteins are shown in Table 1. Despite the identification of eHsp90 interacting proteins, the function of eHsp90 in these complexes is unknown. Elucidation of whether eHsp90 acts as a chaperone is still ongoing. eHsp90, eHsp90α in most cases, has received much attention for its proposed role in cell migration and invasion. Reported targets for eHsp90 stimulated cell migration include MMPs, LRP-1, tyrosine kinase receptors and possible others unidentified. eHsp90 has been shown to stimulate migration through the maturation and activation of MMPs and other extracellular proteases. Extracellular proteases are of crucial significance for migration and invasion (Sabeh et al. 2009; Vérollet et al. 2011). Sims and co-workers propose a model in which the

activation of MMP-2, by an extracellular chaperone/co-chaperone complex containing eHsp90α, increased cell migration and invasion in breast cancer cells (Sims et al. 2011). A report by Song and colleagues show the middle domain (residues 272 to 617) of eHsp90 responsible for the activation of MMP2 (Song et al. 2010). Hance and colleagues further show that eHsp90 plays a dual role in both up-regulating MMP2 and MMP9 transcript levels, as well as increasing proteolytic activity (Hance et al. 2012). Most recently, Correia and colleagues showed a requirement for eHsp90β for MMP3 function in invasion (Correia et al. 2013). Of importance, it must be noted that eHsp90 was also identified as a substrate for proteolytic cleavage by MMP2 (Song et al. 2010). Both Hsp90α and Hsp90β are degraded upon incubation with MMP2 *in vitro*, however Hsp90β is degraded far more rapidly (Song et al. 2010). Apart from the interaction of eHsp90 with MMPs, McCready and colleagues showed that Hsp90α assisted in plasminogen activation and subsequent tumor cell migration (McCready et al. 2010). Suzuki and Kulkarni report that eHsp90β blocks the conversion of latent TGFβ into its active form, decreasing the tumor suppressing activity of TGFβ (Suzuki & Kulkarni 2010).

eHsp90 function appears to be distinct from its intracellular chaperone function, in that it may act via receptor mediated induction of intracellular signaling activity (Hance et al. 2012). A range of receptor associated, signal transduction pathways have been implicated in the eHsp90 stimulated migration and invasion of cancer cells. Sidera and colleagues suggest membrane bound Hsp90α interacts with HER-2 leading to activation of signal pathways that result in increased cell motility and invasion (Sidera et al. 2008). Thuringer and coworkers reported that recombinant Hsp90α activates a toll-like receptor 4 (TLR-4) signal pathway in glioblastoma U87 cells and subsequent transactivation of EGFR and a change in cytosolic calcium concentration patterns (Thuringer et al. 2011). Both outcomes were predicted to facilitate cell migration (Thuringer et al. 2011). Chung and colleagues showed upregulation of transcription of the IL-8 gene by secreted eHsp90 (Chung et al. 2009). TLR-4, mitogen activated protein kinases, NF-κB and reactive oxygen species were shown to be involved in the process (Chung et al. 2009). Elevated production of IL-8 has been shown to be associated with invasiveness and metastatic potential in breast cancer cells (Kim et al. 2012; Yao et al. 2007).

Several reports show the stimulatory effects of eHsp90 on migration in concert with CD91/ LRP-1 (low density lipoprotein receptor-related protein 1), a functional receptor previously

shown to bind Hsp90 (Basu et al. 2001; Gopal et al. 2011). Cheng and colleagues initially show that secreted Hsp90α promoted cell migration through LRP-1 (Chieh-Fang Cheng et al. 2008b). Interestingly, Hsp90β was shown to have no effect on LRP-1 mediated cell migration (Wei Li – personal communication, CSSI VI International Congress on Stress Proteins in Biology and Medicine). Chen and colleagues later reported the induction of colorectal cancer (CRC) cell migration through secreted Hsp90α induced LRP-1 and NF-κB-mediated integrin α_v expression (Chen et al. 2010). Chen further showed that secreted Hsp90α induced LRP-1 and NF-κB-mediated TCF12 protein expression, enhancing CRC cell migration through down-regulation of E-cadherin, connexin-26, connexin-43 and gap junction levels (Chen et al. 2013). Similarly to TCF12 overexpression, secreted or recombinant Hsp90α induced fibronectin expression (Chen et al. 2013). Gopal and colleagues demonstrated eHsp90-LRP-1 dependent AKT signaling and regulation of EphA2 function as an integral component of the aggressive nature of glioblastoma cell invasion (Gopal et al. 2011). Hance and colleagues showed that an eHsp90-LRP signaling pathway promoted cell motility through reduced expression and altered localization of E-cadherin in an ERK and MMP2/MMP9 dependent manner (Hance et al. 2012). Taken together, these reports suggest eHsp90 has multiple downstream targets in its stimulatory effect of cell migration and invasion.

Using sequential deletion mutagenesis, Cheng and colleagues reported that a 115 amino acid fragment (F-5) at the boundary between the linker region and middle domain responsible for the pro-motility effect of eHsp90α-LRP-1 signaling (Cheng et al. 2011). These findings suggested the N-terminal ATPase domain and C-terminal dimerization domain are dispensable for eHsp90α to promote cell migration (Li et al. 2011). Three reports suggest the N-terminal ATP binding site of Hsp90α is still required for functioning of at least some of the roles of eHsp90 (Eustace et al. 2004; Tsutsumi, Scroggins, et al. 2009). DMAG-N-oxide, a geldanamycin/17-AAG derived cell impermeable Hsp90 inhibitor was shown to inhibit cell invasion *in vitro* and tumor invasion *in vivo* (Eustace et al. 2004; Tsutsumi, Scroggins, et al. 2009; Cheng et al. 2011). Chen and colleagues further show that treatment with DMAG-N-oxide blocks Hsp90α, but not F-5, stimulated skin cell migration (Cheng et al. 2011). Li and coworkers therefore hypothesized that binding of the N-terminal ATPase site results in a conformational change in eHsp90α that results in masking of the F-5 epitope (Li et al. 2011). Apart from a role for eHsp90 in migration and invasion, eHsp90 has been shown to possess additional roles in the pathogenicity of bacterial and viral infections. eHsp90 has been implicated in recognizing lipopolysaccharides (LPS) on the surface of gram-negative bacteria

(Triantafilou & Triantafilou 2004). Similarly, eHsp90 has been shown to form part of a receptor complex of the Dengue virus (Reyes-Del Valle et al. 2005) and Infectious bursal disease virus (IBDV) on chicken cells (Lin et al. 2007) and serves as a co-factor for cellular entry of Karposi sarcoma-associated herpesvirus (KSHV).

Li and colleagues strongly concluded that eHsp90 does not act as a chaperone in the extracellular space (Li et al. 2012). The chaperoning activity of the intracellular Hsp90 complex has been thought to rely upon ATP hydrolysis and co-chaperone interaction (Johnson et al. 2000). Despite reports of N-terminal inhibitory effects on eHsp90, to date, all reports state a role for eHsp90 independent of ATP hydrolysis (Li et al. 2012). The secretion of a truncated form of Hsp90α, lacking the EEVD motif (Wang et al. 2009) may suggest an inability of eHsp90 to interact with TPR-containing co-chaperones. Most recently, El Hamidieh and colleagues show the presence of the molecular chaperone Cdc37 on the surface of MDA-MB-453 and MDA-MB-231 human breast cancer cells (El Hamidieh et al. 2012). Surface Cdc37 was shown to interact with membrane associated eHsp90 as well as HER-2 and EGFR (El Hamidieh et al. 2012). Inhibition of Hsp90 with a monoclonal antibody against Hsp90 (MAb 4C5) was shown to disrupt the surface Cdc37/eHsp90 complex (El Hamidieh et al. 2012). Cdc37 blocks closure of the N-terminal Hsp90 ATP binding site and inhibits the ATPase activity of Hsp90 (Siligardi et al. 2002). El Hamidieh and colleagues suggest surface Cdc37 acts as a co-chaperone to eHsp90 in association with the protein kinase receptors (El Hamidieh et al. 2012). To further substantiate a possible chaperoning role for eHsp90, a growing number of Hsp90 co-chaperones have also been reported on the cell surface (Tsutsumi & Neckers 2007; Eustace & Jay 2004; Sims et al. 2011).

Table 1: eHsp90 interacting proteins

Protein	Extracellular Pool of Hsp90	Hsp90 isoform	Reference
Annexin	Membrane	Hsp90α	(Lei et al. 2004)
TLR-1/CD14, CXCR4, GDF-5	Membrane	Hsp90α	(Triantafilou & Triantafilou 2004)
MMP2	Both	Hsp90α	(Eustace et al. 2004)
Hsp70	Membrane	Hsp90α	(Reyes-Del Valle et al. 2005)
HER-2/ErbB-2	Membrane	Both*	(Sidera et al. 2008)
LAP	Both	Hsp90β	(Suzuki & Kulkarni 2010)
tPA	Secreted	Hsp90α	(McCready et al. 2010)
MMP9	Secreted	Both*	(Stellas et al. 2010)
LRP-1/CD91	Undefined	Hsp90α?	(Gopal et al. 2011; Basu et al. 2001)
Cdc37	Membrane	Undefined	(El Hamidieh et al. 2012)
EGFR	Membrane	Undefined	(El Hamidieh et al. 2012)
MMP3	Secreted	Hsp90β	(Correia et al. 2013)

*Identified using a monoclonal antibody against Hsp90 (MAb 4C5) that recognizes the α isoform to a greater extent than the β isoform (Sidera et al. 2008).

1.5 THE EXTRACELLULAR MATRIX (ECM)

A substantial part of the volume of a tissue is extracellular space (Frantz et al. 2010). This space is filled by an intricate network of macromolecules (proteins, glycoproteins, proteoglycans and polysaccharides) secreted and assembled into an organized network by surrounding cells (Hynes 2009; Lu et al. 2012). The extracellular matrix (ECM) components confer unique physical, biochemical and biomechanical properties in a complex three-dimensional network that regulates cell behavior (Lu et al. 2012). ECM macromolecules are bioactive and play a key role in cell adhesion, differentiation, proliferation and migration of cells (Mao & Schwarzbauer 2005; Hynes 2009). The importance of the ECM is demonstrated by the wide range of physical syndromes, minor to severe, arising from abnormalities of the

ECM (Jarvelainen et al. 2009). The concept that local microenvironments, and the importance of non-cellular components, play an important role in cell behavior have become increasingly accepted in cancer biology (Lu et al. 2012).

1.6 FIBRONECTIN (FN)

FN is a ubiquitous ECM glycoprotein that is assembled into a fibrillar matrix in all tissues and throughout all stages of life (Singh et al. 2010). FN forms a fundamental part of the ECM (Dallas et al. 2006; Wierzbicka-Patynowski & Schwarzbauer 2003; To & Midwood 2011). FN plays an important role in cell adhesion, migration, growth and differentiation (Hynes 1990; Pankov 2002; Xu & Mosher 2011). Several ECM proteins, including collagen types I and III and thrombospondin-1 (Mcdonald et al. 1982; Sottile & Hocking 2002; Li et al. 2003), fibrillin-1 (Sabatier et al. 2009), fibulin-1 (Roman & McDonald 1993), fibrinogen (Pereira et al. 2002) and LTBP-1 (Dallas et al. 2005), have been shown to rely upon an extracellular FN matrix for assembly. FN has thus been described as a "master organizer" for biogenesis of the ECM (Dallas et al. 2006).

1.6.1 Fibronectin and cancer

FN is produced and secreted as a soluble dimer by various benign and malignant epithelial and mesenchymal cells. Soluble FN is then assembled into an insoluble network of fibers in the extracellular space (Mao & Schwarzbauer 2005; Schwarzbauer & Sechler 1999; Salicioni et al. 2002; Labat-Robert 2012; Christensen 1992; Wierzbicka-Patynowski & Schwarzbauer 2003). FN has been implicated in the development of numerous human cancers (Waalkes et al. 2010; Jia et al. 2010; Zheng et al. 2007; Hu et al. 2004). Brenner and colleagues have shown that oncogenically transformed cells show a decrease in FN synthesis and an increase in FN degradation (Brenner et al. 2000). A more recent study reports FN expression is related to tumor size, histological grade and MMP-9 expression in breast cancer tissue (Fernandez-Garcia et al. 2013). Tumors with high FN expression were associated with a higher probability of metastasis and poor overall survival in breast cancer patients (Fernandez-Garcia et al. 2013).

1.6.2 Structure

Fibronectin (FN) is an ECM glycoprotein existing as a dimer (~450 kDa) linked by disulfide bonds at the carboxyl terminus (Mao & Schwarzbauer 2005; Schwarzbauer & Sechler 1999; Salicioni et al. 2002). Figure 3 shows the structure of a FN monomer. Each FN subunit is

composed of repeating modules, types I, II and III (Schwarzbauer & Sechler 1999; Wierzbicka-Patynowski & Schwarzbauer 2003). Type I modules have a hydrophobic core, containing highly conserved aromatic amino acids and a pair of disulphide bonds, encased by stacked β sheets (Baron et al. 1990). Type II modules consist of two anti-parallel β-sheets linked by disulphide bonds (Pickford et al. 1997). Type III modules consist of seven β-strands arranged as two anti-parallel β-sheets connected by flexible loops (Dickinson et al. 1994). FN consists of 12 type I modules, 2 type II modules, both types of modules containing two intrachain disulfide bonds, and 15-17 type III modules which do not have disulfide bridges (Mao & Schwarzbauer 2005). Fifteen type III modules are constitutively included while two are alternatively spliced (Hynes 1990). Sets of repeating modules make up domains that bind extracellular and cell surface molecules such as collagen, fibrin, integrins and FN itself (Wierzbicka-Patynowski & Schwarzbauer 2003). Rotary shadowing electron microscopy has shown the FN molecule to have a length of 120 – 160 nm, with each polypeptide chain of the dimeric molecule spanning half the length of each strand (Erickson et al. 1981). Well extended FN molecules are uniform in thickness, with an average diameter of 2 nm (Erickson et al. 1981). Each polypeptide chain of a FN dimer is arranged with its carboxyl termini joined at the center of an extended strand, and its amino termini at the outer ends (Erickson et al. 1981). Erickson and colleagues further observed the presence of a forklike structure at one or both ends of the extended fibronectin strand (Erickson et al. 1981). Additionally a segment of 10 – 30 nm appeared to be missing near the center of each strand; however this was observed less frequently (Erickson et al. 1981). In cell culture, secreted soluble FN forms a complex intricate insoluble network of FN fibrils in the extracellular space (Ohashi & Erickson 2009). Electron microscopy has shown that these matrix fibrils are composed of bundles of fine FN fibers, 5 to 10 nm in diameter (Ohashi & Erickson 2009). Fibrils are dynamic and elastic in nature (Ohashi & Erickson 2009). The variation in length of FN reported by Erickson and colleagues (Erickson et al. 1981) testifies to its dynamic elastic structure as reported by Ohashi and Erickson (Ohashi & Erickson 2009). FN matrix fibrils have long thought to form from disulfide-bonded FN multimers, although no direct evidence for a covalent attachment has been reported (Ohashi & Erickson 2009). This chain of thought was brought about by the appearance of migrating FN multimers on non-reducing SDS gels (Ohashi & Erickson 2009). Ohashi and Erickson showed that the phenomenon of FN migrating as a FN multimer on SDS gels is an artifact rising from other large components of deoxycholate extraction (Ohashi & Erickson 2009). They suggest that

FN matrix fibrils are made of FN dimers that are further cross-linked by non-covalent protein-protein interactions (Ohashi & Erickson 2009).

Structural variants of FN arise from a single gene by alternative splicing and post-translational modification (Salicioni et al. 2002). Fifteen type III modules are invariant whilst two are alternatively spliced (Salicioni et al. 2002).

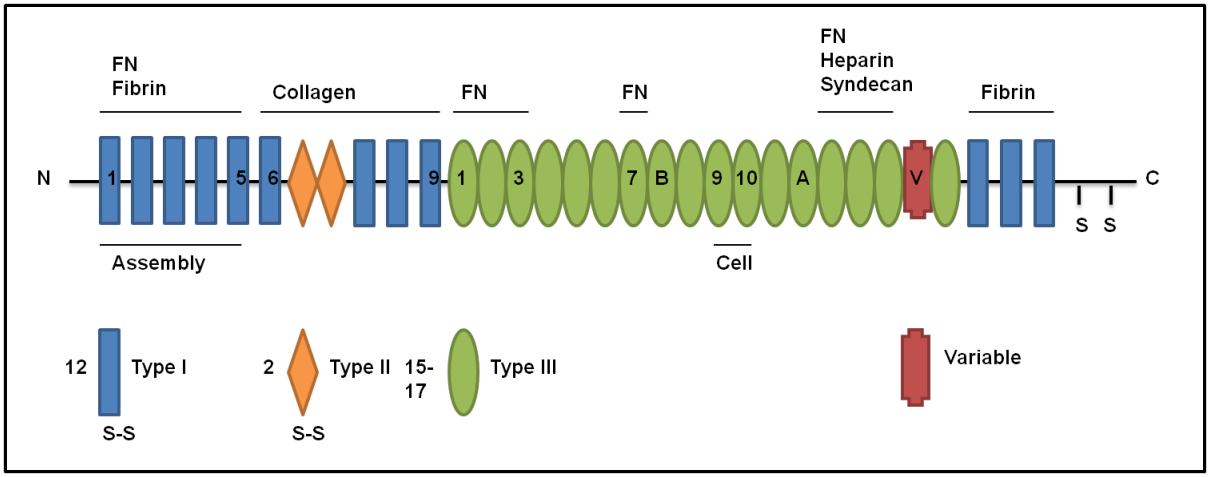

Figure 3: Structure of the FN monomer

Schematic diagram of the structure of a FN monomer. Each FN monomer is composed of three types of repeats: 12 type I (rectangle), 2 type II (diamond) and 15-17 type III (oval). Repeats are numbered according to type of repeat. Cell surface binding, assembly, fibrin, collagen, heparin, syndecan and FN self-association binding domains are shown. Alternatively spliced EIIIA (A) and EIIIB (B) and variable region are shown. Intermolecular dimer cysteines (S) are seen at the C-terminus.

1.7 FIBRONECTIN FIBRILLOGENESIS

FN is secreted by cells as a soluble dimer that is then assembled into an insoluble network of fibers (Figure 4) (Robinson et al. 2004; Wierzbicka-Patynowski & Schwarzbauer 2003; Singh et al. 2010). The interaction of secreted FN with cell surface proteins and the subsequent formation of insoluble FN as a part of the ECM can be termed fibrillogenesis (Mao & Schwarzbauer 2005; Robinson et al. 2004). Fibrillogenesis proceeds stepwise from initiation through to elongation and stabilization (Schwarzbauer & Sechler 1999). Following secretion into the extracellular space, fibrillogenesis is initiated by the binding of soluble FN to cell surface recognition sites (Pankov 2002; Wierzbicka-Patynowski & Schwarzbauer 2003). Reports identify the binding of the RGD (Arg-Gly-Asp) motif, in the type III_9 module, and synergy sequence (PHSRN) in the adjacent type III_{10} module of FN, to cell surface $\alpha5\beta1$ integrin, as a key binding step in the initiation of fibrillogenesis (Pankov 2002; Robinson et

al. 2004; Wierzbicka-Patynowski & Schwarzbauer 2003; Singh et al. 2010). Most recently, Gee and colleagues further identified a 23-residue cryptic peptide (CP1) within the type III_{10} module, exposed upon tension driven unfolding of FN, that initiates FN fibrillogenesis (Gee et al. 2013) Binding of FN to α5β1 integrin is not restricted to III_{9-10} but also interacts with an N-terminal FN fragment containing repeats I_{1-9} and II_{1-2} (Pankov 2002), henceforth referred to as FN70. The RGD motif of FN is reported to bind eight out of twenty-four cell synthesized integrins (Labat-Robert 2012). The α5β1 integrin is reported as the primary receptor for the initiating interaction with FN, however other integrins can perform this function under appropriate conditions (Mao & Schwarzbauer 2005). An RGD-independent mechanism for initiation acts through the binding of α4β1 integrin to the CS1 site within the alternatively spliced V-region near the C-terminus of FN (Sechler et al. 2000). Initiation of fibrillogenesis is thus not dependent upon the central placement of the integrin binding site (Wierzbicka-Patynowski & Schwarzbauer 2003). The binding of FN to integrins increases the affinity of individual integrins for bound FN and induces clustering of integrins along the cell surface site of binding (Labat-Robert 2012; Robinson et al. 2004; Singh et al. 2010). Clustering of FN-bound integrins increases the concentration of local FN promoting FN-FN interactions (Wierzbicka-Patynowski & Schwarzbauer 2003). Monomeric FN lacking the C-terminal cysteines could not assemble into a FN matrix (Kozaki et al. 2003). Cysteine co-ordinated dimerization of soluble FN is thus essential for FN assembly through the binding, and initiation of clustering, of integrins (Wierzbicka-Patynowski & Schwarzbauer 2003). Integrin-FN clusters also result in the connection of extracellular FN to the intracellular actin cytoskeleton via integrin cytoplasmic domain interactions, an important linkage for matrix assembly (Mao & Schwarzbauer 2005; Schwarzbauer & Sechler 1999). The formation of actin stress fibers generates tension and cytoskeletal rearrangements that most likely stretch cell-associated FN, exposing additional sites for FN self-association (Schwarzbauer & Sechler 1999). Evidence for tension induced exposure of FN self-association sites and the elasticity of FN fibrils (Carraher & Schwarzbauer 2013; Erickson 2002), led to the hypothesis that conformational changes and extension of FN is thought to arise from unfolding of individual type III repeats, as they lack intrachain disulfide bonds (Mao & Schwarzbauer 2005; Schwarzbauer & Sechler 1999). In addition to receptor clustering, binding of FN to integrins initiates a conformational change in the FN molecule that exposes FN self-association sites (Vakonakis et al. 2007; Wierzbicka-Patynowski & Schwarzbauer 2003; Singh et al. 2010). At least four FN-FN binding sites are distributed across each subunit with many of these acting as binding partners for the N-terminal assembly domain (Wierzbicka-

Patynowski & Schwarzbauer 2003; Schwarzbauer & Sechler 1999). FN self-association sites involved in FN elongation include the amino-terminal repeats I_{1-5}, the first one or two type III repeats, and the carboxy-terminal heparin domain (Schwarzbauer & Sechler 1999). All known FN self-association sites interact with the amino terminal domain of FN (FN70) (Schwarzbauer & Sechler 1999). FN lacking FN70 is unable to assemble into FN fibrils (Schwarzbauer 1991), and addition of exogenous FN70 blocks FN matrix assembly (McKeown-Longo & Mosher 1985). FN self-association sites in repeat III_1 and the heparin binding domain appear cryptic (Schwarzbauer & Sechler 1999), and are thought to rely upon FN unfolding for exposure and binding of additional FN molecules. Following initiation, fibrils are propagated by the continual addition and extension of FN dimers to growing multimers, resulting in an insoluble FN matrix (Schwarzbauer & Sechler 1999).

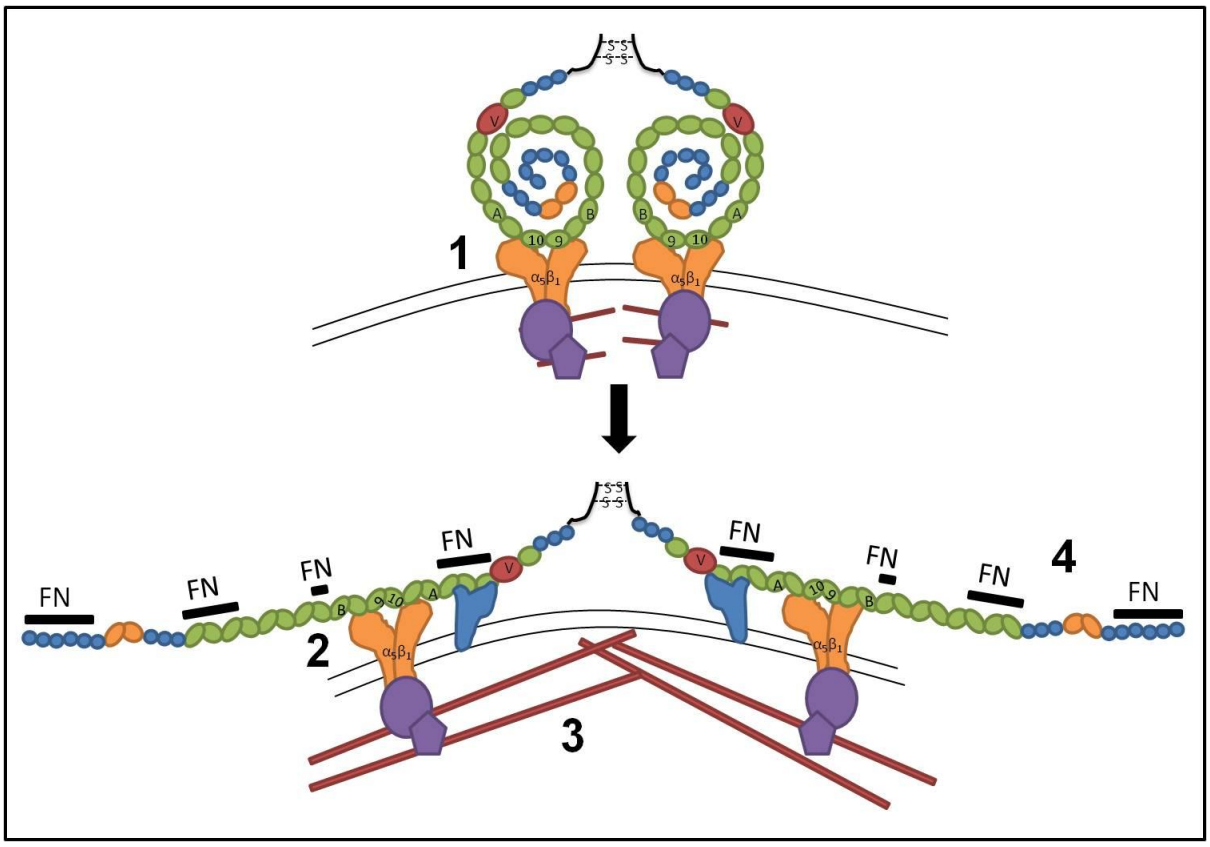

Figure 4: Schematic diagram of the major steps in FN fibrillogenesis

Schematic diagram describing the major steps in FN matrix assembly. (1) Binding of the RGD (Arg-Gly-Asp) motif, in the type III_9 module, and synergy sequence (PHSRN) in the adjacent type III_{10} module of FN, to cell surface α5β1 integrins. (2) Binding of FN to cell surface integrins leads to clustering of ligand (FN) bound integrins and connection of FN to the actin cytoskeleton via receptor cytoplasmic domain interactions. (3) The formation of actin stress fibers results in generated tension and cytoskeletal rearrangements that most likely stretch cell-associated FN, which together with conformational changes of FN upon integrin binding (4) reveal additional sites for FN self-association. Fibrils are propagated by the continual addition and extension of FN dimers to growing multimers, resulting in an insoluble FN matrix

1.8 FIBRONECTIN TURNOVER

FN matrix stability is dynamic and involves the balance of FN matrix assembly and turnover. Two molecular mechanisms are currently believed to be involved in the degradation and turnover of ECM proteins, namely extracellular degradation of ECM proteins by proteases, and internalization of ECM proteins and intracellular degradation in lysosomes (Shi & Sottile 2009). These molecular mechanisms are not mutually exclusive and are believed to act collaboratively in the turnover of ECM proteins (Shi & Sottile 2009).

1.8.1 Extracellular fibronectin degradation

Given the large size and macromolecular structure of FN (Schwarzbauer & Sechler 1999) it is likely some degree of degradation occurs extracellularly prior to internalization (Shi & Sottile 2009; Shi & Sottile 2011). Numerous proteolytic enzymes have been reported for the degradation of ECM proteins (Etique et al. 2013). A wide range of extracellular proteases have been implicated in the degradation of FN (Berry et al. 1998; Zhang et al. 2012). These include plasmin (Gold et al. 1989; Bonnefoy & Legrand 2000), matrix metalloproteinases (MMPs) MMP1, MMP3, MMP13 and MMP14 (Zhang et al. 2012; Shi & Sottile 2011). Urokinase-type plasminogen activator (uPA) and tissue-type PA (tPA) catalyze the conversion of plasminogen to the active serine protease plasmin (Etique et al. 2013). Plasmin has been implicated in the degradation of numerous ECM macromolecules, including FN, and additionally triggers the maturation of MMPs (Etique et al. 2013). MMPs are secreted as a proenzyme that is then enzymatically activated by the proteolytic removal of the pro-domain by other extracellular proteases (Stellas et al. 2010; Etique et al. 2013). A primary characteristic of invasive tumors is their capacity to enhance degradation of the ECM via the catalytic activity of MMPs (Stellas et al. 2010). Shi and Sottile show MMP14 as a crucial regular of FN turnover by promoting extracellular degradation of FN and by regulating α5β1 integrin endocytosis (Shi & Sottile 2011). Zhang and colleagues further report the cleavage of FN by MMP1, MMP3, MMP13 and MMP14 (Zhang et al. 2012). Two levels of control are applied for the activity of extracellular proteases, namely inhibition of their catalytic activities and receptor-mediated endocytosis and lysosomal catabolism (Etique et al. 2013). Extracellular proteases also regulate the production of biologically active ECM fragments that can have potent biological effects (Shi & Sottile 2011). Proteolytic fragments of FN can have distinct biological activity from intact FN (Lohr et al. 1990). Zhang and colleagues report that cleavage of FN by MMP3, MMP13 and MMP14 all generated the 70-kDa N-

terminal FN fragment, FN70 (Zhang et al. 2012). MMP2 has been shown to cleave FN into 120, FN70, 45 and 11 kDa fragments (Kenny et al. 2008). As previously stated, FN70 has been shown to play a fundamental role in the assembly of FN (Schwarzbauer & Sechler 1999; McKeown-Longo & Mosher 1985; Aguirre et al. 1994; Wierzbicka-Patynowski & Schwarzbauer 2003). FN70 has also been shown to have distinct biological activity to its role in FN assembly. FN70 fragments play an important role in the initiation and progression of arthritic diseases through the induction of a pro-inflammatory response (Zhang et al. 2012). FN70 has also been shown to act as chemoattractant for human peripheral blood monocytes (Lohr et al. 1990) and modulate proliferation of human retinal endothelial cells (Wilson 2003). In addition to FN70 as a proteolytic fragment of FN degradation, Migration Stimulating Factor (MSF), a truncated isoform of FN, consists of FN70 coupled with a unique 10 amino acid C-terminus (Ellis et al. 2010). MSF is derived from a transcription read-through of the intron separating exons III-1a and III-1b of the FN gene, followed by message cleavage and polyadenylation (Ellis et al. 2010). MSF has been shown to be a potent motogenic factor, stimulating migration of fibroblasts, epithelial and endothelial cells (Ellis et al. 2010). In addition to FN70, other proteolytic fragments of FN have profound biological effects. Treatment of TM-6 cells with a 120 kDa FN fragment (FN120) induced matrix degrading protease activity (Schedin et al. 2000).

1.8.2 Fibronectin endocytosis

FN degradation occurs intracellularly after endocytosis (Sottile & Chandler 2005a). Endocytosis of extracellular FN is reported to be regulated by both β1 integrins and LRP-1 (Etique et al., 2013; Shi & Sottile, 2009; Sottile & Chandler, 2005a). Both cell surface integrins (Bretscher 1989; Bretscher 1992) and LRP-1 (Wu & Gonias 2005) undergo constitutive endocytosis and recycling in their regulation of FN turnover. The α5β1 integrin, one of the membrane bound cell surface integrins that binds FN, is known to undergo endocytosis (Bretscher 1989). Salicioni and co-workers thus proposed that under certain circumstances, FN may be internalized with α5β1 integrin (Salicioni et al. 2002). Salicioni and colleagues report the LRP-1 as a major regulator of FN endocytosis and degradation (Salicioni et al. 2002). LRP-1 is a 600 kDa member of the low density lipoprotein (LDL) receptor family that is constitutively recycled in clathrin-coated pits through endocytosis (Salicioni et al. 2002; Etique et al. 2013). LRP-1 binds a diverse range of ligands, such as plasminogen activators, apolipoprotein E and thrombospondin 2 (a primary ligand that mediates the endocytosis of MMP-2) that are then recycled or delivered to lysosomes for

degradation (Salicioni et al. 2002; Gaultier et al. 2011). Salicioni and co-workers proceed further to show that FN accumulated in the ECM in LRP-1 deficient fibroblasts, thus concluding that LRP-1 bound directly to FN and mediated its catabolism (Salicioni et al. 2002). The LRP-1 antagonist, receptor associated protein (RAP) was shown to block the association of FN with LRP-1 providing evidence that the FN-LRP interaction is specific (Salicioni et al. 2002). However, LRP-1 may indirectly regulate FN accumulation in the ECM as LRP-1 has been shown to decrease cell-surface levels of urokinase-type plasminogen activator receptor (uPAR), a receptor that Aguirre-Ghiso and colleagues show associates with α5β1 integrin (Salicioni et al. 2002; Aguirre et al. 1994). Salicioni and colleagues further report a model in which LRP-1 directly or indirectly promotes the maturation of β1 integrin precursor, increasing the cell surface level of β1 integrins (Salicioni et al. 2004)

1.9 FORMER WORK AND MOTIVATION

The chaperone activity of Hsp90 plays a vital role in the stability, refolding and maturation of key oncogenic proteins expressed in tumor cells. Hsp90 is thus considered a bona fide drug target. Mounting evidence suggests that Hsp90 is present and functionally active in the extracellular space, although the function of eHsp90 is relatively uncharacterized compared to its intracellular counterpart. Recent unpublished work within the Biomedical Biotechnology Research Unit, Rhodes University, has shown the presence of both cell surface associated eHsp90 as well as soluble eHsp90α. Hsp90α, and to a greater extent, Hsp90β, were isolated in a complex containing FN on the surface of MDA-MB-231 cells. The interaction of Hsp90 with FN has not been analyzed. Previous unpublished data showed that treatment of Hs578T cells with novobiocin results in a loss of extracellular FN matrix and subsequent endocytosis of FN and colocalization with key vesicular trafficking markers (Rab-5 and LAMP-1). Most interestingly geldanamycin showed no effect on the extracellular FN matrix. It has been proposed that inhibition of Hsp90 results in FN matrix instability and degradation of FN through an endocytosis-mediated pathway. It has been shown that LRP-1 is able to regulate FN endocytosis and degradation, and endocytosis of Hsp90 in macrophages and dendritic cells. Whether Hsp90 is responsible for the chaperoning of FN to LRP-1 followed by subsequent endocytosis of the complex is unknown.

1.10 HYPOTHESIS

Inhibition of the direct interaction of Hsp90 and FN with novobiocin results in FN endocytosis.

1.11 OBJECTIVES

The broad aim of the project was further elucidation of the role of Hsp90 in FN matrix dynamics. The following objectives were addressed:

1. Analysis of the Hsp90-FN interaction *in vitro*
2. Analysis of the effect of Hsp90β on the extracellular FN matrix dynamics

CHAPTER 2: METHODS

2.1 MATERIALS

2.1.1 Reagents

All general reagents were from Sigma Aldrich, USA, unless otherwise specified. GlutaMAX^{TM}-I, Fetal Calf Serum (FCS) and Oregon Green 488 Carboxylic Acid (O-6147) were from Invitrogen, UK. Penicillin/streptomycin was from Biowhittaker, UK. Insulin was from Novorapid, Canada. Complete, EDTA-free Protease Inhibitor Cocktail Tablets (11873580001) were from Roche, UK. ELISA microplates (655061) were from Greiner Bio-One, UK. Protino® Glutathione Agarose (GSH) 4B (745500) was from Macherey-Nagel, Germany. ECL Advance Western Blotting Detection Kit was from Amersham, UK. Tetramethylrhodamine-5-maleimide (94506), 3, 3'-Dithiobis [sulfosuccinmidylpropionated] (21578), Zeba spin desalting columns (89882), Pierce high capacity endotoxin removal spin columns (88273) and Pierce LAL chromogenic endotoxin quantitation kit (88282) were from Thermo Scientific, USA. MagReSyn™ NTA and MagReSyn™ Protein A were from ReSyn Biosciences, South Africa.

2.1.1 Proteins

Human FN (sc-29011) was from Santa Cruz Biotechnology, USA. FN70 (F0287) was from Sigma, USA. Hsp90α (SPR-101/A/B/C) and Hsp90β (SPR-102/A/B/C) was from StressMarq Biosciences, USA.

2.1.3 Antibodies

Mouse anti-human FN (F0916) and rabbit anti-human FN (F3648) primary antibodies were from Sigma Aldrich, USA. Mouse monoclonal Hsp90α/β IgG_{2a} antibody (sc-13119), goat polyclonal anti-Hsp90α/β (sc-1055), rabbit polyclonal anti-His-probe (sc-804) primary antibodies and donkey anti-goat IgG-HRP (sc-2020) secondary antibody were from Santa Cruz Biotechnology, USA. Mouse monoclonal anti-Hsp90β (ab119833), rabbit monoclonal anti-LRP1 (ab92544) primary antibodies and donkey anti-mouse Dylight® 488 (ab96875), donkey anti-rabbit Dylight® 555 (ab96892) and donkey anti-goat Dylight® 650 (ab96934) secondary antibodies were from Abcam, UK. Rat monoclonal anti-human Hsp90α (ADI-SPA-840) primary antibody was from Enzo Life Sciences, USA. Goat polyclonal anti-schistosomal GST (27457701) primary antibody and donkey anti-rabbit IgG-HRP (NA934V) secondary antibody was from GE Healthcare, UK. Goat anti-mouse IgG-HRP (474-1806)

secondary antibody was from Kirkegaard and Perry Laboratories, USA. Mouse monoclonal anti-LRP (515 kDa) LRP-1 used in blocking experiments was from GeneTex, USA.

2.2 METHODS

2.2.1 Cell culture

The Hs578T (HTB-126) and MDA-MB-231 (HTB-26) breast cancer cell lines were obtained from American Type Culture Collection (ATCC). MDA-MB-231 cells were maintained in Dulbecco's Modified Eagle Medium (DMEM) supplemented with GlutaMAX^{TM}-I, 5 % (v/v) FCS and penicillin/streptomycin (100 U.ml^{-1}). Hs578T cells were maintained in DMEM supplemented with GlutaMAX^{TM}-I, 10 % (v/v) FCS, penicillin/streptomycin (100 U.ml^{-1}) and 2 mM insulin. All cells were maintained at 37 °C in a humidified atmosphere with 10 % CO_2.

2.2.2 Optimization of induction conditions of GST-Hsp90β and GST

Plasmids pGEX-4T-1-GST-Hsp90β encoding human Hsp90β with an N-terminal GST tag, and pGEX-4T-1-GST encoding the GST tag alone, were previously cloned (Hunter 2011). The pGEX-4T-1-Hsp90β and pGEX-4T-1-GST (Figure 5) constructs (0.5 µM) were transformed into competent DnaK null *Escherichia coli* BB1994 (MC4100 *dnaK52 sidB1::Tc pDMI, 1::CmR KanR)* cells (Mayer et al. 2000). All growth media used for selection included the antibiotics ampicillin (100 µg.ml^{-1}) and kanamycin (50 µg.ml^{-1}). Transformed colonies were inoculated into 25 ml yeast extract and tryptone (YT) broth and incubated overnight with shaking at 37 °C. Overnight cultures were each added to 225 ml YT broth and incubated at 37 °C with shaking until an OD_{600} between 0.6 - 0.8 was obtained. Protein expression was induced with isopropyl β-D-1-thiogalactopyranoside (IPTG; [1 mM]) and cultures were incubated at 37 °C. At each time interval after induction (0, 1, 2, 3, 4, 5, 6 hours and overnight) an OD_{600} reading was recorded and 1 ml sample centrifuged at 13000 ×*g* for 1 minute. The pellet was resuspended in phosphate buffered saline (PBS; 137 mM NaCl, 2.7 mM KCl, 10 mM Na_2PO_4, 2 mM KH_2O_4) to a volume of equal cell density. The resuspended pellet was mixed with SDS sample buffer (60 mM Tris-HCl, pH 6.8, 2 % [w/v] SDS, 10 % [v/v] glycerol, 0.01 % [w/v] bromophenol blue, 5 % [v/v] β-mercaptoethanol) and boiled for 5 minutes. Induction samples were analyzed as per the SDS-PAGE and immunoblotting analysis methodology.

2.2.3 Purification of GST-Hsp90β and GST

GST-Hsp90β and GST were purified from induced *E. coli* BB1994 according to an adapted protocol of the batch purification of GST-tagged proteins in the Protino® Glutathione Agarose (GSH) user manual. Briefly, 250 ml pGEX-4T-1-Hsp90β and pGEX-4T-1-GST culture (OD_{600} between 0.6 - 0.8) was incubated at 37 °C and protein overproduction induced with IPTG (1 mM) for 3 hours. Cells were harvested at 6000 ×*g* for 15 minutes at 4 °C and the pellet resuspended in PBS. Cells were then lysed with the addition of lysozyme (1 mg/ml) in the presence of Complete, EDTA-free Protease Inhibitor Cocktail Tablets. Sonication subsequently followed at 50 Hz for 6 repeats, alternating 30 seconds on/30 seconds off using a Vibra-cell™ sonicator. Cell lysates were centrifuged at 10 000 ×*g* for 30 minutes at 4 °C and mixed with a bed volume of 0.5 ml GSH agarose. Pelleted beads were washed with PBS followed by centrifugation at 500 ×*g* for 5 minutes. Proteins were eluted with elution buffer (50 mM Tris, 10 mM glutathione) as outlined in the user manual. Samples were collected at each step of the purification and analyzed as per the SDS-PAGE and immunoblotting analysis methodology.

2.2.4 SDS-PAGE and Immunoblotting Analysis

Proteins were separated by discontinuous SDS-PAGE using the Laemmli buffer system (Laemmli 1970). Resolved proteins were transferred onto nitrocellulose membrane using transfer buffer (25 mM Tris, 192 mM glycine, 20 % [v/v] methanol), at 100 V for 2 hours on ice with stirring (Towbin et al. 1979). Each membrane was blocked in blocking solution (5 % [w/v] non-fat milk powder in TBS [50 mM Tris, 150 mM NaCl]) for 1 hour. Membranes were incubated with primary antibody at 4 °C overnight with shaking. Membranes were subsequently washed with TBST (TBS containing 1 % [v/v] Tween 20). Fresh blocking solution was added with the addition of HRP-linked species specific secondary antibodies. Incubation with species matched secondary antibodies was performed for 1 hour at room temperature, after which the membranes were washed with TBST. Proteins were detected using the ECL Advance Western Blotting Detection Kit and visualized using the Chemidoc™ system (Biorad).

2.2.5 Solid phase binding assay for the binding of GST-Hsp90β to FN

FN (100 $\mu g.ml^{-1}$) in 50 µl buffer A (20 mM Tris-HCl, 150 mM NaCl, pH 7.4, 1 mM ATP, 5 mM $CaCl_2$, 0.05 % [v/v] Tween 20) was incubated in the wells of a flat-bottomed high binding 96-well microplate for 5 hours at 22 °C. Non-specific binding sites were blocked

with 3 % (w/v) BSA in buffer A. Blocking solution was removed and either GST (negative control) or GST-Hsp90β (0 – 2500 nM) incubated in each well for 12 hours at 4 °C. Wells were subsequently washed three times with 1 % (w/v) BSA in buffer A and incubated with primary antibody in buffer A (1:1000) for 2 hours at 22 °C. Wells were washed three times with 1 % (w/v) BSA followed by the addition of secondary antibody in buffer A (1:4000) for 1 hour at 22 °C. 3,3',5,5'-Tetramethylbenzidine (TMB) substrate solution (in 0.05 M Phosphate-Citrate, pH 5.0) was added to each well for 25 minutes, and the reaction was stopped with 2 M H_2SO_4. The absorbance at 450 nm was recorded and data analysis performed using GraphPad Prism 4.03. FN adsorption to the ELISA plate and specificity of the Hsp90β antibody for GST-Hsp90β was confirmed using a similar protocol.

2.2.6 Determination of extracellular soluble Hsp90β

Hs578T cells were grown in maintenance media such that they reached confluency after 4 days. Conditioned media was centrifuged at 1 500 rpm in a microfuge for 10 minutes at 4 ºC. Conditioned media was incubated in the wells of a microplate Hsp90β detected as outlined previously. Recombinant commercial Hsp90β was used to establish a standard curve for the determination of the concentration of extracellular soluble Hsp90β.

2.2.7 Surface Plasmon Resonance (SPR) spectroscopy of the Hsp90-FN interaction

2.2.7.1 Kinetic analysis of the Hsp90-FN interaction

SPR spectroscopy was performed on a ProteOn^{TM} XPR36 Protein Interaction Array System (Bio-Rad, US) at 37 °C using running buffer (40 mM HEPES-NaOH, pH 7.4, 150 mM KCl, 5 mM $MgCl_2$). A ProteOn^{TM} GLM Sensor chip (#176-5012, Bio-Rad, US) was initialized with 50 % (v/v) glycerol and preconditioned at 30 µl.min^{-1} with successive 60 µl pulses of 0.05 % SDS (w/v) and 100 mM HCl in both the horizontal and vertical direction. Activation of the GLM chip surface followed with a 150 µl pulse of a 1:1 mixture of 1-ethyl-3-(3-dimethylaminopropyl)carbodiimide (EDAC) and Sulfo-NHS at 30 µl.min^{-1}. Recombinant Hsp90β (2, 10 and 50 µg.ml^{-1}), in 10 mM sodium acetate, pH 4.5 (determined by pre-concentration pH scouting), was immobilized at a level equivalent to ± 100 RU, ± 1900 RU and ± 350 RU respectively. Free amines on a fourth ligand channel were blocked with 1 M ethanolamine and used as an inline reference. FN sensorgrams were collected as either a 100 µl.min^{-1} injection for 180 seconds followed by a 600 second delay used to monitor dissociation (or as otherwise stated in figure legends). Regeneration was performed with an 18 second pulse injection of 10 mM Tris, pH 8.0, 3 M guanidine-HCl. Blank buffer injections

were used as a double reference subtraction. Kinetic curves were fit with a simultaneous K_a/K_d (Langmuir binding) to each of four independent experimental sets (10 $\mu g.ml^{-1}$) of sensorgrams using BIAevaluation 4.1.1. Further analysis was conducted in GraphPad Prism 4.03. Reported R_{eq} values were plotted against concentration and fit with a non-linear curve (one site binding). A Scatchard transformation was performed using one of Prism's built-in Pharmacology and biochemistry transforms with the superimposition of a straight line with points B_{max} and B_{max}/K_d. Analysis of the binding of FN70 to Hsp90β (10 $\mu g.ml^{-1}$) was performed as outlined above.

2.2.7.2 Analysis of Hsp90α and Hsp90β isoform specific binding of FN

SPR spectroscopy was performed on a ProteOn^{TM} XPR36 Protein Interaction Array System as outlined above with the following exceptions: Recombinant Hsp90α (10 $\mu g.ml^{-1}$) and Hsp90β (10 $\mu g.ml^{-1}$) were immobilized on the surface of a ProteOn^{TM} GLC Sensor chip (#176-5011, Bio-Rad, US) at a level equivalent to ± 3500 RU and ± 2400 RU respectively. Sensorgrams were collected as a 100 $\mu l.min^{-1}$ injection for 120 seconds followed by a 600 second delay used to monitor dissociation. Further analysis was conducted in GraphPad Prism 4.03.

2.2.8 Cell surface biotinylation and streptavidin-agarose affinity chromatography

Surface proteins of confluent Hs578T, MDA-MB-231 and MCF-7 cells were biotinylated by incubation with NHS-biotin (1 $mg.ml^{-1}$) for 30 minutes at 4 °C. Cells were quenched with 1 M Tris-HCl (pH 7.5) before washing twice with PBS to remove unbound NHS-biotin. Cells were subsequently lysed in RIPA buffer (50 mM Tris-HCl, pH7.4, 150 mM NaCl, 1 mM ethyleneglycol-bis[beta-aminoethylether] N'N'N'N-tetraacetic acid/ethylenediaminetetraacetic acid [EGTA/EDTA], 1 mM Na_3VO_4, 1 % [v/v] NP40, 1 mM sodium deoxycholate [DOC], 1 mM phenylmethylsulfonyl fluoride [PMSF] and 0.05 % [v/v] protease inhibitor cocktail) after being lifted either by scraping or by trypsin treatment. Cell supernatants were incubated with streptavidin-agarose for 1 hour at 4 °C and bound protein harvested by centrifugation at 13 000 rpm in a microfuge for 1 minute at 4 °C. Purified proteins were released in SDS-PAGE sample buffer by boiling for 8 minutes and analyzed as per the SDS-PAGE and immunoblotting analysis methodology.

2.2.9 Confocal microscopy

Cells were seeded at a density of 4.5×10^5 cells.ml^{-1} onto sterile glass cover slips and allowed to adhere overnight followed by treatments indicated in figure legends. Cells on coverslips were fixed with ethanol and blocked with 1 % (w/v) BSA/PBS. Fixed cells were incubated with primary antibody in 1 % (w/v) BSA/PBS (1:100), washed with 1 % (w/v) BSA/PBS, and subsequently incubated with species specific fluorescently tagged secondary antibody in 1% (w/v) BSA/PBS (1:500). Antibodies used are specified in figure legends. Nuclei were stained with Hoechst 33342 (1 μg.ml^{-1}). Images were captured using the Zeiss LSM 510 Meta laser scanning confocal microscope and analyzed using Zen software (blue edition, Zeiss, Germany) or AxiovisionLE 1.4.7 (Carl Zeiss Imaging Solutions, Germany). Product of the Differences from the Mean (PDM) values and a Colour Scatter Plot were generated using the Intensity Correlation Analysis tool of the Colocalization Analysis plug-in of Image J 1.43m. Mean grey values and the number of nuclei were measured using Image J 1.43m following threshold adjustment. The ratio of the mean grey value per nuclei were averaged from three images and compared using a one-way ANOVA with a Tukey Post Test.

2.2.10 Fluorescent labeling of commercial FN

FN exists as a large multidomain homodimer with two free cysteine residues per subunit, located in modules $FNIII_7$ and $FNIII_{15}$ (Baugh & Vogel 2004). The presence of these free cysteine residues permitted the labeling of FN with the cysteine reactive fluorescent dye, Tetramethylrhodamine-5-Maleimide (TMR). Oregon Green 488 Carboxylic Acid (OG) was used for the fluorescent labeling of random amines. Batches of FN (1 mg) in 0.1 M sodium bicarbonate (pH 8.3) were denatured in 4M guanidine hydrochloride for 15 minutes to expose free cysteines. Denatured FN was subsequently incubated with a 20-fold molar excess of TMR for 2 hours at room temperature, producing FN-TMR. FN-TMR was separated from unbound TMR using a Zeba spin desalting column. Unlabeled FN, or FN-TMR, was incubated with a 20-fold molar excess of OG for 1 hour at room temperature, producing FN-OG and FN-TMR-OG respectively. Fluorescently labeled FN was separated from unbound OG using a Zeba spin desalting column. Labeling ratios were calculated from the solution absorbance at 280, 488 and 543 nm. Extinction coefficient values 364560, 87000 and 70000 M^{-1}cm^{-1} were used for FN, TMR and OG, respectively. FN was labeled with an average of 2.92 ± 1.89 TMR fluorophores and 15.78 ± 7.44 OG fluorophores per FN dimer.

2.2.11 Flow cytometry

FN-OG fluorescence was detected by excitation at 488 nm and emission collection using the FITC channel on a FACSAria II flow cytometer. FN-TMR fluorescence was detected by excitation at 488 nm and emission collection using the PE channel on a FACSAria II flow cytometer. A total of 10 000 live events were captured for all analyses.

2.2.12 Optimization of induction conditions of RAP1

Plasmid pQTEV-LRPAP1, encoding His-tagged human low density lipoprotein RAP1 with an N-terminal His tag was obtained from Addgene (Plasmid 31327; Figure 5). pQTEV-LRPAP1 construct (0.5 µM) was transformed into competent *E. coli* BL21 (*E. coli* B F- *dcm ompT hsdS*[r_B- m_B-] gal [$malB^+$]$_{K-12}$[λ^S]) cells. All growth media used for selection included the ampicillin (100 $\mu g.ml^{-1}$). Transformed colonies were inoculated into 25 ml yeast extract and tryptone (YT) broth and incubated overnight with shaking at 37 °C. Overnight cultures were each added to 225 ml YT broth and incubated at 37 °C with shaking until an OD_{600} between 0.4 – 0.6 was obtained. Protein expression was induced with IPTG (0.42 mM) and cultures were incubated at 30 °C. At each time interval after induction (0, 1, 2, 3, 4, 5, 6 hours and overnight) an OD_{600} reading was recorded and 1 ml sample centrifuged at 13000 $\times g$ for 1 minute. The pellet was resuspended in PBS to a volume of equal cell density. The resuspended pellet was mixed with SDS sample buffer and boiled for 5 minutes. Induction samples were analyzed as per the SDS-PAGE and immunoblotting analysis methodology.

2.2.13 Purification of RAP1

Overproduction of RAP1 occurred in *E. coli* BL21 cells. RAP1 was purified according to an adapted protocol of the purification of HIS-tagged proteins in the MagReSyn™ NTA user manual. Briefly, 250 ml pQTEV-LRPAP1 culture (OD_{600} between 0.4 - 0.6) was incubated at 30 °C and protein overproduction induced with IPTG (0.42 mM) for 4 hours. Cells were harvested at 6000 $\times g$ for 30 minutes at 4 °C and the pellet resuspended in wash buffer (10 mM Tris-HCl, pH 7.5, 300 mM NaCl, 50 mM imidazole) with lysozyme (1 mg/ml) and in the presence of Complete, EDTA-free Protease Inhibitor Cocktail Tablets. Sonication subsequently followed at 50 Hz for 6 repeats alternating 30 seconds on/30 seconds off using a Vibra-cell™ sonicator. Cell lysates were then centrifuged at 10 000 $\times g$ for 30 minutes at 4 °C and mixed with a bed volume of 50 µl MagReSyn™ NTA overnight at 4 ºC. Magnetically separated beads were washed with wash buffer followed by magnetic separation. Proteins were eluted with elution buffer (10 mM Tris-HCl, pH 7.5, 300 mM NaCl, 500 mM

imidazole) for 3 minutes at room temperature. Purified protein was separated from eluting imidazole by buffer exchange into buffer F (10 mM Tris-HCl, pH 7.5, 300 mM NaCl) using a Zeba spin desalting column. Contaminating endotoxin was removed using Pierce High Capacity Endotoxin Removal Resin and endotoxin levels determined using a Pierce LAL Chromogenic Endotoxin Quantitation Kit. Protein concentrations were quantified on the NanoDrop 2000™ or by Bradford's assay (Bradford 1976). Samples were collected at each step of the purification and analyzed as per the SDS-PAGE and immunoblotting analysis methodology.

2.2.14 Immunoprecipitation

An equal number of Hs578T cells were seeded overnight at 37 ºC. Adherent cells remained untreated or were treated with either novobiocin (250 μM) or exogenous Hsp90β (100 ng.ml^{-1}) at 37 °C for 1 hour and subsequently at 4 ° for 1 hour. Cells were shifted to 37 °C for 7 minutes to allow initiation of endocytosis. Cells were washed twice with PBS followed by crosslinking of protein interactions with DTSSP (3 mg.ml^{-1}) at 4 °C for 2 hours. DTSSP was quenched with 1 M Tris-HCl (pH 7.5) at 4 ºC for 15 minutes. Cells were lysed in RIPA buffer and lifted with gentle scraping. Immunoprecipitation of LRP-1 protein complexes was performed using an adapted immunoprecipitation (IP) protocol from the MagReSyn™ Protein A user manual. MagReSyn™ Protein A was equilibrated as outlined in the user manual. Equilibrated MagReSyn™ Protein A was incubated with 1 μg Rb anti-LRP-1 at room temperature for 30 minutes. Magnetically separated beads were washed with wash buffer 2 (50 mM Tris-HCl, pH 7.5, 150 mM NaCl, 0.025 % [v/v] Tween 20) and with RIPA lysate (prepared above) overnight at 4 ºC. Magnetically separated beads were washed with wash buffer 2 and subsequently with dH_2O. LRP-1 immunoprecipitated complexes were eluted from MagReSyn™ Protein A in SDS-PAGE sample buffer by boiling for 10 minutes. Samples were collected at each step of the purification and analyzed as per the SDS-PAGE and immunoblotting analysis methodology.

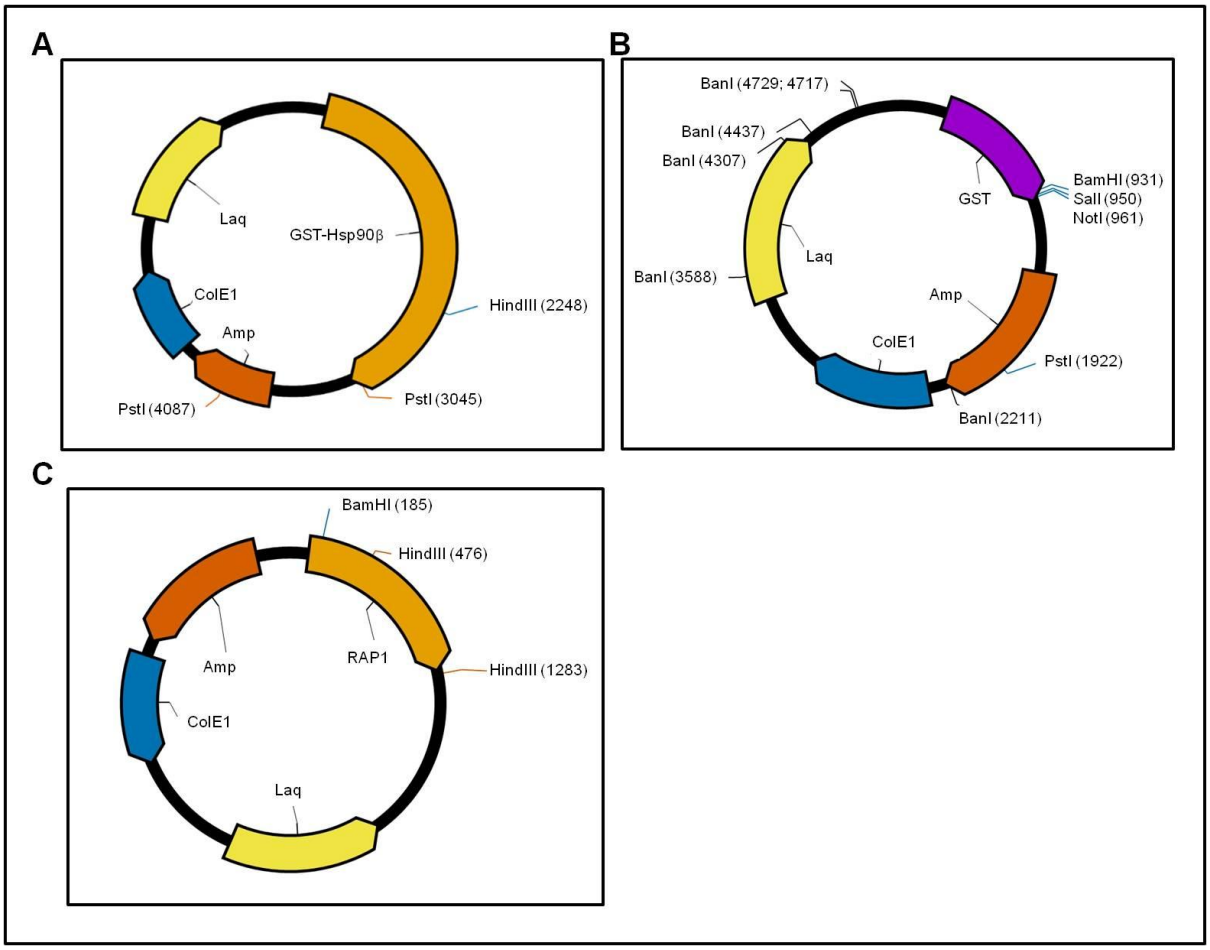

Figure 5: Plasmid maps of pGEX-4T-1-Hsp90β, pGEX-4T-1-GST and pQTEV-LRPAP1 vectors

Plasmid maps (A) pGEX-4T-1-GST-Hsp90β, (B) pGEX-4T-1-GST and (C) pQTEV-LRPAP1 show an ampicillin resistance gene (Amp), colicin E1 gene (ColE1), Lac operon (Laq) and genes for either GST-Hsp90β, GST, or RAP1 respectively. Restriction enzyme recognition sites used in a restriction digest to confirm the identity of the plasmids are shown.

CHAPTER 3: RESULTS

3. 1 HSP90 INTERACTS DIRECTLY WITH FN *IN VITRO*

In order to confirm a direct interaction between Hsp90 and FN, the binding of purified Hsp90 to FN was investigated *in vitro*.

3.1.1 Overexpression and purification of GST-Hsp90β

The pGEX-4T-1-GST-Hsp90β plasmid was used for the expression and purification of recombinant human Hsp90β for the analysis of the binding of Hsp90 to FN. Expression and purification of GST tag alone served as a control for any observed binding of GST-Hsp90β to FN. The pGEX-4T-1-GST-Hsp90β and pGEX-4T-1-GST plasmid identities were previously confirmed by restriction enzyme diagnostic digests and sequencing (*data not shown*).

Purification of GST-Hsp90β and GST were previously optimized, however low amounts of contaminating DnaK were observed. In order to prevent co-purification of DnaK in GST-Hsp90β and GST purifications, pGEX-4T-1-GST-Hsp90β and pGEX-4T-1-GST were transformed into DnaK null *E. coli* BB 1994 (MC4100 *dnaK52 sidB1::Tc pDMI, 1::CmR KanR*) cells. To optimize the expression of GST-Hsp90β and GST in *E. coli* BB 1994 cells, an induction study of the expression of GST-Hsp90β was performed. Figure 6 shows the induction of expression of GST-Hsp90β in *E. coli* BB 1994 cells. Immunoblot analysis to detect GST-Hsp90β using an anti-GST primary antibody showed a GST-tagged protein with approximate molecular weight of 110kDa (Figure 6A). Hsp90β has an approximate molecular weight of 84 kDa and together with the GST tag (26kDa), GST-Hsp90β has a predicted size of 110 kDa. A range of lower molecular weight proteins were also detected using the anti-GST antibody (Figure 6A). Detection of GST-Hsp90β using an anti-Hsp90β primary antibody (Figure 6B) confirmed the expression of GST-Hsp90β as a single band at 110 kDa and validated that the lower molecular weight GST-tagged proteins (Figure 6A) were GST-tagged degradation or truncation products. The absence of a band in non-transformed *E. coli* lysate (L) indicated the absence of endogenous expression of GST-Hsp90β in uninduced *E. coli* BB 1994 cells. The presence of protein expression, seen at time zero, was indicative of leaky expression from the *taq* promoter in pGEX-4T-1 (Saluta & Bell 1998). Figure 6A and 6B both confirmed that a time of three hours post induction was optimal for harvesting of GST-Hsp90β expressing *E. coli* BB 1994 cells for purification (Figure 6A and 6B, lane marked 3). An induction study of expression of GST was previously performed in *E. coli* BL21 cells (Figure 6C). High amounts of protein expression throughout induction were observed and thus it was decided, similarly to the induction of GST-Hsp90β,

that three hours post induction was sufficient for harvesting of GST expressing *E. coli* BB 1994 cells.

Following a 3 hour induction of expression of GST-Hsp90β and GST in *E. coli* BB 1994 cells, GST-Hsp90β and GST were purified using GSH affinity chromatography (Figure 7). The purification fractions collected for GST-Hsp90β and GST were resolved by SDS-PAGE (Figure 7A) and analyzed by immunoblotting (Figure 7B and 7C). SDS-PAGE analysis of the collected fractions of the purification of GST-Hsp90β showed the presence of a band of the anticipated size (110 kDa) observed in the elution fractions (Figure 7A). Low levels of lower molecular weight proteins were observed in the elution fractions (Figure 7A). Immunoblot analysis for GST (Figure 7B) and Hsp90β (Figure 7C) confirmed successful purification of GST-Hsp90β. The lower molecular weight bands observed on the SDS-PAGE were detected on the immunoblot for GST, indicating the presence of GST-tagged degradation/truncation products in the elution fractions. The lower sized GST-tagged degradation/truncation products were not observed in an immunoblot for Hsp90β using an Hsp90-specific antibody (Figure 7C). The degree of purity of GST-Hsp90β was thus deemed sufficient for subsequent experiments. SDS-PAGE (Figure 7D) and immunoblot (Figure 7E) analysis of the collected fractions of the purification of GST showed successful purification of GST in the elution fractions. Immunoblot analysis for GST showed a single band at the expected molecular weight in all eluted fractions (Figure 7E). Purification of GST-Hsp90β and GST showed yields of 3.724 and 1.966 $mg.L^{-1}$ respectively. Purified GST-Hsp90β and GST elution fractions were subsequently used in the further development of a solid phase binding assay used in the determination of the binding of Hsp90β to FN.

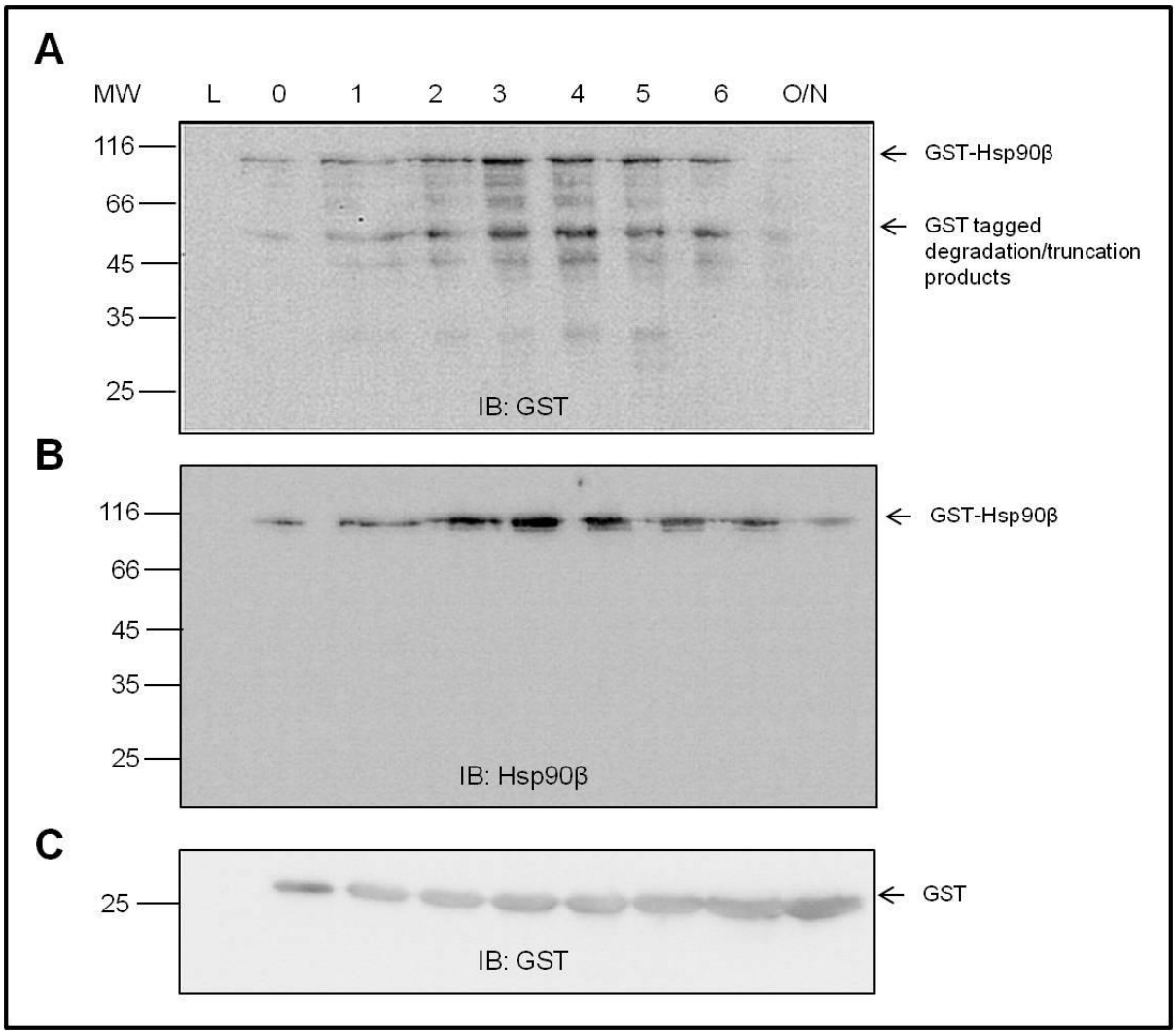

Figure 6: Induction of expression of GST-Hsp90β and GST

GST-Hsp90β expression was induced (1 mM IPTG; 37 °C) in E. *coli* BB1994 cells and induction samples collected hourly and overnight and probed using (A) anti-schistosomal GST and (B) anti-human Hsp90β primary antibodies. (C) GST expression was induced (1 mM IPTG; 37 °C) in *E. coli* BL21 cells and induction samples collected and probed using anti-schistosomal GST primary antibody. Numbers on the left hand side show the molecular weight (kDa) of the prestained protein molecular weight marker (MW). Letters show the (L) non-transformed E. *coli* lysate and (O/N) overnight induced sample. Numbers (0 – 6) show the hourly time intervals post induction. Arrows show the expression of GST-Hsp90β, GST and GST tagged degradation/truncation products.

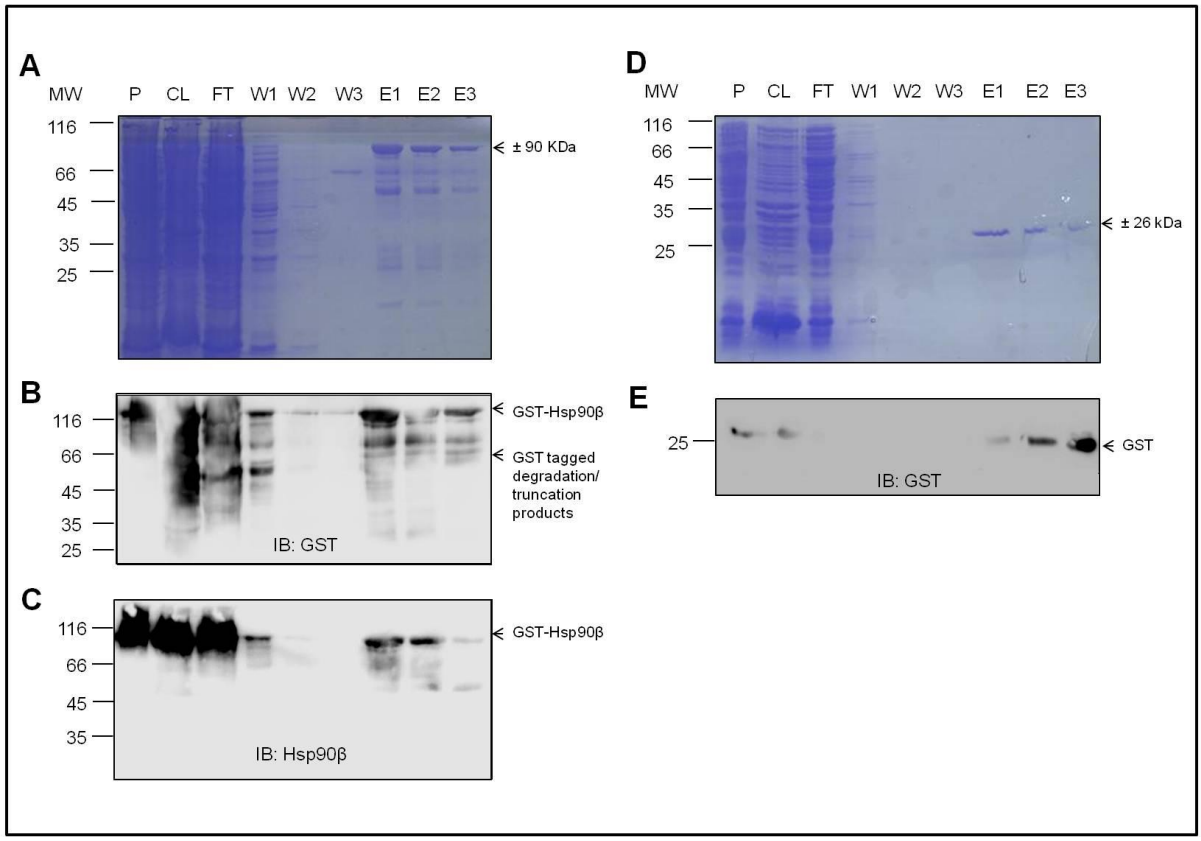

Figure 7: Overexpression and Purification of GST-Hsp90β and GST

GST-Hsp90β and GST were purified from E. *coli* BB1994 cells 3 hours post induction with 1 mM IPTG. Fractions collected during (A) GST-Hsp90β purification were resolved by SDS-PAGE and probed using (B) anti-schistosomal GST and (C) anti-human Hsp90β primary antibodies. Fractions collected during (D) GST purification were resolved by SDS-PAGE and probed using (E) anti-schistosomal GST primary antibody. Numbers on the left hand side show the molecular weight (kDa) of the prestained protein molecular weight marker (MW). Letters above show the (P) pellet, (CL) cleared lysate, (FT) flow through, (W) wash and (E) elution fractions. Arrows show the purified GST-Hsp90β and GST tagged degradation/truncation products.

3.1.2 GST-Hsp90β bound FN in a solid phase binding assay

The binding of GST-Hsp90β to FN was determined in a solid phase binding assay using a modified enzyme-linked immunosorbent assay (ELISA) (Figure 8). GST-Hsp90β was incubated with adsorbed FN and binding occurred. Purified GST was used as a negative control for any non-specific binding of the GST tag to FN. Bound GST-Hsp90β or GST was detected using either anti-schistosomal GST (Figure 8A and 8B) or anti-human Hsp90β primary antibodies (Figure 8C). Anti-schistosomal GST and/or anti-human Hsp90β primary antibody were in turn bound by horseradish peroxidase (HRP) conjugated species matched secondary antibody. The addition of HRP substrate resulted in the generation of a colorimetric signal that was measured at 450 nm. Absorbance at 450 nm was used as a quantitative measure of the binding of GST-Hsp90β and GST to adsorbed FN. FN adsorption to the ELISA plate surface (Figure 8D) and specificity of the Hsp90β antibody for GST-Hsp90β (*data not shown*) was confirmed using a similar protocol.

Figure 8A shows the binding of GST-Hsp90β to adsorbed FN (100 $\mu g.ml^{-1}$) detected using anti-schistosomal GST primary antibody. Increasing concentrations of GST-Hsp90β (0 – 2500 nM) showed a dose dependent increase in absorbance at 450 nm. A dose dependent increase in absorbance at 450 nm suggested a concentration dependent interaction between GST-Hsp90β and FN. Saturation of absorbance at 450 nm at higher GST-Hsp90β concentrations (2000 – 2500 nM) suggested saturated binding of GST-Hsp90β and FN. Non-specific binding of GST to FN was below the level of the binding of GST-Hsp90β to FN. A non-linear regression curve fit of the data resulted in r^2 values of 0.9481 and 0.7670 for GST-Hsp90β and GST respectively. An F-test showed a statistically significant difference in the curve fits of GST-Hsp90β and GST ($p < 0.0001$). The saturation binding data was transformed using a built in pharmacology and biochemistry transformation in GraphPad Prism to demonstrate a Scatchard plot with the superimposition of a straight line with points (B_{max}; B_{max}/K_d) (Figure 8B). Scatchard plot analysis showed the solid phase binding data for GST-Hsp90β binding to FN conformed to a straight line, suggesting a single class of binding sites (Weder et al. 1974). A K_d value of 289.8 nM and 541.1 nM for GST-Hsp90β and GST, respectively, was reported by Scatchard plot analysis of solid phase binding data.

Binding of GST-Hsp90β to FN was also observed using anti-human Hsp90β primary antibody for detection (Figure 8C). A linear increase in absorbance at 450 nm was seen for increasing concentrations of GST-Hsp90β (0 – 2500 nM) at both 10 $\mu g.ml^{-1}$ (*data not shown*)

and 100 μg.ml^{-1} (Figure 8C) FN adsorption concentrations. Higher absorbance readings recorded for the binding of GST-Hsp90β to a higher concentration of immobilized FN further validated the dose dependant binding of GST-Hsp90β to FN. Adsorption of FN to the ELISA plate surface was validated using a FN specific primary antibody (Figure 8D). Detection of adsorbed GST-Hsp90β, and not GST, using anti-human Hsp90β primary antibody confirmed specificity of the Hsp90β antibody for GST-Hsp90β (*data not shown*).

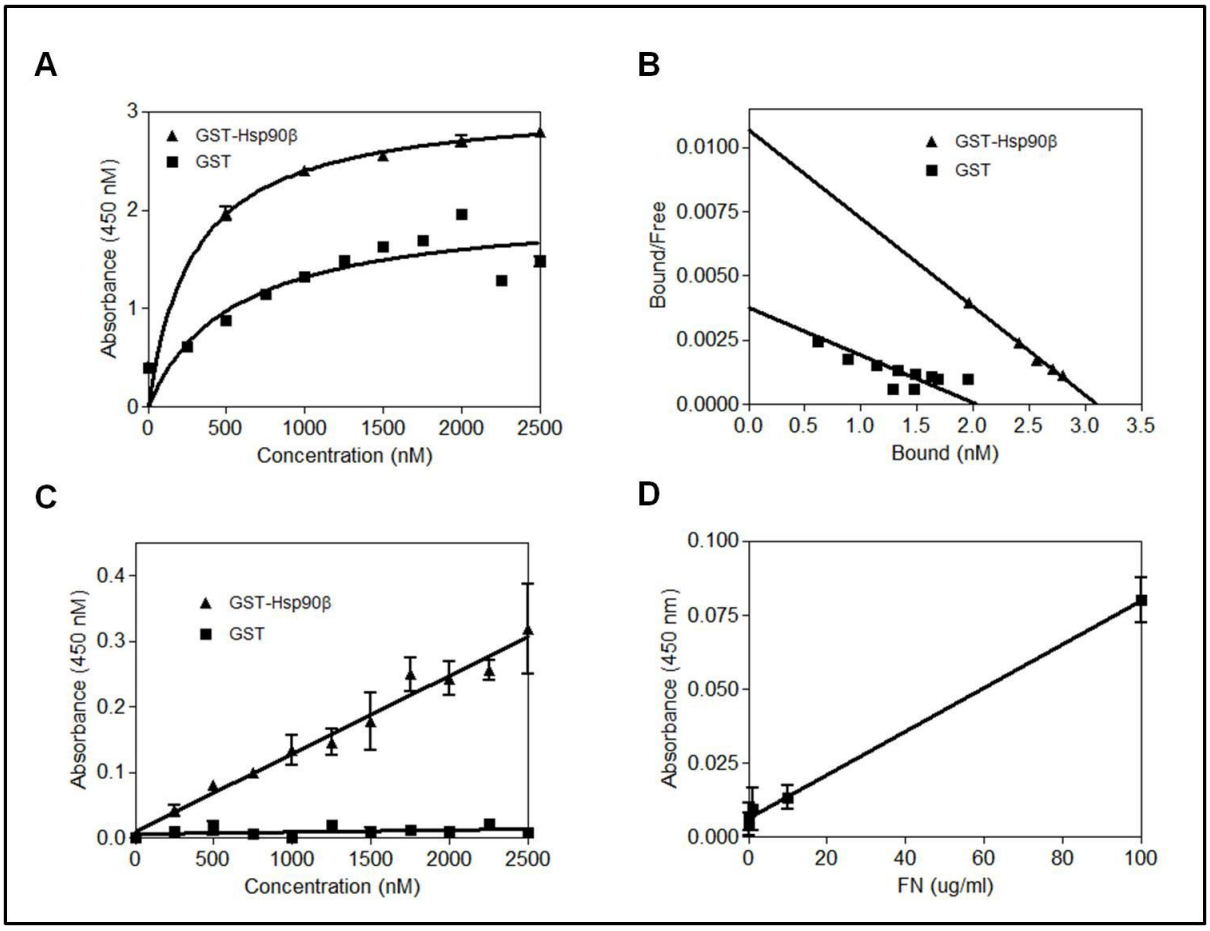

Figure 8: GST-Hsp90β bound adsorbed FN in a solid phase binding assay

Solid phase binding assay showed that recombinant GST-Hsp90β and GST (negative control) bound to adsorbed FN (100 μg.ml^{-1}) in a dose dependant manner. Absorbance at 450 nm (as a measure of binding) was plotted against concentration of GST-Hsp90β and GST. (A) Binding of GST-Hsp90β and GST to adsorbed FN detected using anti-schistosomal GST primary antibody. Data were fit with a non-linear curve fit (one site binding; hyperbola) and showed R^2 values equal to 0.9481 and 0.7670 for GST-Hsp90β and GST respectively. An F-test showed significant difference in the curve fits of GST-Hsp90β and GST with $p<0.0001$. (B) Saturation binding data were transformed using Prism's built in pharmacology and biochemistry transformations to demonstrate a Scatchard plot with the superimposition of a straight line with points (B_{max}; B_{max}/K_d). (C) Binding of GST-Hsp90β and GST to adsorbed FN detected using anti-human Hsp90β primary antibody. (D) Validation of FN adsorption to the surface of the microplate. All data analysis was performed in GraphPad Prism 4.03. The data shown are from triplicate experiments.

3.1.3 FN bound Hsp90 by Surface Plasmon Resonance spectroscopy

In order to define the kinetics of the Hsp90-FN interaction, binding of FN to Hsp90β was determined in real-time by SPR spectroscopy using the ProteOn™ XPR36 Protein Interaction Array System. Recombinant untagged Hsp90β (2, 10 and 50 $\mu g.ml^{-1}$) was immobilized onto the surface of a GLM Sensor chip. In order to determine potential kinetics of the Hsp90-FN interaction, increasing concentrations (0 – 1000 nM) of commercial FN in solution (analyte) was allowed to associate with Hsp90β on the chip (ligand). BSA in solution was used as a negative control analyte for any non-specific binding effects. Sensorgrams collected as a 100 $\mu l.min^{-1}$ injection for 180 seconds followed by a 600 second delay were used to monitor dissociation (or as otherwise stated in figure legends).

Figure 9 shows the binding of FN to immobilized Hsp90β as seen by SPR. Representative sensorgrams demonstrated the dose dependent binding of FN to all concentrations of Hsp90β (Figure 9A-C). No binding of BSA to all concentrations of Hsp90β was observed (*data not shown*). Binding of FN to Hsp90 did not require the presence of ATP (*data not shown*). A shorter injection time (association phase) showed dose dependent linear binding of FN to Hsp90β (Figures 9A and 9C). A longer association phase showed dose dependent binding of FN to Hsp90β reaching a state of equilibrium (Figure 9B). With good immobilization levels, and dose dependent binding reaching equilibrium, these data were used for kinetic analysis. Kinetic curves were fit to three experimental sets of five analyte (FN) concentrations using a simultaneous K_a/K_d (Langmuir binding model). Chi^2 values were reported as below 10 % of the R_{max}. Kinetic fits of the sensorgrams reported a dissociation constant (K_d) equal to 17.4 ± 12.1 nM. In order to confirm Hsp90-FN binding followed 1:1 Langmuir binding kinetics (fitted model) and improve estimation of the K_d value, the output RU_{eq} values from each of the kinetic fits were plotted against concentration of FN and a binding saturation curve (non-linear curve one site binding) generated (Figure 9D). The data was transformed using a built in pharmacology and biochemistry transformation in GraphPad Prism to demonstrate a Scatchard plot with the superimposition of a straight line with points (B_{max}; B_{max}/K_d) (Figure 9E). A K_d equal to 29.9 ± 6.1 nM for the binding of FN to Hsp90β was obtained. Fitting of the data to a straight line by Scatchard Plot analysis (Figure 9E) confirmed successful fit of the 1:1 Langmuir binding kinetic model.

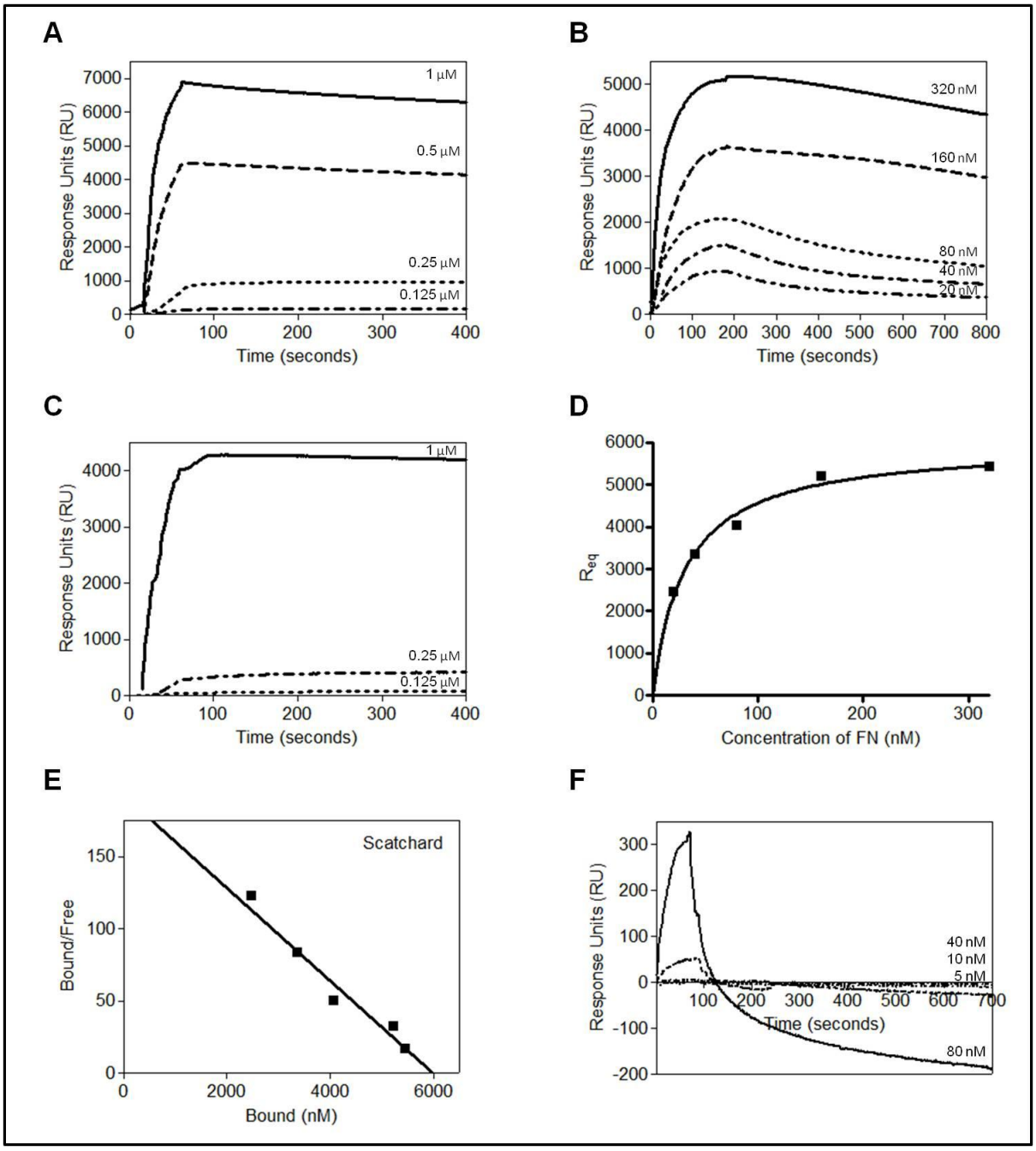

Figure 9: legend over page

Figure 9: Kinetic analysis of FN binding to Hsp90β by SPR

Representative sensorgrams of observed binding of FN (0 – 1000 nM) to immobilized Hsp90β (A) 2 $\mu g.ml^{-1}$, (B) 10 $\mu g.ml^{-1}$ and (C) 50 $\mu g.ml^{-1}$. Hsp90β was immobilized onto the surface of a Proteon GLM sensor chip and increasing concentrations of FN allowed to flow over the surface of the chip. Sensorgrams are representative of duplicate experiments at varying FN concentrations, both in the presence and absence of ATP (1 mM). Four independent experimental replicates of binding of FN to immobilized Hsp90β (10 $\mu g.ml^{-1}$) were fit with a simultaneous K_a/K_d (Langmuir binding) model. Kinetic fits showed Chi^2 values below 10% of the R_{max} and reported a dissociation constant (K_d) equal to 32.45 ± 30.20 nM. (D) Saturation binding curve (E) Scatchard plot of FN-Hsp90β SPR binding data (10 $\mu g.ml^{-1}$). Reported R_{eq} values were plot against concentration of FN and fit with a non-linear curve (one site binding). Saturation binding data in were transformed using Prism's built in pharmacology and biochemistry transformations to demonstrate a Scatchard plot with the superimposition of a straight line with points (B_{max}; B_{max}/K_d). The straight line shows the best possible estimate of K_d. Scatchard plot analysis reported a K_d equal to 28.88 ± 3.26 nM. (F) Representative sensorgrams of observed binding of FN70 (0 – 80 nM) to immobilized Hsp90β (10 $\mu g.ml^{-1}$).

A preliminary study of the binding of FN70, the 70 kDa amino-terminal fragment of FN (McKeown-Longo & Mosher 1985), to Hsp90β was determined. Increasing concentrations (0 – 80 nM) of commercial FN70 was allowed to associate with immobilized Hsp90β and resulting sensorgrams collected as a 100 $\mu l.min^{-1}$ injection for 90 seconds followed by a 600 second delay used to monitor dissociation. Due to limited FN70 availability, a single replicate of FN70 concentrations (0 – 160 nM) was performed at different Hsp90β immobilization concentrations (2, 10 and 50 $\mu g.ml^{-1}$). Figure 9F shows the binding of FN70 to immobilized Hsp90β (10 $\mu g.ml^{-1}$). Binding of FN70 to Hsp90β was observed at 80 and 40 nM analyte (FN70) concentrations but data collected were not sufficient for kinetic analyses (Figure 9E).

In order to define the binding of FN to Hsp90α or Hsp90β isoforms, interaction of FN with Hsp90α and Hsp90β was performed. Hsp90α (10 $\mu g.ml^{-1}$) and Hsp90β (10 $\mu g.ml^{-1}$) were immobilized onto the surface of a GLC Sensor chip. Increasing concentrations (0 – 15 nM) of commercial FN (analyte) was allowed to associate with Hsp90α and/or Hsp90β (ligand). Sensorgrams were collected as a 100 $\mu l.min^{-1}$ injection for 120 seconds followed by a 600 second delay used to monitor dissociation. Figure 10A and 10B show the binding of FN to immobilized Hsp90α and Hsp90β, respectively. Representative sensorgrams demonstrated dose dependent binding of FN to all concentrations of immobilized Hsp90α and Hsp90β (Figure 10A and 10B, respectively). Linear binding, without equilibrium, was observed for both Hsp90α and Hsp90β at all analyte concentrations. Binding of FN to Hsp90α showed a higher association phase RU in comparison to Hsp90β at all analyte concentrations, which was most likely due to higher immobilization levels of Hsp90α on the surface of the GLC Sensor chip (Methods - Analysis of Hsp90α and Hsp90β isoform specific binding of FN). Attempts to fit kinetic curves to three experimental sets of five analyte (FN) concentrations using a simultaneous K_a/K_d (Langmuir binding model) yielded inconsistent K_d values.

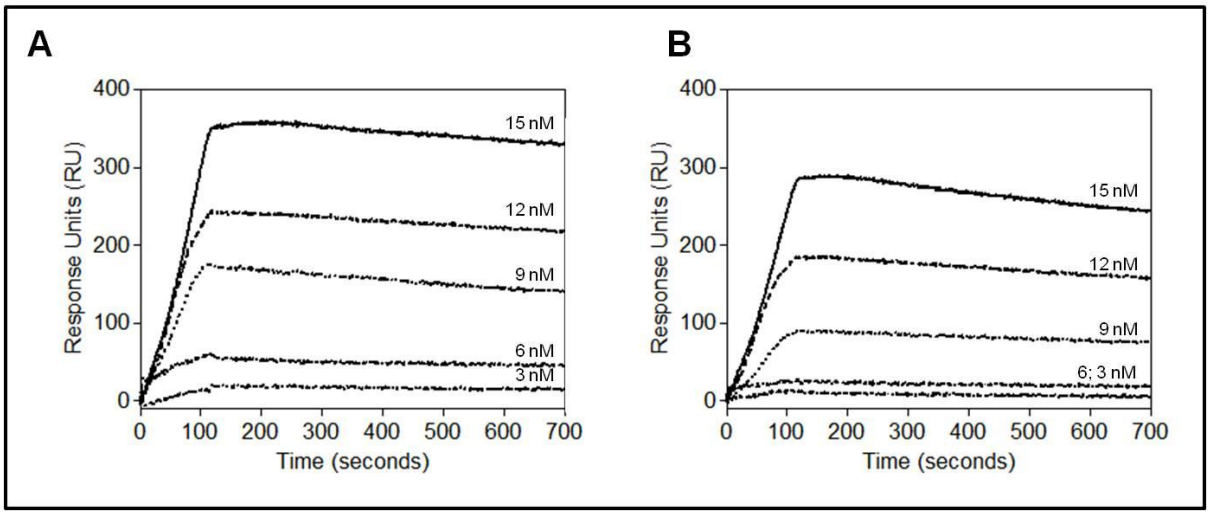

Figure 10: Analysis of binding of FN to isoform specific Hsp90 by SPR

Representative sensorgrams of observed binding of FN (0 – 15 nM) to immobilized (A) Hsp90α (3500 RU) and (B) Hsp90β (2400 RU). Hsp90α or Hsp90β (10 $\mu g.ml^{-1}$) was immobilized onto the surface of a Proteon GLC sensor chip and increasing concentrations of FN allowed to flow over the surface of the chip. Sensorgrams are representative of triplicate experiments at varying FN concentrations.

3.2 HSP90 INTERACTED WITH FN IN MAMMALIAN CANCER CELL LINES

3.2.1 Mammalian cancer cell lines expressed FN and Hsp90

Having determined that FN and Hsp90 can interact in vitro, we subsequently investigated whether this interaction was functionally relevant in cells. The expression of cytosolic Hsp90 and FN was determined in cancer cell lines available in the laboratory by immunoblot analysis (Figure 11A). Figure 11A shows an immunoblot analysis for the expression of FN (220 kDa) and Hsp90 (90 kDa) in MDA-MB-231, MCF-7, Hs578T breast cancer, A549 lung cancer, and SW480 and SW620 colon cancer cell lines. An immunoblot for Histone H3 (17 kDa) was used as a control for equal protein loading. Both MDA-MB-231 and Hs578T breast cancer cell lines showed expression of FN (Figure 11A, lanes 1 and 3; 220 kDa). MCF-7, A549, SW480 and SW620 cancer cell lines showed undetectable levels of FN (220 kDa). Lower molecular weight FN bands were detected in MDA-MB-231, MCF-7, SW480 and SW620 cancer cell lines. An immunoblot for Hsp90 showed similar levels of expression in all available mammalian cancer cell lines (Figure 11A, all lanes; 90 kDa).

The presence of Hsp90α and Hsp90β on the surface of breast cancer cells was investigated. Equal cell numbers of MDA-MB-231, Hs578T and MCF-7 breast cancer cells were treated with cell impermeable NHS-biotin, lifted by scraping or with trypsin and the biotinylated purified fractions purified by streptavidin affinity purification and probed for the presence of either Hsp90α or Hsp90β using isoform specific antibodies. Figure 11A shows an immunoblot analysis for the detection of surface associated and extracellular soluble pools of Hsp90α and Hsp90β in the lysates of cells lifted by scraping. Both Hs578T and MDA-MB-231 cells showed the presence of Hsp90α and Hsp90β in the surface biotinylated purified fraction (Figure 11B, lanes 2 and 3). MCF-7 cells showed the presence of Hsp90β, but not Hsp90α, in the surface biotinylated purified fraction (Figure 11B, lane 4). In all cases, cells treated with trypsin showed a loss of these proteins in the biotinylated fractions. The whole cell lysate (WCL) from Hs578T cells was used as a positive control for immunoblotting.

The presence of extracellular soluble Hsp90β in the spent media of Hs578T cells was investigated using a solid phase binding assay similar to that described previously (Figure 8). Spent media from Hs578T cells was adsorbed onto the surface of a high-binding ELISA microplate and, following blocking with BSA and subsequent washing, bound Hsp90β detected using an Hsp90β isoform specific antibody. Media alone acted as a negative control. Recombinant commercial Hsp90β was used to establish a standard curve (Figure 11C) for the

determination of the concentration of extracellular soluble Hsp90β. The concentration of extracellular soluble Hsp90β in spent media of Hs578T cells was determined as 89.25 ± 68.05 $ng.ml^{-1}$.

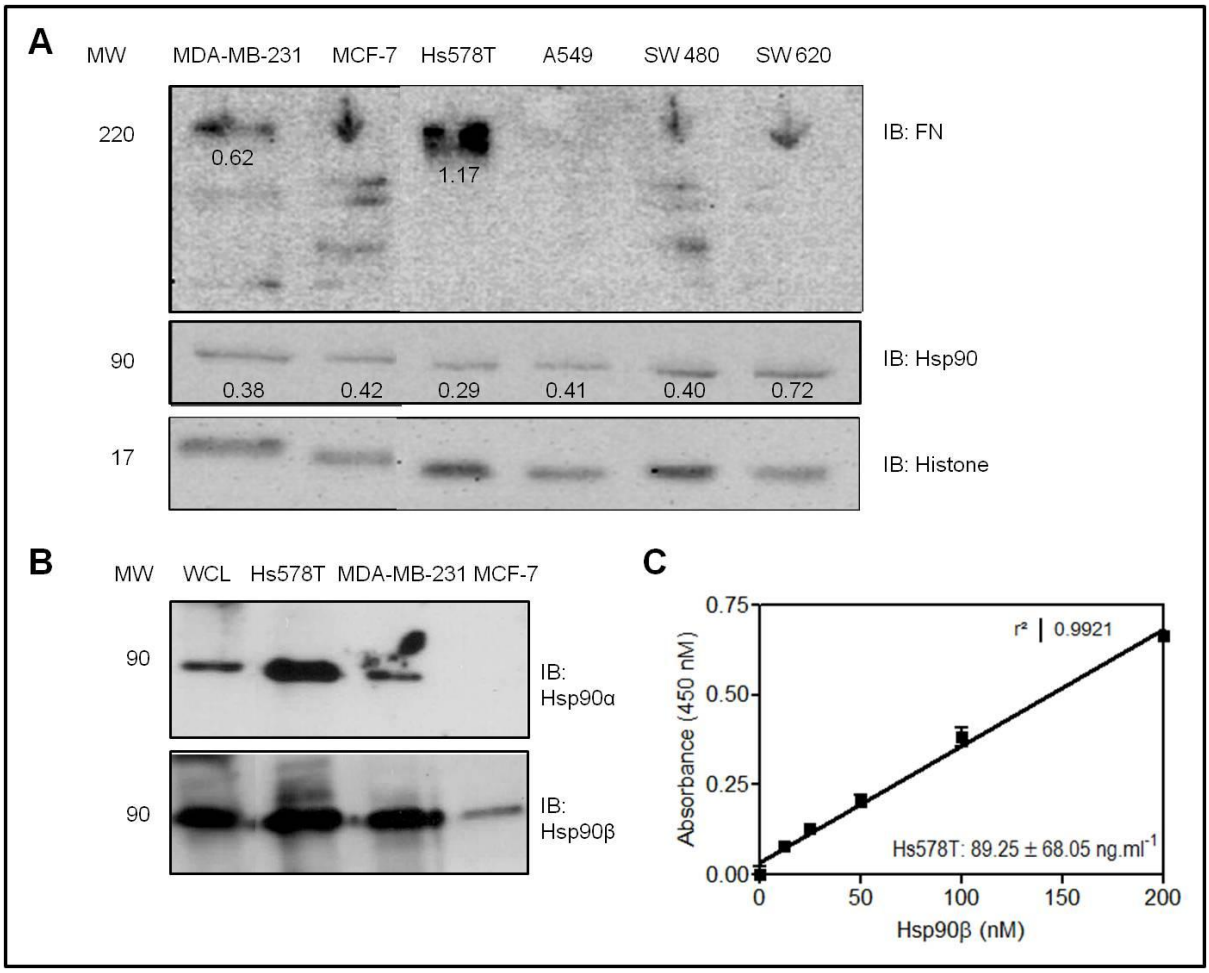

Figure 11: Expression of FN and Hsp90 in mammalian cell lines

(A) Lysates of mammalian breast (MDA-MB-231, MCF-7 and Hs578T), lung (A549) and colon (SW480 and SW620) cancer cell lines were probed using anti-human FN, anti-human Hsp90 and anti-human Histone H3 primary antibodies by immunoblot (IB) analysis. Densitometry values relative to Histone H3 are shown below respective bands. (B) Equal cell numbers of Hs578T, MDA-MB-231 and MCF-7 breast cancer cells were treated with cell impermeable NHS-biotin and lifted with gentle scraping. Surface biotinylated purified fractions were probed using anti-human Hsp90α or anti-human Hsp90β by immunoblot analysis. The WCL from Hs578T cells was used as a positive control for immunoblotting. (C) A solid phase binding assay of spent media from Hs578T cells revealed the presence of extracellular soluble Hsp90β in Hs578T cells. A standard curve of commercial Hsp90β in media was used to determine the concentration of extracellular soluble Hsp90β in Hs578T spent media (Hs578T).

3.2.2 FN and Hsp90 partially colocalize in mammalian breast cancer cell lines

We next investigated the subcellular localization of FN (green) and Hsp90 (red) in MDA-MB-231 and Hs578T breast cancer cells using confocal microscopy (Figure 12). Merged images show overlapping green and red intensities. The PDM values show the product of the differences from the mean for each pixel, with highlighted (orange) PDM values showing regions of possible colocalization (Figure 12) (Reitan et al. 2012). FN and Hsp90 expression were detected in MDA-MB-231 and Hs578T breast cancer cell lines (Figure 12). A dispersed intracellular localization pattern for FN was observed in both cell lines (Figure 12). Hs578T cells showed intracellular staining for FN as well as extracellular FN fibrils. The MDA-MB-231 cell line showed less of an extracellular fibrillar FN matrix in comparison to the Hs578T cell line.

A dispersed staining pattern for Hsp90 was seen in both cells lines. Hsp90, in MDA-MB-231 cells, showed a diffuse localization pattern distinct from FN, although selected regions of partial colocalization were identified (Figure 12, yellow arrows). Hsp90, in Hs578T cells, showed a similar diffuse localization pattern, however, selective regions of Hsp90 staining (Figure 12, yellow arrows) appeared to partially colocalize with extracellular FN fibrils as seen in the PDM values output.

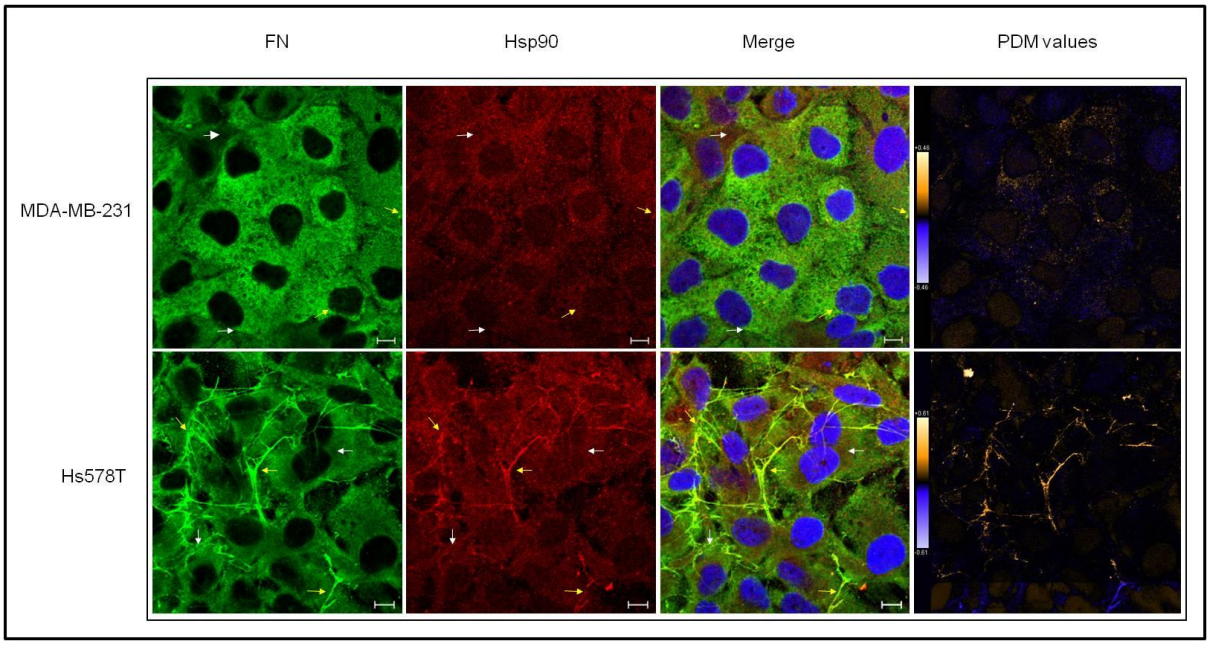

Figure 12: FN and Hsp90 show regions of partial colocalization in MDA-MB-231 and Hs578T cancer cell lines

MDA-MB-231 and Hs578T cells were stained using mouse anti-human FN and goat anti-human Hsp90α/β primary antibodies followed by donkey anti mouse DyLight® 488 and donkey anti goat DyLight® 650 fluorescent secondary antibodies, respectively. Nuclei were stained with Hoechst 33342 (1 $\mu g.ml^{-1}$). Images were captured using a Zeiss LSM 510 Meta laser scanning confocal microscope and analyzed using Zen software, blue edition (Zeiss, Germany). Yellow arrows show regions of interest for partial colocalization, white arrows show regions where colocalisation was not observed. PDM values were generated using Image J 1.43m. Positive and negative PDM values are indicated in orange and blue respectively. Scale bars are equivalent to 10 μm. The data shown are representative of images obtained from triplicate experiments.

3.2.3 Loss of extracellular FN in response to novobiocin is partially rescued by soluble Hsp90

We tested the effect of Hsp90 inhibition with novobiocin on the extracellular FN matrix. Hs578T cells were treated with or without increasing concentrations of novobiocin and the resulting FN phenotype observed with and without addition of exogenous endotoxin-free Hsp90β (Figure 13). Cells were treated with novobiocin concentrations previously shown to have no effect on cell viability (O'Hagan 2012). Treatment of Hs578T cells with novobiocin has previously been shown to have no effect on the synthesis of FN (Unpublished Observations). Treated cells were fixed and stained for FN. The ratio of FN fluorescence intensity per cell number (as measured by the number of nuclei per image) in multiple images was quantified using ImageJ in order to compare the FN staining between samples.

Hs578T cells showed a dose dependent, and statistically significant (500μM Novo; $p<0.001$) decrease in the extracellular FN matrix upon treatment with increasing concentrations of novobiocin compared to the untreated cells (Figure 13, Novo). Hs578T cells showed a significant ($p<0.01$) recovery of the extracellular FN matrix upon addition of exogenous Hsp90β to novobiocin treated cells (Figure 13, + Hsp90β). Moreover, a greater recovery of the extracellular FN matrix was observed in Hs578T cells treated with Hsp90 and a lower novobiocin concentration (Figure 13A, + Hsp90β, 250 versus 500 μM Novo). Treatment of Hs578T cells with Hsp90β alone showed no significant effect on the extracellular FN matrix, although better defined FN matrix fibrils were observed.

Novobiocin, although a known inhibitor of Hsp90, also binds DNA gyrase, a type II topoisomerase (Ali et al. 1993). In order to confirm that the observed FN phenotype was not a result of inhibition of topoisomerase, Hs578T cells were treated with etoposide, a published type II topoisomerase inhibitor (Hande 1998). Cells were treated with etoposide at a concentration half of the determined IC_{50} value determined in Hs578T cells (Hou & Wang 2012). Figure 13 shows that treatment with etoposide had no significant (0.5 μM Etop; $p>0.05$) effect on the extracellular FN matrix in Hs578T cells and thus suggested that the effect of novobiocin on the FN matrix was not as a result of novobiocin inhibiting a type II topoisomerase within Hs578T cells.

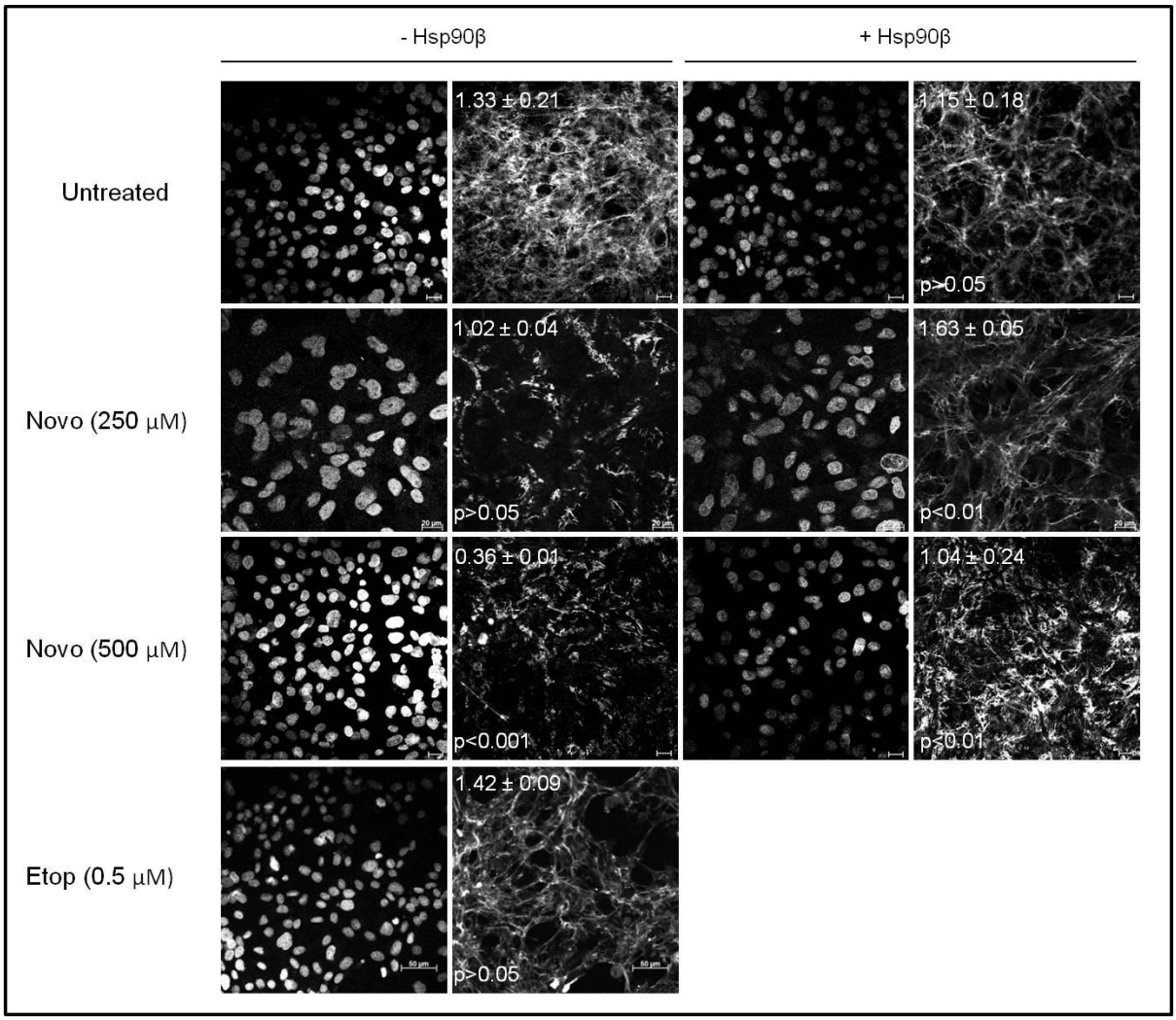

Figure 13: Treatment of Hs578T cells with novobiocin results in a loss of the FN matrix; exogenous Hsp9β partially rescues this effect

(A) Hs578T cells either remained untreated or were treated with novobiocin (Novo; 250 or 500 μM) or etoposide (Etop; 0.5 μM) for 1 hour followed by treatment with media (- Hsp90β) or exogenous Hsp90β (+ Hsp90β; 100 ng.ml^{-1}) overnight. Fixed cells were stained using mouse anti-human FN followed by donkey anti mouse DyLight® 488 secondary antibody. Nuclei were stained with Hoechst 33342 (1 μg.ml^{-1}). Images were captured using a Zeiss LSM 510 Meta laser scanning confocal microscope. Images were analyzed using Zen software, blue edition (Zeiss, Germany). Scale bars are equivalent to 20 μm or 50 μm (Etop). Values (in white) at the top of each frame represent the mean grey values (± standard deviation) per nuclei for each treatment. Mean grey values were compared using a one-way ANOVA with a Tukey Post Test. The mean grey value of novobiocin treated (Novo; 250 or 500 μM) and etoposide treated (Etop; 0.5 μM) cells were compared to untreated cells. The mean grey value of exogenous Hsp90β (+ Hsp90β) treated cells were compared to the equivalent treatment without exogenous Hsp90β (-Hsp90β). Statistical p-values are shown in the bottom left of each frame. The data shown are representative of triplicate images collected from duplicate experiments.

3.2.4 Inhibition of Hsp90 with novobiocin leads to FN internalization

Inhibition of Hsp90 with novobiocin showed a loss of the extracellular FN matrix (Figure 13). In order to determine whether loss of the extracellular FN matrix was due to the endocytosis of extracellular FN, we examined the uptake of fluorescently labeled FN in Hs578T breast cancer cells. FN was fluorescently labeled with TMR (FN-TMR) and OG (FN-OG) or a combination of both TMR and OG (FN-TMR-OG).

To confirm incorporation of fluorescently labeled FN into the extracellular FN matrix, Hs578T cells were treated with fluorescently labeled FN and allowed to incorporate the labeled FN into an extracellular FN matrix overnight. Confocal microscopy confirmed incorporation of fluorescently labeled FN into an extracellular FN matrix (Figure 14). Figure 14 shows the incorporation of FN-OG, FN-TMR and FN-OG-TMR into the extracellular FN matrix of Hs578T cells. FN labeled with both OG and TMR showed overlapping green (λ = 488 nm) and red (λ = 550 nm) signals (Figure 14, FN-OG-TMR, Merge). Incorporation of exogenous fluorescently labeled FN into the extracellular FN matrix permitted the study of the dynamics of only extracellular, exogenous FN. Following incorporation of fluorescently labeled FN into the extracellular FN matrix, Hs578T cells were treated with increasing concentrations of novobiocin to induce proposed endocytosis of FN. Cells were lifted with either accutase and gentle scraping or by trypsin and proteinase K treatment. Cells were lifted with accutase and gentle scraping to preserve the integrity of extracellular cell associated FN. Cells were lifted with trypsin and proteinase K to remove extracellular FN. Flow cytometry for TMR and OG fluorescence was used to monitor endocytosis of extracellular fluorescently labeled FN using a FACSAria II instrument. Gating was used to define the live cell population and restrict histogram analysis to these cells only. The live population was analyzed for fluorescence using the FITC (λ = 488 nm) or PE (λ = 550 nm) channel. The level of fluorescence correlated to the level of internalized labeled FN in Hs578T cells lifted with trypsin and proteinase K.

Figure 15 shows the internalization of fluorescently labeled FN upon inhibition of Hsp90 with novobiocin. FN-TMR fluorescence, measured in the PE channel, was used as a measure of internalization of fluorescently labeled FN-TMR and/or FN-TMR-OG. Cells treated with unlabeled FN (unstained) served as a negative control for fluorescence. Cells treated with unlabeled FN showed a background level of fluorescence (Figure 15A, unstained). Cells treated with fluorescently labeled FN and lifted with accutase and gentle scraping served as

positive control for fluorescence that would arise from both intracellular and extracellular fluorescent FN (Figure 15A). Cells treated with fluorescently labeled FN showed a shift increase in the log fluorescence compared to cells treated with unlabeled FN (Figure 15A). Cells lifted with trypsin/proteinase K showed a lower level of fluorescence by half a log scale in comparison to cells lifted with accutase (Figure 15A). This drop in fluorescence intensity was assumed to be as a result of the loss of extracellular fluorescent FN by trypsin treatment. Cells treated with fluorescently labeled FN and increasing concentrations of novobiocin were compared to cells treated with fluorescently labeled FN alone (untreated). In all cases, cells were treated with trypsin/proteinase K to remove extracellular fluorescent FN. Figure 15B shows a shift in the FN-TMR fluorescence of Hs578T cells upon treatment with novobiocin. A dose dependent increase in the fluorescent signal was observed upon treatment with novobiocin (Figure 15B). Figure 15C shows the mean fluorescence intensity of unstained, untreated, and novobiocin treated Hs578T cells for a set of triplicate experiments. Replicate results showed a dose dependent, although not statistically significant, increase in the mean fluorescence for treatment with 62.5, 125 and 250 μM novobiocin in comparison to the untreated control (Figure 15C). Treatment with 500 μM novobiocin showed a statistically significant increase in the mean FN-TMR fluorescence compared to the untreated control ($p<0.05$; Figure 15C). A similar but less pronounced FN response to novobiocin treatment was observed in MDA-MB-231 cells, presumably due to the lower levels of extracellular FN fibrils in these cells (*data not shown*).

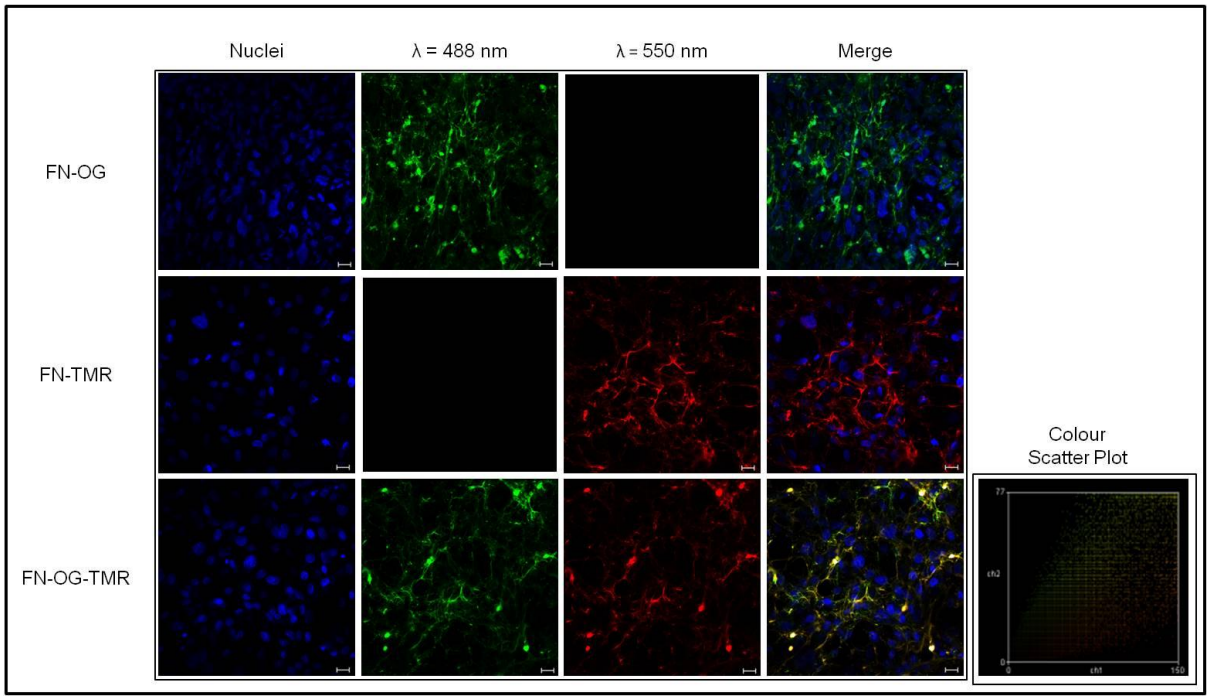

Figure 14: Fluorescently labeled FN was incorporated into the ECM of Hs578T cells

Hs578T cells were seeded with the addition of fluorescently labelled FN-OG, FN-TMR or FN-OG-TMR (50 nM) overnight at 37 °C. Cells were fixed and nuclei stained with Hoechst 33342 (1 $\mu g.ml^{-1}$). Images were captured using a Zeiss LSM 510 Meta laser scanning confocal microscope and analyzed using Zen software, blue edition (Zeiss, Germany). A colour scatter plot output of the 488 and 550 nm fluorescence signals are shown in the lower panel for FN-OG-TMR. Scale bars are equivalent to 20 μm.

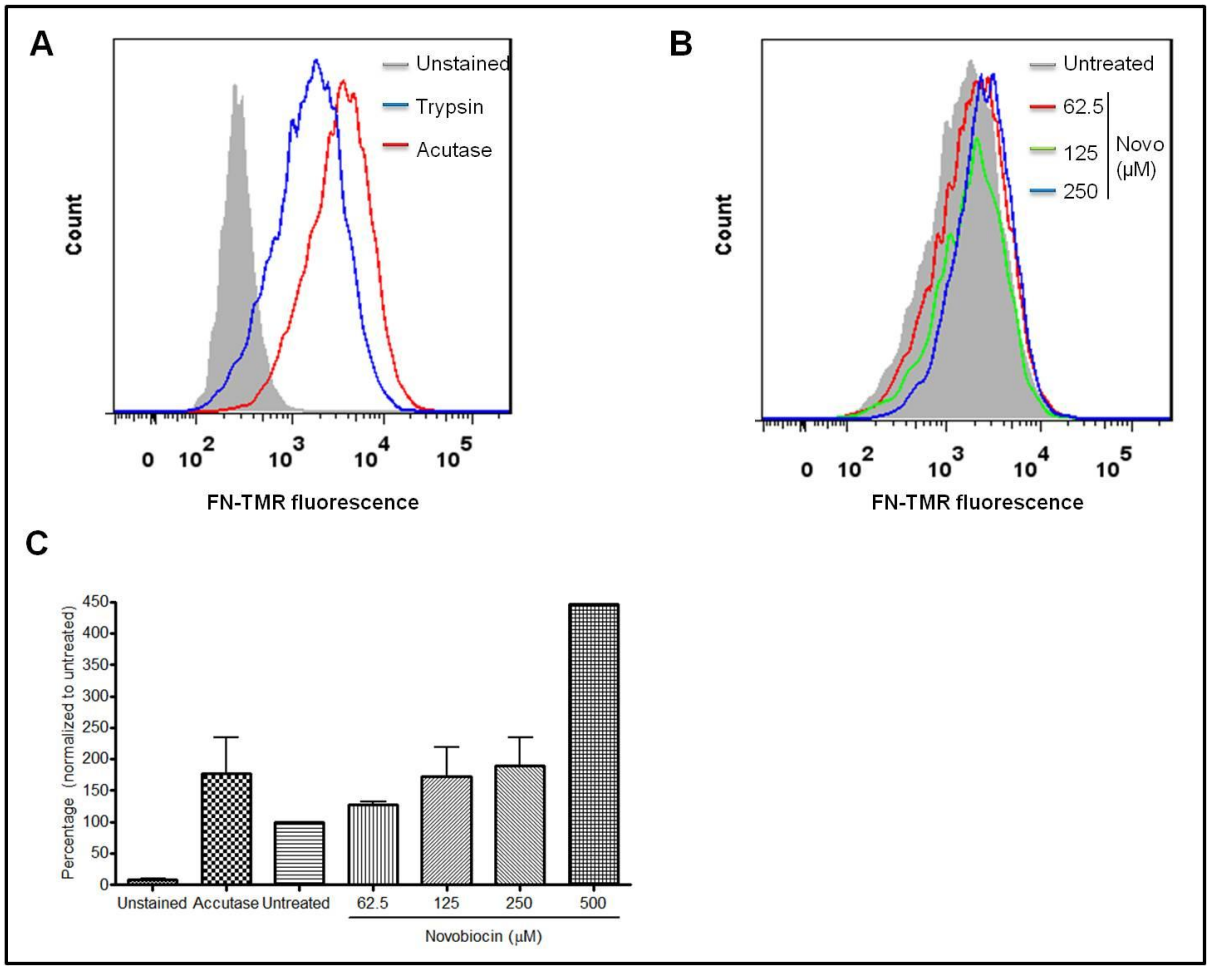

Figure 15: Inhibition of Hsp90 leads to FN internalization

An equal number (5×10^5) of Hs578T cells were seeded in a 6-well culture dish and allowed to adhere overnight at 37°C. Cells were treated with fluorescently labelled FN (50 nM) for 8 hours followed by treatment with 62.5, 125, 250 or 500 μM novobiocin overnight. Cells were lifted with either accutase and gentle scraping (negative control) or 0.03% EDTA, 0.1% trypsin and 200 μg/ml proteinase K. Cells were washed with PBS and analyzed for fluorescence by flow cytometry using the FITC or PE channel of a FACSAria II instrument. (A) Cells treated with unlabeled FN (Unstained) and cells treated with fluorescently labelled FN lifted with either accutase and gentle scraping (negative control) or trypsin. (B) Untreated and novobiocin treated cells lifted with trypsin. (C) Mean fluorescence (FITC-Height) values of cells that were treated with unlabeled FN (Unstained; triplicate) or were treated with labelled FN but remained untreated (Untreated; triplicate), or were treated with 62.5 (duplicate), 125 (triplicate), 250 (triplicate) and 500 (single) novobiocin (Novobiocin). Cells treated with unstained FN (Unstained), labelled FN (Untreated) and labelled FN and novobiocin (Novobiocin) were lifted with trypsin/proteinase K treatment. Cells lifted with accutase and gentle scraping (Accutase; triplicate) remained untreated. Fluorescence values were normalized against the untreated control.

3.3 ROLE OF LRP-1 AND HSP90 IN FN ENDOCYTOSIS

Inhibition of Hsp90 with novobiocin showed internalization of extracellular FN that is known to occur via endocytosis (Figure 15). LRP-1 has previously been shown to bind FN and function as a catabolic receptor for FN (Salicioni et al. 2002). We investigated the role of LRP-1 in the endocytosis of FN following inhibition of Hsp90 with novobiocin. LRP-1 has been shown to bind Hsp90 (Chieh-Fang Cheng et al. 2008a). We investigated the role of Hsp90 in LRP-1 mediated endocytosis of FN.

3.3.1 MDA-MB-231 and Hs578T cells express LRP-1

The expression of LRP-1 in breast, colon and lung cancer cell line lysates was determined by immunoblot analysis. Figure 16A shows the expression of LRP-1 in MDA-MB-231, MCF-7, Hs578T, A549, SW480 and SW620 cancer cell lines. Expression of LRP-1 (85 kDa) was detected in MDA-MB-231 and Hs578T breast cancer cells (Figure 16A, upper panel). Histone H3 (17 kDa) was used as a control for equal protein loading. LRP-1 expression was undetectable in MCF-7, A549, SW480 and SW620 cancer cells (Figure 16A, upper panel). Interestingly, MDA-MB-231 and Hs578T cells were also the only two of the cell lines tested to express detectable levels of full length FN (Figure 11A).

Fluorescence microscopy was used to evaluate the subcellular localization of LRP-1 in MDA-MB-231 and Hs578T breast cancer cells relative to the subcellular localizations of FN and Hsp90 (Figure 16B). Fluorescence microscopy confirmed expression of LRP-1 in MDA-MB-231 and Hs578T breast cancer cells. A dispersed intracellular localization pattern for LRP-1 was observed in both MDA-MB-231 and Hs578T breast cancer cell lines (Figure 16B, LRP-1).

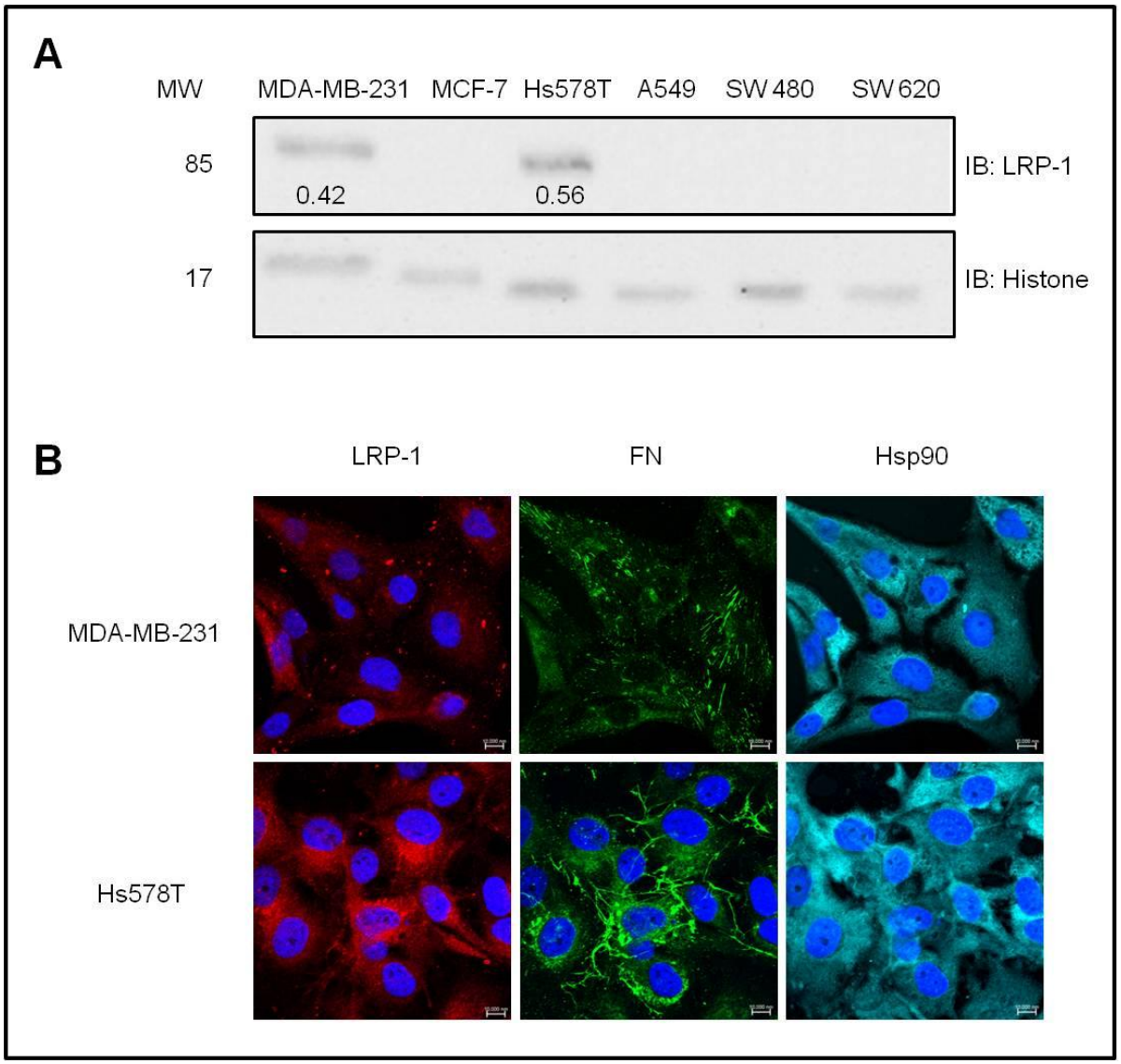

Figure 16: MDA-MB-231 and Hs578T cells show expression of LRP-1

(A) Lysates of mammalian breast (MDA-MB-231, MCF-7, and Hs578T), lung (A549) and colon (SW480 and SW620) cancer cell lines showed expression of LRP-1 and Histone H3 by immunoblot analysis. Densitometry values relative to Histone H3 are shown below respective bands. (B) Fixed MDA-MB-231 and Hs578T cells were stained using rabbit anti-human LRP-1, mouse anti-human FN and goat anti-human Hsp90α/β followed by donkey anti-rabbit DyLight® 550, donkey anti mouse DyLight® 488 and donkey anti goat DyLight® 650 fluorescent secondary antibodies respectively. Nuclei were stained with Hoechst 33342. Images were captured using a Zeiss LSM 510 Meta laser scanning confocal microscope and analyzed using Zen software, blue edition (Zeiss, Germany). Scale bars are equivalent to 10 μm. The data shown are representative of images obtained from duplicate independent experiments.

3.3.2 LRP-1 and FN colocalize in novobiocin treated Hs578T breast cancer cells

We next determined the effects of novobiocin on the localization of LRP-1 relative to FN in Hs578T breast cancer cells. Hs578T cells untreated, or treated with novobiocin, Hsp90β, or a combination of both treatments, were fixed and stained for LRP-1 and FN (Figure 17). Highlighted (orange) PDM values showed regions of possible colocalization (Reitan et al. 2012). Untreated Hs578T cells showed little to no colocalization of FN and LRP-1 signals (Figure 17, untreated). Treatment with novobiocin resulted in partial perinuclear colocalization between LRP-1 and FN signals (yellow arrows) in Hs578T cells (Figure 17, Novo). Similar to treatment with novobiocin, treatment with novobiocin in combination with exogenous Hsp90β showed similar regions of partial LRP-1 and FN perinuclear colocalization (Figure 17, Novo + Hsp90). Treatment with exogenous Hsp90β alone showed little to no colocalization of FN and LRP-1, similar to that of untreated Hs578T cells (Hsp90).

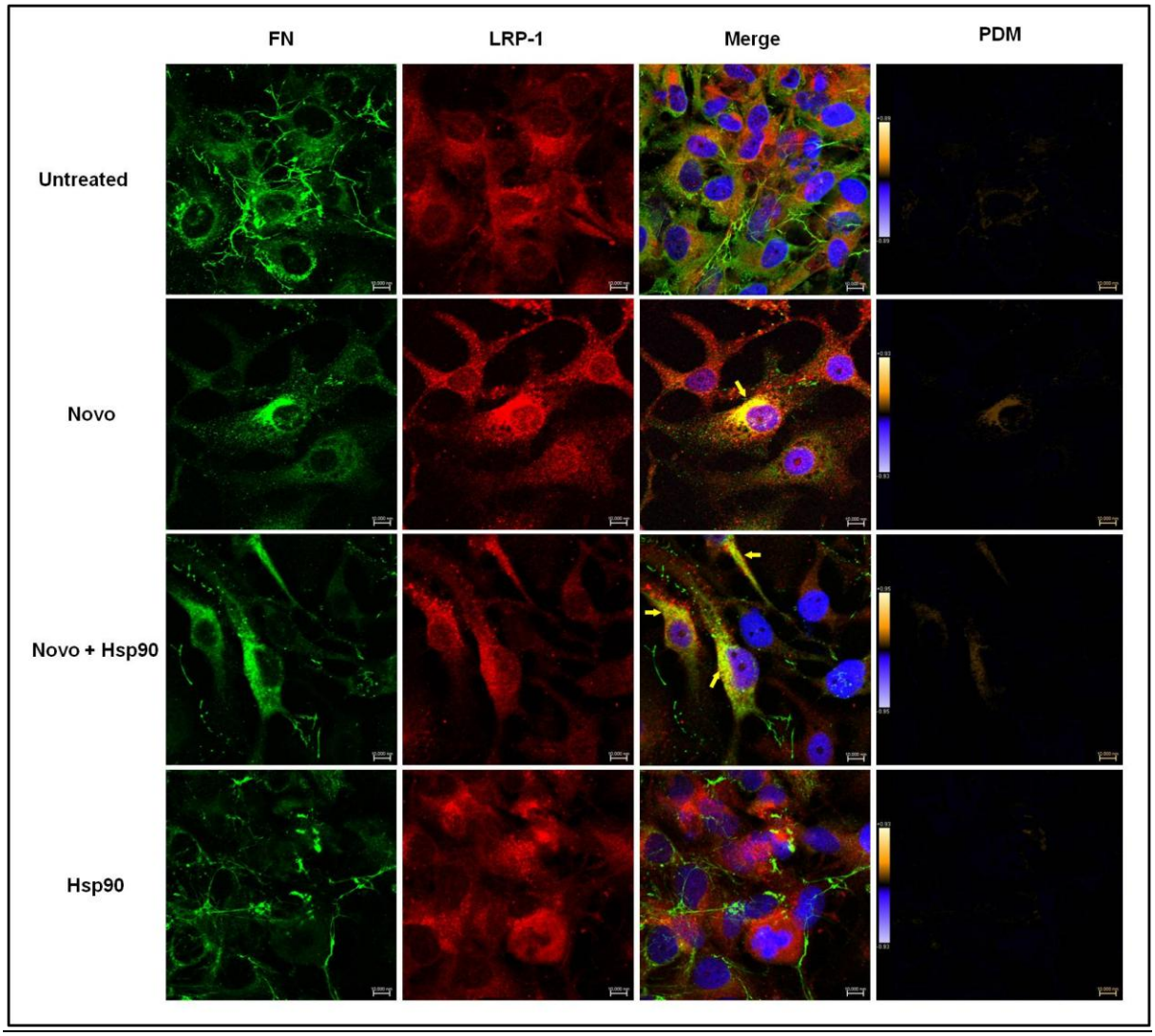

Figure 17: Novobiocin treatment results in LRP-1 and FN partial colocalization in Hs578T cells.

Adherent Hs578T cells were treated with novobiocin (Novo; 500 μM) in fresh media for 1 hour at 37 °C and then with exogenous Hsp90β (100 $ng.ml^{-1}$) directly overnight. Fixed cells were stained using mouse anti-human FN and rabbit anti-human LRP-1 followed by donkey anti mouse DyLight® 488 and donkey anti-rabbit DyLight® 550 fluorescent secondary antibodies respectively. Nuclei were stained with Hoechst 33342 (1 $\mu g.ml^{-1}$). Images were captured using a Zeiss LSM 510 Meta laser scanning confocal microscope and analyzed using Zen software, blue edition (Zeiss, Germany). Yellow arrows show regions of interest for partial colocalization. PDM values were generated using Image J 1.43m. Positive and negative PDM values are indicated in orange and blue respectively. Scale bars are equivalent to 10 μm. The data shown are representative of images obtained from triplicate experiments.

3.3.3 Overexpression and purification of RAP1

LRP-1 was shown to partially colocalize with FN in Hs578T cells upon treatment with novobiocin (Figure 17). We wanted to investigate the effects of LRP-1 inhibition on the endocytosis of FN following inhibition of Hsp90 with novobiocin. We investigated known inhibitors of LRP-1 and found Receptor-associated protein (RAP1). RAP1 has previously been shown to bind LRP-1 and prevent binding of all known ligands, including HSPs (Willnow et al. 1995; Binder & Srivastava 2004). Plasmid pQTEV-LRPAP1, encoding His-tagged human low density lipoprotein RAP1 with an N-terminal His tag was obtained from Addgene (Plasmid 31327). The pQTEV-LRPAP1 plasmid identity was confirmed by sequence analysis. Expression and purification of His-tagged RAP1 protein was adapted from the published protocol (Herz et al. 1991). In order to optimize the overexpression of RAP1, pQTEV-LRPAP1 was transformed into *E. coli* BL21 cells. Protein expression was induced with IPTG and cell lysate fractions collected hourly and overnight. Fractions collected were resolved by SDS-PAGE and analyzed by immunoblotting for His-tagged protein expression. Figure 18A shows resolved proteins of the induction of expression of RAP1 in *E. coli* BL21 cells. Non-transformed *E.coli* BL21 lysate (L) served as a negative control for expression of RAP1. Expression of a band (indicated with an arrow) correlating with the estimated size of His-tagged RAP1 (± 45 kDa) was seen post induction with IPTG with increasing intensity up until six hours (Figure 18A, lanes marked 0 to 6). Immunoblot analysis to detect RAP1 using an anti-His primary antibody confirmed expression of a His-tagged protein with approximate molecular weight of 45 kDa (Figure 18B). The absence of a band in non-transformed *E. coli* BL21 lysate (L) indicated the absence of endogenous expression of RAP1 in *E. coli* BL21 cells. Expression of His-tagged RAP1 protein was seen in all samples post induction (Figure 18B, lanes marked 1 to O/N). Figure 18B confirmed that four hours post induction was optimal for harvesting of RAP1 expressing E. coli BL21 cells (Figure 18B, lane marked 4).

Following a 4 hour induction of expression of RAP1 in *E. coli* BL21 cells, RAP1 was purified using His affinity chromatography (Figure 18C and 18D). The fractions collected from the purification of RAP1 were resolved by SDS-PAGE (Figure 18C) and analyzed by immunoblotting (Figure 18D). A band (indicated with an arrow) of the anticipated size of RAP1 (45 kDa) was observed in the elution fractions; although a number of contaminating bands were also present (Figure 18C). Elution one showed high levels of contaminating protein (Figure 18C). Lower levels of contaminating protein were observed in elution

fractions two and three (Figure 18C). Immunoblot analysis for His-tagged protein confirmed purification of RAP1 (Figure 18D).

In order to further optimize the purification of RAP1, the incubation time of induced cell lysate with MagReSyn-NTA was increased. Figure 18E shows the resolved protein fractions of RAP1 purification round two. A longer incubation time of the induced cell lysate with MagReSyn-NTA greatly improved the degree of purity of RAP1 in elution fractions (compare elution fractions of Figure 18E to Figure 18C). Contaminating endotoxin was removed and elutions determined to be endotoxin free. However, no quantifiable protein was detected after this procedure. Given the project time constraints and the availability of a commercial alternative LRP-1 inhibitor, optimization of the purification of RAP1 was halted for future study.

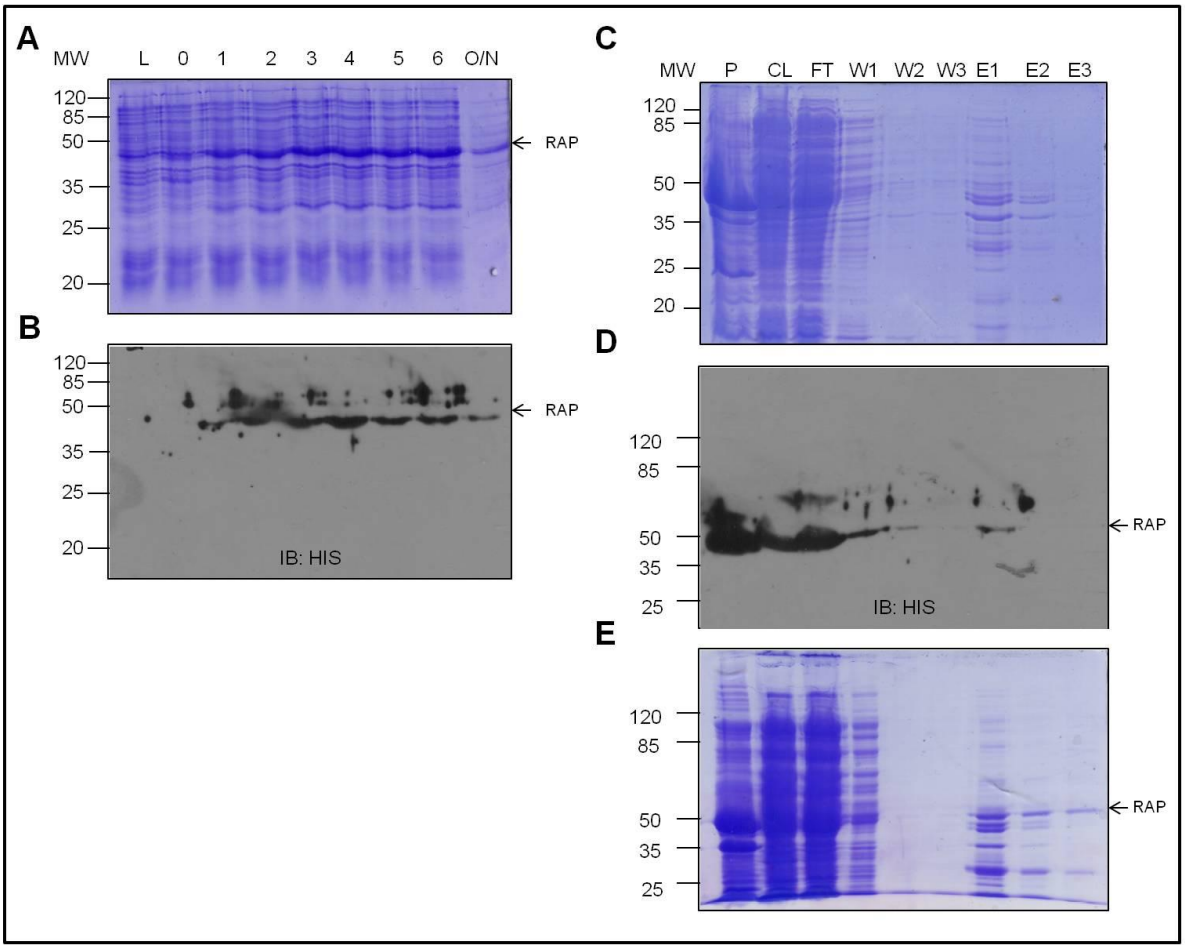

Figure 18: Expression and Purification of RAP1

RAP1 expression was induced (0.42 mM IPTG; 30 °C) in E. *coli* BL21 cells and induction samples collected and resolved by (A) SDS-PAGE and (B) probed using anti-human His. Numbers on the left hand side show the molecular weight (kDa) of the prestained protein molecular weight marker (MW). Letters above the figure show the (L) Non-transformed E. *coli* lysate and (O/N) overnight induced sample. Numbers (0 – 6) above the figure show hourly time interval post induction. Arrows show the expressed RAP1. RAP1 was purified from E. *coli* BL21 cells 4 hours post induction with 0.42 mM IPTG. Collected fractions of RAP1 purification were resolved by (C) SDS-PAGE and (D) probed using anti-human His. (E) Fractions collected from RAP1 purification round 2 were resolved by SDS-PAGE. Numbers on the left hand side show the molecular weight (kDa) of the prestained protein molecular weight marker (MW). Letters above each figure show the (P) pellet, (CL) cleared lysate, (FT) flow through, (W) wash and (E) elution collected fractions. Arrows show the purified RAP1.

3.3.4 Loss of extracellular FN in response to LRP-1 blocking antibody was partially rescued by soluble Hsp90

A commercial LRP-1 blocking antibody was used to study the effects of LRP-1 on the endocytosis of FN. Mouse monoclonal LRP-1 antibody [8G1] is reported to bind the 515 kDa alpha chain of LRP-1 and prevent binding of ligand molecules (Scilabra et al. 2013). The role of Hsp90 on the endocytosis of FN was studied in combination with this LRP-1 blocking antibody by inhibition of Hsp90 with novobiocin, or by supplementation with exogenous Hsp90β. Figure 19 shows the FN phenotype upon treatment with novobiocin (Novo; 500 μM), LRP-1 blocking antibody (LRPab; 2 $\mu g.ml^{-1}$), both LRPab and exogenous Hsp90β (LRPab + Hsp90β; $100ng.ml^{-1}$), and a combination of novobiocin, LRPab and Hsp90β (Novo + LRPab + Hsp90β). Adherent Hs578T cells were treated as described and the resulting extracellular FN matrix phenotype determined using confocal microscopy after fluorescent staining for FN. The intensity of the FN signal as a ratio of the number of cell nuclei for multiple images was compared for the different treatments. As noted previously (Figure 13), treatment of Hs578T cells with novobiocin showed a significant ($p<0.001$) loss of the extracellular FN matrix in comparison to the untreated control (Figure 19B). Treatment of Hs578T cells with a LRP-1 blocking antibody showed a significant ($p<0.001$) loss of the extracellular FN matrix in comparison to the untreated control (Figure 19C). A FN phenotype similar to that of novobiocin treated Hs578T cells was observed (Figure 19B and 19C). The addition of exogenous Hsp90β was able to significantly ($p<0.05$) overcome the observed FN phenotype in LRPab treated Hs578T cells (Figure 19D) and restored the extracellular FN matrix phenotype of LRPab treated Hs578T cells similar to that of the untreated control (Figure 19A). Treatment with a combination of novobiocin, LRPab and exogenous Hsp90β resulted in a loss of the extracellular FN matrix similar to that of novobiocin treated (Novo) and LRPab treated (LRPab) Hs578T cells (Figure 20, Novo + LRPab + Hsp90β). Hsp90β was partially ($p<0.05$) able to restore the extracellular FN matrix phenotype of novobiocin in combination with LRPab treated Hs578T cells (Figure 19E).

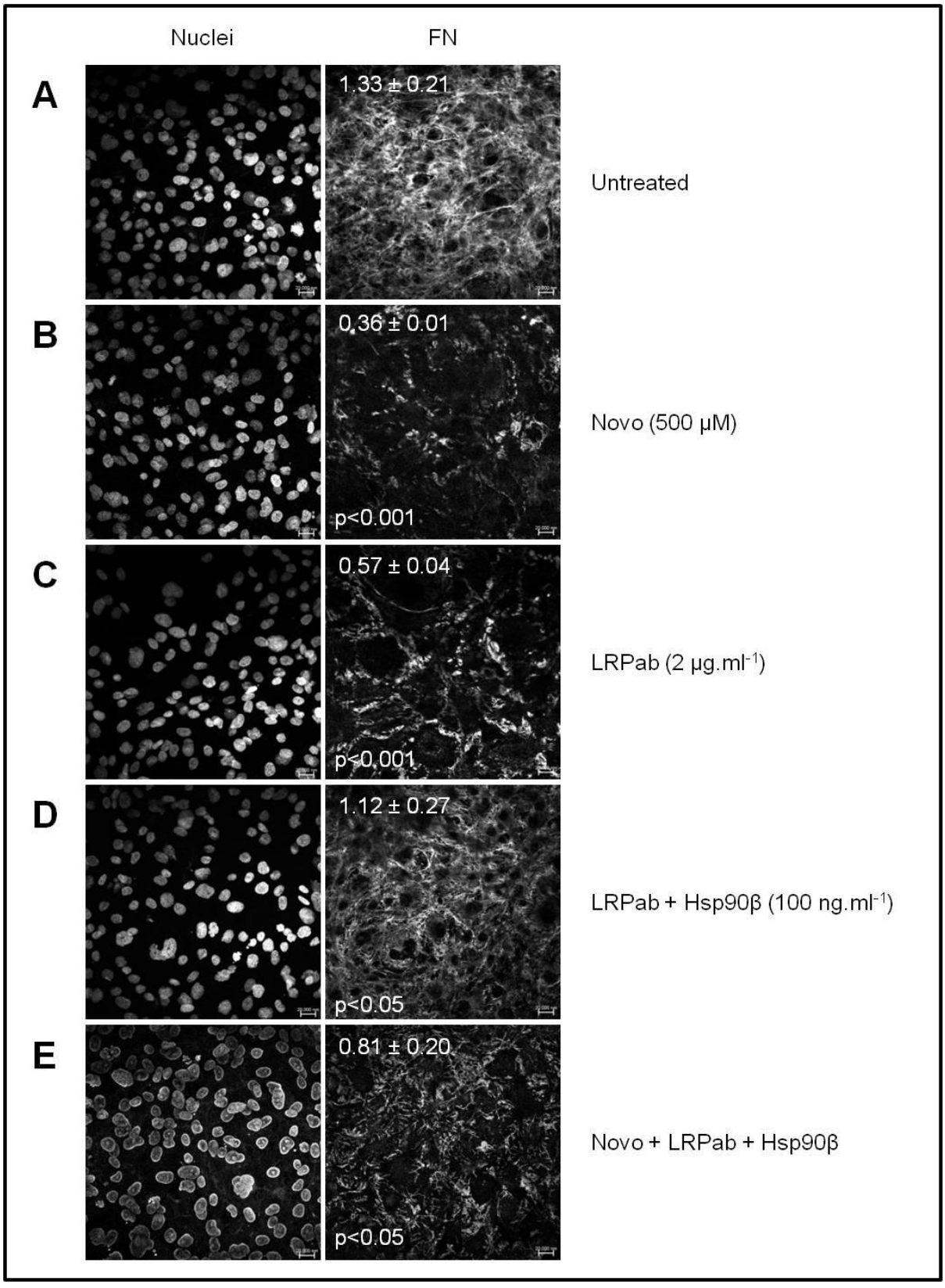

Figure 19: legend over page

Figure 19: Loss of extracellular FN in response to LRP-1 blocking antibody is partially rescued by soluble Hsp90B

Adherent Hs578T cells were treated with novobiocin (Novo; 500 μM) in fresh media for 1 hour at 37 °C followed by treatment with a blocking LRP-1 antibody (LRPab; 2 $\mu g.ml^{-1}$) for 10 minutes before direct addition of exogenous Hsp90β (100 $ng.ml^{-1}$) overnight. Fixed cells were stained using rabbit anti-human FN followed by donkey anti-rabbit DyLight® 488 fluorescent secondary antibodies. Nuclei were stained with Hoechst 33342 (1 $\mu g.ml^{-1}$). Images were captured using a Zeiss LSM 510 Meta laser scanning confocal microscope and analyzed using Zen software, blue edition (Zeiss, Germany). Scale bars are equivalent to 20 μm. Values (in white) at the top of each frame represent the mean grey values (± standard deviation) per nuclei for each treatment. Mean grey values were compared using a one-way ANOVA with a Tukey Post Test comparing all values. The mean grey value of novobiocin treated (Novo) and LRP-1 blocking antibody treated (LRPab) were compared to untreated cells. The mean grey value of LRP-1 blocking antibody and exogenous Hsp90β treated (LRPab + Hsp90β) cells were compared to the equivalent treatment without exogenous Hsp90β (LRPab). The mean grey value of a combination of all three treatments (Novo + LRPab + Hsp90β) was compared to untreated cells. Statistical p-values are shown in the bottom left of each frame. The data shown are representative of triplicate images collected from duplicate experiments.

3.3.4 Immunoprecipitation of a LRP-1 complex containing FN and Hsp90

LRP-1 co-immunoprecipitation experiments were performed. Immunoprecipitation of LRP-1 was carried out as outlined previously with modifications (Muratoglu et al. 2010). Adherent Hs578T cells were chilled before being shifted to 37 ºC for seven minutes to allow endocytosis to initiate. Protein interactions were cross-linked with a cell-impermeable crosslinker to select for complexes containing extracellular FN. LRP-1 containing complexes were immunoprecipitated using LRP-1 antibody coupled MagReSyn™ Protein A and eluting complexes resolved by SDS-PAGE (Figure 20A) and analyzed by immunoblotting (Figure 20B). MagReSyn™ Protein A alone served as a negative control for non-specific binding of protein to Protein A.

Figure 20A shows flow-through (FT, cell lysate proteins that were not immunoprecipitated), wash (W), and elution (E) fractions of the immunoprecipitation of LRP-1 containing complexes by MagReSyn™ Protein A alone (Beads) or LRP-1 antibody coupled MagReSyn™ Protein A (Beads – LRPab). Fractions were resolved in the absence of β-mercaptoethanol to prevent cleavage of the DTSSP cross-linker. Non-specific binding of proteins to MagReSyn™ was noted in fractions from both samples (Beads and Beads-LRPab) (Figure 20A). The elution fraction of the Beads-LRPab immunoprecipitation showed two unique bands (*A* and *B*) in comparison to the negative control (Beads) elution fraction (Figure 20A, compare E of Beads-LRPab to E of Beads). To confirm successful immunoprecipitation of LRP-1, immunoblot analysis of the elution fractions of the test and control immunoprecipitations was performed (Figure 20B). Figure 20B shows successful immunoprecipitation of LRP-1. The presence of a band at 85 kDa in the Beads-LRPab elution fraction confirmed immunoprecipitation of LRP-1 (Figure 20B, LRP-1). The lysate of Hs578T cells (L) served as a control for immunoblotting and sizing of LRP-1. Lower molecular weight bands, 55 kDa and 35 kDa, possibly corresponding to the size of the heavy and light chain of LRP IgG used in the immunoprecipitation, were also observed in the Beads-LRPab elution fraction (Figure 20B). A band detected at 35 kDa in the Beads and Beads-LRPab elution fractions was possibly Protein A (45 kDa) from the MagReSyn™. (Figure 20B).

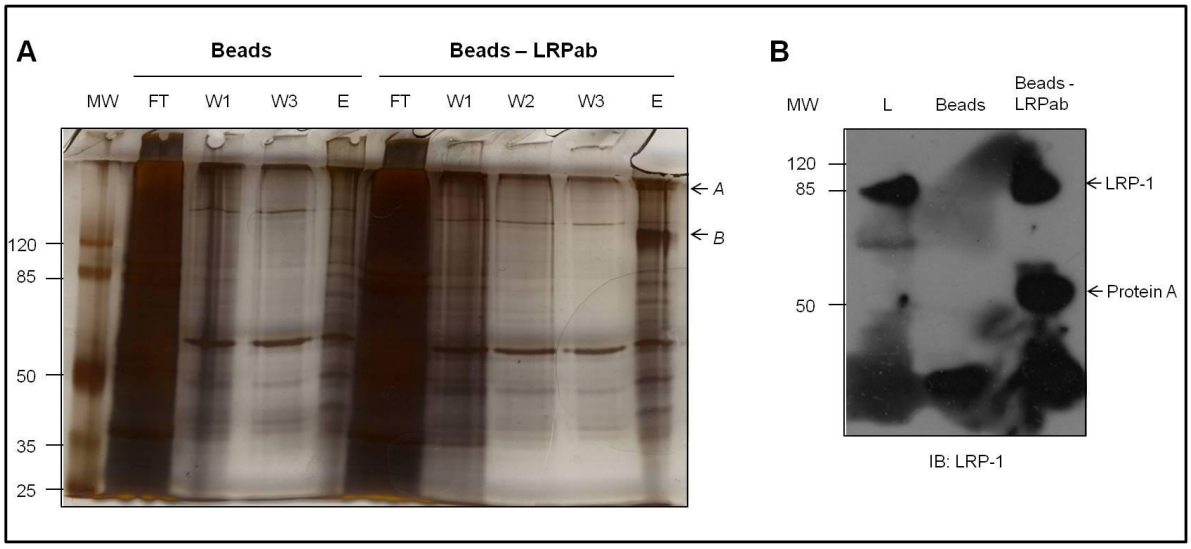

Figure 20: Immunoprecipitation of higher molecular weight LRP-1 complexes

Confluent Hs578T cells were chilled to 4 °C for 1 hour. Cells were shifted to 37 °C for 7 minutes to allow endocytosis to initiate followed by crosslinking of protein interactions with DTSSP at 4 °C for 2 hours. Cells were lysed with RIPA buffer and LRP-1 protein complexes immunoprecipitated using MagReSyn™ Protein A alone (Beads; negative control) or LRP-1 antibody coupled MagReSyn™ Protein A (Beads – LRPab). (A) LRP-1 immunoprecipitation fractions (in the absence of β-mercaptoethanol) were resolved by SDS-PAGE on an 8 % polyacrylamide gel and stained using the Fermentas PageSilver™ Silver Staining Kit. Numbers on the left hand side show the molecular weight (kDa) of the prestained protein molecular weight marker (MW). Letters above each lane indicate the (FT) Flow Through, (W) Washes and (E) Elution fractions of the LRP-1 immunoprecipitation. (B) LRP-1 protein complexes were immunoprecipitated using MagReSyn™ Protein A alone (Beads) or LRP-1 antibody coupled MagReSyn™ Protein A (Beads-LRPab) and elution fractions probed for LRP-1 using anti-human LRP-1 primary antibody by immunoblotting (IB). Hs578T (L) lysate was used as a control for immunoblotting of LRP-1. Arrows show the immunoprecipitated LRP-1 and Protein A respectively. Numbers on the left hand side show the molecular weight (kDa) of the prestained protein molecular weight marker (MW).

The effect of novobiocin and exogenous Hsp90β on the immunoprecipitated LRP-1 complexes was investigated. Equal numbers of Hs578T cells were seeded and allowed to adhere overnight. Adherent cells remained untreated or were treated with either novobiocin or exogenous Hsp90β at 37 ºC for 1 hour prior to processing as previously described. In order to determine the input levels of LRP-1, FN and Hsp90, untreated, novobiocin treated, and Hsp90β treated cell lysates were probed for LRP-1, FN and Hsp90 prior to immunoprecipitation of LRP-1 containing complexes (Figure 21A). LRP-1, FN and Hsp90 expression was observed in all cell lysates. Similar levels of LRP-1 (85 kDa) expression was observed in all cell lysates (Figure 21A, upper panel). Similar levels of FN (220 kDa) expression was observed in all cell lysates, however lower molecular FN products were detected in novobiocin treated (± 70 kDa product) and exogenous Hsp90β treated (± 85, 70, 40 kDa products) lysates (Figure 21A, middle panel). Treatment with novobiocin, and exogenous Hsp90β appeared to reduce the levels of Hsp90 in comparison to the untreated control (Figure 21A, lower panel).

Immunoprecipitation of LRP-1 containing complexes from untreated, novobiocin treated and exogenous Hsp90β treated cell lysates was performed. Figure 21B shows the immunoblot analysis for LRP-1, FN and Hsp90 in the immunoprecipitated fraction of untreated (Un), novobiocin treated (Novo) and exogenous Hsp90β (90β) treated cell lysates. Lysates were prepared from the same number of cells. The detection of LRP-1 (85 kDa) in all cell lysates confirmed successful immunoprecipitation of LRP-1 containing complexes (Figure 21B, upper panel). Given the use of Protein A in the immunoprecipitation of LRP-1 containing complexes, bands detected at ~ 45 kDa in the elution fractions (Figure 21B) were most likely the detection of Protein A by the secondary antibodies used in immunoblot analysis. None of the treatments appeared to have a major effect on the level of LRP-1 that was immunoprecipitated (Figure 21B, upper panel). An immunoblot for FN showed the presence of FN in all elution fractions (Figure 21B, middle panel). Non-specific binding of FN (bands detected at both >120 kDa and 70 kDa) to beads was observed in the beads alone and LRPab immunoprecipitation fractions (Figure 21B, middle panel). The band intensity of FN in the LRPab immunoprecipitation fraction was thus compared to the beads alone fraction (negative control). Untreated cells showed a band detected at 70 kDa. The FN band at 70 kDa was greater in intensity in the LRPab immunoprecipitation fraction (+) when compared to the beads alone fraction (-) (Figure 21B, middle panel). This suggested the presence of a 70 kDa FN fragment in an LRP-1 containing complex (Figure 21B, middle panel). Treatment with

novobiocin showed a band of equal intensity of the 70 kDa fragment in the LRPab immunoprecipitation (+) when compared to the beads alone fraction (-) (Figure 21B, middle panel). This suggested absence of/or a decrease in the level of the 70 kDa band in the LRPab immunoprecipitation fraction treated with novobiocin in comparison to the untreated control. Treatment with exogenous Hsp90β showed a 70 kDa FN band of lower intensity in the overexposed LRPab immunoprecipitation (+) image, when compared to the beads alone fraction (-) (Figure 21B, middle panel). This suggested absence of a 70 kDa FN band in the LRPab immunoprecipitation fraction treated with exogenous Hsp90β.

Additionally, untreated cells showed FN bands detected at > 120 kDa, henceforth referred to as FN120+. Untreated cells showed a lower level of FN120+ in the LRPab immunoprecipitation fraction (+) when compared to the beads alone fraction (-) (Figure 21B, middle panel). Treatment with novobiocin showed an increase in the level of the FN120+ detected in the LRPab immunoprecipitation fraction (+) in comparison to the beads alone fraction (-) (Figure 21B, middle panel). This suggested an increase in the level of FN120+ in the LRPab immunoprecipitation fraction treated with novobiocin in comparison to the untreated control. Treatment with exogenous Hsp90β showed the absence of FN120+ in both the LRPab immunoprecipitation fraction (+) and the beads alone fraction (-) (Figure 21B, middle panel). This could suggest Hsp90β addition resulted in a decrease in the higher molecular weight FN120+ in the LRPab elution fraction (+) in comparison to the untreated cells.

An immunoblot for Hsp90 showed the presence of Hsp90 in all LRPab immunoprecipitation fractions (Figure 21B, lower panel). Hsp90 was detected in the untreated LRPab immunoprecipitation fraction (+), confirming the presence of Hsp90 in the LRP-1 and FN containing complex (Figure 21B, lower panel). Treatment with novobiocin had no effect on the level of Hsp90 in comparison to the untreated LRP1 immunoprecipitation (Figure 21B, lower panel). A slight decrease in Hsp90 was observed in the immunoprecipitates from Hsp90β treated cells in comparison to the untreated LRP1 immunoprecipitation (Figure 21B, lower panel). The data showed the successful immunoprecipitation of an LRP-1 containing complex composed of FN and Hsp90.

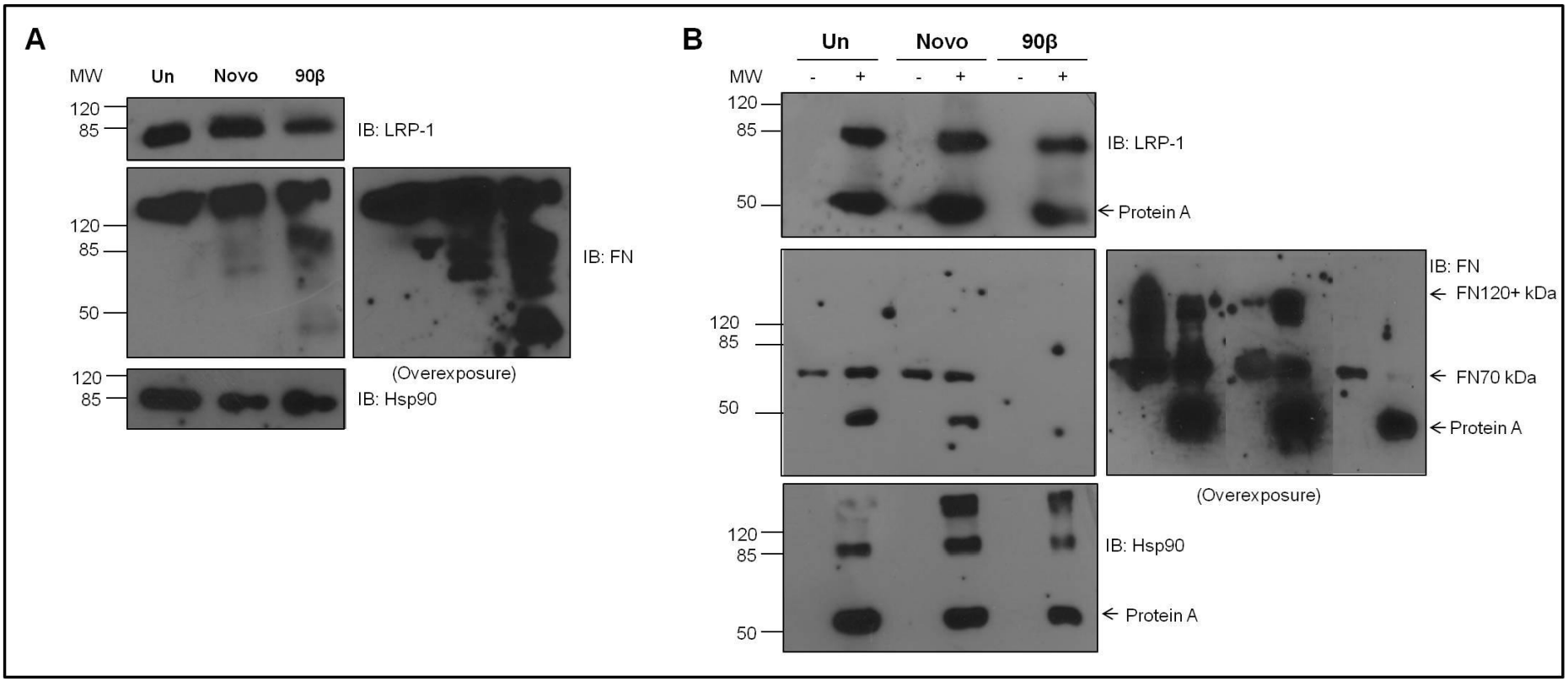

Figure 21: legend over page

Figure 21: LRP-1 immunoprecipitation from untreated, novobiocin treated and exogenous Hsp90β treated Hs578T cells

An equal number of Hs578T cells were seeded overnight at 37 ºC. Adherent cells remained untreated (Un) or were treated with either novobiocin (Novo; 250 µM) or exogenous Hsp90β (90β; 100 ng.ml^{-1}) at 37 °C for 1 hour and subsequently at 4 ° for 1 hour. Cells were shifted to 37 °C for 7 minutes to allow endocytosis to occur followed by crosslinking of protein interactions with DTSSP at 4 °C for 2 hours. Cells were lysed with RIPA buffer. (A) Cell lysates were probed for LRP-1, FN and Hsp90. (B) LRP-1 protein complexes were immunoprecipitated using MagReSyn™ Protein A alone (-) or LRP-1 antibody coupled MagReSyn™ Protein A (+) and elution fractions probed for LRP-1, FN and Hsp90. Numbers on the left hand side show the molecular weight (kDa) of the prestained protein molecular weight marker (MW). Data shown as representative of duplicate experiments with similar results.

CHAPTER 4: DISCUSSION

4.1 SUMMARY OF KEY FINDINGS

The biological function of eHsp90 remains relatively uncharacterized compared to that of intracellular Hsp90. Limited studies have alluded to a role for eHsp90 in cell migration and invasion, potentially contributing to the metastatic process of cancer cells (Eustace & Jay 2004). In this study, we provided evidence for a direct role of eHsp90 in FN matrix remodeling.

Previous results in our laboratory have shown the presence of cell surface associated Hsp90 as well as extracellular soluble Hsp90α in cancers of different origin, cell type and malignancy. Hsp90 was isolated in a complex containing FN on the surface of MDA-MB-231 cells. In addition, Hs578T cells treated with novobiocin showed a loss of extracellular FN matrix and subsequent endocytosis of FN and colocalization with key vesicular trafficking markers (Rab-5 and LAMP-1). Treatment with methyl-β-cyclodextrin, a vesicular trafficking inhibitor, resulted in recovery of the extracellular FN matrix following treatment with novobiocin. These data suggested a role for Hsp90 in FN matrix dynamics. Interestingly, the N-terminal Hsp90 inhibitor, geldanamycin, showed no effect on the extracellular FN matrix of Hs578T cells and loss of extracellular FN matrix was specific to novobiocin treatment.

In this report, we further defined the presence of both cell surface associated Hsp90α and Hsp90β isoforms in breast cancer cell lines. We reported the presence of extracellular soluble Hsp90β in Hs578T cells and showed colocalization of Hsp90 with extracellular FN fibrils. Moreover, we showed direct binding of Hsp90α and Hsp90β to FN and FN70 *in vitro*. We confirmed that treatment of Hs578T cells with novobiocin resulted in a loss of extracellular FN matrix, and further showed partial rescue of the phenotype with the addition of exogenous Hsp90β. We showed that treatment with novobiocin resulted in FN endocytosis and partial colocalization with LRP-1. Treatment with blocking antibody against LRP-1 resulted in a loss of the FN matrix and exogenous Hsp90β partially rescued this response. We further reported a complex containing LRP-1, FN fragments and Hsp90 on the surface of Hs578T cells. Treatment with novobiocin was shown to increase the binding of higher molecular weight FN fragments (greater than 120 kDa) and decrease the binding of a 70 kDa FN fragment to LRP-1. Treatment with exogenous Hsp90β resulted in the loss of both high (>120 kDa) and low (70 kDa) molecular weight FN fragments in the LRP-1 immunoprecipitates.

4.2 IDENTIFICATION OF FN AS A HSP90 INTERACTING PROTEIN

To the best of our knowledge, this is the first published report of an interaction between Hsp90 and FN. Direct association of FN and Hsp90 *in vitro* and colocalization of Hsp90 with FN in Hs578T cells suggested FN as an Hsp90 interacting protein. The affinity of the interaction between FN and Hsp90β was compared to known intracellular Hsp90 client proteins and co-chaperones (Table 2). Given the use of label-free Hsp90β in SPR experiments, and the improved accuracy of binding quantification using multichannel SPR sensing technology (Palumbo et al. 2005), the reported K_d value of 29.9 ± 6.1 nM was deemed more accurate for the Hsp90-FN interaction than that derived from the solid phase binding assay. Despite differences in determined K_d values from the different studies, all K_d values for the binding of Hsp90β to FN were reported in the nanomolar range (Table 2). The K_d (29.9 ± 6.1 nM) for the binding of Hsp90β to FN correlated closely to the K_d (59.9 ± 44.9) of the binding of Hsp90β to the intracellular Signal transducer and activator of transcription 3 beta (STAT3β) client protein. The K_d (690 ± 40 nM; 1700 nM) values for the binding of Hsp90β to co-chaperones Hop and p23 are between 10 and 100 fold higher than the K_d (29.9 ± 6.1 nM) for the binding of Hsp90β to FN. FN plays an important role in cell morphology, adhesion and migration (Humphries et al. 1989; Ruoslahti 1984; Akiyama et al. 1995; Labat-Robert 2002; Bendas & Borsig 2012); a role thought to rely upon weak, transient binding of associated proteins. Due to the dynamics of cell migration and adhesion, weak binding has been described for numerous interactions involved in such processes (Anton et al. 1994; Dustin et al. 1997; Friedl et al. 1998; Loskutoff et al. 1999; Palecek et al. 1999), roles that are consistent with those alluded for eHsp90. Conversely, we report a K_d value in the nanomolar range, alluding to higher affinity binding of Hsp90 to FN.

Analysis of isoform dependent binding indicated that FN bound to both Hsp90α and Hsp90β. Although Hsp90α and Hsp90β are highly homologous (86 % sequence identity, 93 % sequence similarity) (Solier et al. 2012; Chadli et al. 2008; Peterson et al. 2013), certain regions of differing amino acid sequence raise the possibility of differential binding to interacting proteins (Sreedhar et al. 2004). Hsp90α and Hsp90β sequence differences are most evident near the N-terminal, although the crystal structures of their N-terminal domains are very similar (Wright et al. 2004). Hsp90α and Hsp90β have been shown to share similar interactions with co-chaperones, but different behaviors with client proteins under stress conditions have been observed (Taherian et al. 2008). More recent evidence suggests Hsp90α

and Hsp90β isoforms interact with co-chaperones and client proteins in a unique manner (Johnson 2012). Chadli and colleagues reported the binding of general cell UNC45 (GCUNC45), an Hsp90 co-chaperone implicated in the chaperoning of myosins and progesterone receptor, preferentially to Hsp90β *in vitro* (Chadli et al. 2008). Peterson and colleagues report human ether a-go-go (hERG) channel as an Hsp90α isoform-dependent client protein (Peterson et al. 2013). Although Hsp90 exists as a constitutive dimer, Hsp90α has a higher dimer-forming potential than that of Hsp90β (Kobayakawa et al. 2008). Such a structural determinant could have an effect on the binding of co-chaperones and client proteins (Kobayakawa et al. 2008). Hsp90α and Hsp90β structural differences and isoform specific co-chaperone and client protein interactions give distinct functions for Hsp90α and Hsp90β (Johnson 2012).

Table 2: Binding and kinetics dissociation constants of the Hsp90 and FN interaction

Protein	Partner	K_d value (nM)	Method of analysis	Reference
GST	FN	541.1	Solid phase binding assay	*Current report*
GST-Hsp90β	FN	289.8	Solid phase binding assay	*Current report*
Hsp90β	FN	17.4 ± 12.1 (*F) 29.9 ± 6.1 (*S)	SPR	*Current report*
Hsp90β	FN70	-	SPR	*Current report*
Hsp90β	STAT3β	59.9 ± 44.9	SPR	(Prinsloo et al. 2012)
Hsp90β	p23	1700	SPR	(McLaughlin et al. 2006)
Hsp90β	Hop	690 ± 40	Isotermal titration calorimetry (ITC)	(Onuoha et al. 2008)
Hsp90α	FN	-	SPR	*Current report*

*F (determined from kinetic fit model)
*S (determined from Scatchard plot analysis of saturated binding data)

Whether the interaction of Hsp90 with FN occurs intracellularly, within the plasma membrane, or only in the extracellular space, remains to be determined. Most reports to date show the presence of, and suggest a role for, eHsp90α, and not eHsp90β, in cancer cell migration (Li et al. 2011). Our results, in combination with previous results from our laboratory, show the presence of both cell surface associated, and extracellular soluble,

Hsp90α and Hsp90β. Similar to our findings, previous studies have identified both Hsp90α and Hsp90β in a soluble extracellular form (Hegmans et al. 2004), while others showed the presence of Hsp90α on the surface of cancer cells coupled with secretion of Hsp90α, and not Hsp90β, into the extracellular space (Eustace & Jay 2004; Li et al. 2007; Liao et al. 2000). Colocalization of Hsp90 with extracellular FN fibrils surrounding Hs578T cells suggested that eHsp90 associated with extracellular FN fibrils. Isolation of Hsp90 and FN in a common complex on the extracellular surface of MDA-MB-231 and Hs578T cells suggested Hsp90 and FN interact within, or closely associated with, the plasma membrane. An interaction of eHsp90 with FN on the surface of cells, or in the extracellular space associated with FN fibrils, are not mutually exclusive.

In addition to direct association of Hsp90 and FN, loss of extracellular FN matrix upon treatment with novobiocin suggested that FN was a possible "client protein" of Hsp90. Recovery of the FN matrix upon treatment with exogenous Hsp90β, and no apparent change in the FN matrix upon treatment with etoposide, supports the fact that the phenotype was specific to the inhibition of Hsp90. Client proteins of intracellular Hsp90 are defined by their direct association with Hsp90, and their dependence on the interaction with Hsp90 for stability or conformational regulation (Theodoraki & Caplam 2013; Citri et al. 2006; Zuehlke & Johnson 2011). Our data suggested that inhibition of Hsp90 with the small molecule inhibitor, novobiocin, resulted in FN endocytosis and colocalization with LRP-1 in intracellular vesicles. In support of previous findings showing a direct interaction of LRP-1 with FN (Salicioni et al. 2002), LRP-1 colocalized with FN in novobiocin treated MDA-MB-231 and Hs578T cells. This data correlates with reports that showed the constitutive endocytosis of LRP-1 (Wu & Gonias 2005) and LRP-1 dependent endocytic trafficking of FN for intracellular degradation (Sottile & Chandler 2005b). It is possible that enhanced LRP-1 and FN colocalization upon treatment with novobiocin was a result of the destabilization of the FN matrix, and subsequent enhanced FN endocytosis. Previous results in our laboratory showed colocalization of FN with lysosomal markers Rab-5 and LAMP-1 upon treatment with novobiocin. It is well reported that inhibition of Hsp90 with small molecule inhibitors results in proteosomal degradation of "client proteins" via the ubiquitin/proteasome pathway (Theodoraki & Caplam 2013). Moreover, recent studies suggest some membrane proteins are removed from the plasma membrane in a chaperone dependent manner and degraded in lysosomes (Okiyoneda et al. 2012).

Co-chaperones act as key regulators in the maturation of intracellular Hsp90 client proteins (Li & Buchner 2013). Most authors report a role for eHsp90 independent of co-chaperone and ATPase activity, suggesting that eHsp90 does not act as a chaperone extracellularly. eHsp90 associated proteins are thus perhaps better defined as eHsp90 interacting proteins than clients. However, most recently, El Hamidieh and colleagues showed the presence of an eHsp90-Cdc37 complex on the surface of MDA-MB-453 and MDA-MB-231 human breast cancer cells (El Hamidieh et al. 2012). El Hamidieh and colleagues suggested surface Cdc37, the co-chaperone of intracellular kinases, acts as a co-chaperone to eHsp90 in association with protein kinase receptors (El Hamidieh et al. 2012). In addition, Sims and colleagues report an eHsp90 multichaperone complex composed of Hsp70, Hsp40, Hop and p23 in the condition media of MDA-MB-231 breast cancer cells (Sims et al. 2011). Whether eHsp90 fulfils its role in complex with co-chaperones remains to be fully determined. Given the detection of both surface associated and extracellular soluble eHsp90 it is plausible membrane associated eHsp90 acts in complex with co-chaperones whilst soluble eHsp90 acts independently of co-chaperone activity, or vice versa. Our data supported a role for eHsp90 in FN dynamics, however further studies would be required to confirm FN as a "client protein" of Hsp90 as defined by Theodoraki & Caplam (Theodoraki & Caplam 2013).

Previous data in our laboratory showed that geldanamycin had no profound effect on the extracellular FN matrix. Differences in the effects of geldanamycin and novobiocin on the extracellular FN matrix may be explained by the sites at which they bind and their mode of inhibition. Geldanamycin is reported to compete with ATP for binding of the Hsp90 N-terminal ATP binding pocket and inhibit N-terminal dimerization of Hsp90, blocking the formation of the active conformation (Holzbeierlein et al. 2010; Donnelly & Blagg 2009). Novobiocin is reported to bind the C-terminal nucleotide binding pocket of Hsp90, preventing dimerization of Hsp90 (Holzbeierlein et al. 2010). Novobiocin competes with ATP for binding, and association with co-chaperones (e.g. p23) is disrupted by novobiocin (Donnelly & Blagg 2009; Marcu et al. 2000). Differential effects of geldanamycin and novobiocin inhibition of Hsp90 have been reported. Conde and colleagues show geldanamycin and novobiocin have alternate effects for Hsp90 modulated activity of HSF-1 (Conde et al. 2009). In addition, geldanamycin has previously been shown to induce different phenotypes in different cell lines (López-Maderuelo et al. 2001). The fact that geldanamycin showed no effect on the extracellular FN matrix suggested an ATPase independent role for Hsp90 in its interaction with FN; consistent with our findings that binding of Hsp90 to FN

was independent of ATP. Recent development of a novel plasma membrane luciferase probe showed that ATP may reach concentrations up to 80 μM surrounding the plasma membrane of HEK293 cells (Falzoni et al. 2013). Scheibel and colleagues report half-maximal binding of ATP to Hsp90 in the high micromolar range (400 μM) (Scheibel et al. 1997). The concentration of ATP in the extracellular environment is therefore likely to be below the threshold for binding of Hsp90. An ATP-independent role for eHsp90 is not without precedent. The interaction of eHsp90α with MMP-2 was shown to be both isoform-specific and ATP-independent (Song et al. 2010; Sims et al. 2011). The putative extracellular Hsp90N isoform was shown to be functional despite lacking the ATPase domain. Loss of the extracellular FN matrix upon inhibition of Hsp90 with novobiocin suggested the C-terminal domain of Hsp90 may be important in its interaction with FN and may also hint at a requirement for extracellular co-chaperones in this process.

4.3 THE ROLE OF HSP90 AND LRP-1 IN FN MATRIX DYNAMICS

In accordance with a recent report on the correlation of FN expression to metastatic probability, aggressive MDA-MB-231 and Hs578T metastatic breast cancer cells showed high levels of FN expression (Fernandez-Garcia et al. 2013). Hs578T cells showed a denser extracellular FN matrix in comparison to MDA-MB-231 cells. Several factors influence the extent of the extracellular FN matrix surrounding a cell. The adhesion of cells *in vitro* is related to the expression or lack of expression of FN, the polymerization of soluble FN into an extracellular FN matrix surrounding the cells, and the extent to which cells interact with matrix-bound FN (Ruoslahti 1984; Liu et al. 2010). Malignant cells have been shown to retain their FN expression, if they originally possessed it, however usually fail to polymerize soluble FN into an extracellular FN matrix (Ruoslahti 1984; Winters et al. 2006). Cell culture studies also implicate several proteases in the loss of extracellular FN matrix associated with malignant cells (Ruoslahti 1984; Shi & Sottile 2011). A lack of FN matrix in malignant cells has generally been shown to reflect a generalized absence of ECM.

Treatment with novobiocin and inhibition of LRP-1 with a blocking antibody both showed a loss of extracellular FN matrix fibrils surrounding Hs578T cells. FN matrix was recovered upon subsequent addition of exogenous Hsp90β in both experiments. Given the reported binding of Hsp90 to LRP-1 (Basu et al. 2001), and our data demonstrating coimmunoprecipitation of Hsp90 in a FN and LRP-1 containing complex, this data supports a direct role for Hsp90 in LRP-1 mediated FN matrix remodeling. Interestingly, LRP-1

expression was only detected in cell lines (MDA-MB-213 and Hs578T) shown previously to express FN. These data, together with the loss of FN matrix upon treatment with an LRP-1 blocking antibody, suggests a role for LRP-1 in FN matrix dynamics. Salicioni and colleagues previously show that LRP-deficient MEF-2 cells accumulate greatly increased levels of cell surface FN (Salicioni et al. 2004). Evidence showed that eHsp90 binds LRP-1 (Basu et al. 2001) and binding of Hsp90α to LRP-1 has been mapped to a 27-amino acid peptide located at the boundary between the linker region and the middle domain of Hsp90α (Sahu et al. 2012). The binding site of novobiocin has been mapped around the $K^{559}KQEEKK^{564}$ sequence in the C-terminal domain of Hsp90. LRP-1 bound Hsp90 may still permit the binding of novobiocin. Immunoprecipitation of LRP-1 showed the presence of low (70 kDa) and high molecular weight FN fragments (> 120 kDa) in complex with LRP-1 and Hsp90 in both untreated and novobiocin treated Hs578T cells. Use of a cell impermeable cross-linker enhanced for complexes containing extracellular FN. SPR spectroscopy showed that Hsp90 was able to interact with the N terminal FN fragment, FN70. Given the specific cleavage of FN by MMPs and other extracellular proteases (reviewed in Hynes, 1990; Mosher, 2012), we proposed that the FN70 fragment observed in our study may be the functional 70 kDa N-terminal assembly fragment of FN (FN70). FN70 has been shown to play a fundamental role in the assembly of FN (Schwarzbauer & Sechler 1999; McKeown-Longo & Mosher 1985; Aguirre et al. 1994; Wierzbicka-Patynowski & Schwarzbauer 2003). A change in the level of different FN fragments in the LRP-1 complex upon treatment with novobiocin when compared to treatment with eHsp90β suggested that Hsp90 may play a role in FN matrix turnover in complex with LRP-1 and FN. Xu & Mosher suggested that FN70 binds to cell surface receptors initiating a conformational unfolding of FN, exposing the RGD motif in module III_{10} for binding with cell surface integrins and subsequent fibrillogenesis (Xu & Mosher 2011). LRP-1 may be a receptor for binding of FN70. Inhibition of Hsp90 may prevent binding of FN70 to LRP-1 and altered fibrillogenesis may account for loss of the FN matrix upon treatment with novobiocin. Loss of FN matrix upon treatment with LRPab supports a role for LRP-1 mediated FN fibrillogenesis. Hsp90β induced recovery of the FN matrix following treatment with LRPab supports a role for the possible "chaperoning" of FN or even FN70 to LRP-1 and subsequent fibrillogenesis. Immunoprecipitation of LRP-1 complexes following treatment with LRPab, with and without the addition of exogenous Hsp90β, would further define the binding of FN70 to LRP-1 and the role of Hsp90 in this process.

A wide range of extracellular proteases have been implicated in the degradation of FN (Berry et al. 1998; Zhang et al. 2012): these include plasmin and urokinase-type plasminogen activator (uPA) (Gold et al. 1989; Bonnefoy & Legrand 2000), matrix metalloproteinases MTI-MMP1 (Shi & Sottile 2011), MMP1, MMP3, MMP13 and MMP14 (Zhang et al. 2012). We speculate that the FN fragments observed in the Hsp90 treated whole cell lysates may have arisen from the proteolytic cleavage of FN by MMPs or other proteases in the extracellular space. Interestingly, there was a loss of FN fragments in the LRP-1 immunoprecipitate from eHsp90β treated cells, despite the fact that higher levels of lower molecular weight FN fragments were detected in this cell lysate compared to the other treatments. An increase in FN120+ in the LRP-1 immunoprecipitate upon treatment with novobiocin suggested treatment with novobiocin enhanced binding of proteolytic fragments (FN120+) to LRP-1. Several reports show a role for Hsp90 in both up-regulation of MMP transcript and MMP activation (Hance et al. 2012; Correia et al. 2013; Stellas et al. 2010). Inhibition of Hsp90 with novobiocin may alter the expression levels of extracellular MMPs or other proteases. Treatment with a monoclonal antibody against Hsp90 (MAb 4C5) has been shown to inhibit the activation of MMP2 and MMP9 (Stellas et al. 2010). Moreover, our results show that exogenous Hsp90β decreased the level of low and high molecular weight FN fragments in a complex with LRP-1. Treatment with exogenous Hsp90β appeared to reduce binding of FN species to LRP-1 to below that of the non-specific binding of FN to the beads alone. Whether this was a measure of a true result or a technical artifact could not be determined. Interestingly, proteolytically inactive pro-cathepsin D has been reported to bind extracellular residues 349-394 of the 85 kDa transmembrane β chain of LRP-1 (Beaujouin et al. 2010). Proteolytic digestion of FN with cathepsin D results in a FN70 proteolytic fragment (Pankov 2002) and pro-cathepsin D is overexpressed and highly secreted in breast cancer cells (Beaujouin et al. 2010). The proteolytic activity of cathepsin D in the extracellular space, or closely associated with the membrane is questionable (Beaujouin et al. 2010). However, Laurent-Matha and colleagues suggest that cathepsin D may self-activate in cancer cells due to a lower pH in tumor microenvironments (Laurent-Matha et al. 2012). Cathepsin D is partly endocytosed by LRP-1 (Derocq et al. 2012) and has been shown to digest ECM in large acidic vesicles in breast cancer cells (Montcourrier et al. 1990). These large acidic vesicles show a similar phenotype to those identified in novobiocin treated MDA-MB-231 and Hs578T cells. Further study of the role of extracellular proteases in the breakdown of FN matrix would clarify some highlighted points.

Two molecular mechanisms are believed to be involved in the degradation and turnover of ECM proteins: extracellular degradation of ECM proteins by proteases; and internalization of ECM proteins and intracellular degradation in lysosomes (Shi & Sottile 2009). These molecular mechanisms are not mutually exclusive and are believed to act collaboratively in the turnover of ECM proteins (Shi & Sottile 2009). Our data may suggest a dual role for Hsp90 in both the extracellular degradation and LRP-1 mediated turnover of FN. Following secretion of FN, eHsp90 may play a crucial role in the maturation of MMP proteins. Active MMP2 and other MMP proteins may proteolytically cleave FN into degradation products, which include FN70. Hsp90 coordinated binding of FN70 to LRP-1 may stimulate subsequent FN fibrillogenesis either directly at LRP-1 or an alternative site. Kenny and colleagues show that MMP2 increased adhesive capability of ovarian cancer cells by specific cleavage of FN (120 and 70 kDa fragments) allowing for enhanced attachment to FN through α5β1 and αVβ3 integrin (Kenny et al. 2008). Loss of FN70 in complex with LRP-1 upon treatment with exogenous Hsp90β may result from a negative feedback mechanism in the regulation of FN matrix assembly. Negative feedback mechanisms associated with the FN matrix have been described previously (Orr et al. 2006). It is reasonable to consider that a negative feedback mechanism would be required to regulate the extracellular FN matrix.

Hsp90 was found in complex with LRP-1 in untreated, novobiocin treated and exogenous Hsp90β treated Hs578T cells. Several authors suggest a role for eHsp90α in LRP-1 receptor mediated signaling (Woodley et al. 2009; Chieh-Fang Cheng et al. 2008b; Sahu et al. 2012). eHsp90α induces activity of ERK, PI3K/Akt and NF-κB p65 and possible others (Chen et al. 2010; Gopal et al. 2011). It is possible that loss of the FN matrix upon treatment with novobiocin was a result of altered LRP-1 signaling and downstream pathways that regulate FN matrix assembly. In support of this, Somanath and colleagues show Akt1 signaling to regulate integrin activation and FN matrix assembly (Somanath et al. 2007). However, Green and colleagues later showed that expression of constitutively active Akt-1 in W775A β1 integrin mutant GD25 cells defective in Akt-1 signaling did not reverse defective FN fibrillogenesis (Green et al. 2009). They however suggest talin recruitment to an intact β1 integrin may be required for Akt-1 regulated FN matrix assembly (Green et al. 2009). Chen and colleagues show Hsp90α induced LRP-1 signaling results in NF-κB mediated TCF12 expression and similarly FN expression (Chen et al. 2013). Loss of FN matrix upon treatment with novobiocin may in part be a result of reduced FN expression. In contrast to these former suggestions, most notably, no reports to date show a role for Hsp90β in LRP-1 signaling.

Moreover, Li and colleagues state that Hsp90β has no effect on LRP-1 mediated cell migration (Wei Li – personal communication, CSSI VI International Congress on Stress Proteins in Biology and Medicine 2013). A comparison of the downstream pathways activated by eHsp90α and eHsp90β stimulated LRP-1 signaling would expound these suggestions.

Given the complexity of FN matrix synthesis, fibrillogenesis and endocytosis, and dynamics of FN turnover, it is possible some of the effects of novobiocin on the FN matrix are indirect of the LRP-1 complex and/or due to effects of other Hsp90 clients. Adverse effects of Hsp90 inhibition on the secretory pathway have been reported (Lotz et al. 2008; Chen & Balch 2006). These reports are however limited in their study to N-terminal specific Hsp90 inhibitors, of which, geldanamycin was shown to have no effect on the FN matrix. No studies to date show the effect of Hsp90 C-terminal inhibitors on the secretory pathway of proteins. Several reports show a role for Hsp90 in integrin (Luo et al. 2011; Liu et al. 2011) and actin (Koyasu et al. 1986; Chaturvedi & Sreedhar 2010) function. In addition, inhibition of Hsp90 in the PC3 prostate cancer line led to reduced adhesion between FN and the β_1-integrin (Liu et al. 2011). Loss of FN matrix upon treatment with novobiocin may be a result of reduced FN fibrillogenesis brought about by altered FN-integrin interactions or altered cytoskeletal arrangements. In addition to actin and cell surface integrins, FN fibrillogenesis may be dependent upon other proteins, some of which may be Hsp90 client proteins.

4.4 CONCLUSION

Only a handful of eHsp90 interacting proteins have been defined. Herein, we provide the first evidence of a direct *in vitro* interaction between Hsp90 and FN. Given the direct binding of Hsp90 to FN *in vitro*, colocalization of Hsp90 with FN fibrils, and loss of FN matrix upon treatment with novobiocin, our data suggests a more direct role for Hsp90 in stability of the FN matrix. The loss of FN matrix upon treatment with an LRP-1 blocking antibody suggests a role for LRP-1 in FN matrix dynamics, possibly other than that in FN endocytosis. Given the recovery of FN matrix of Hs578T cells treated with LRP-1 blocking antibody upon addition of exogenous Hsp90β and the immunoprecipitation of an LRP-1 complex containing Hsp90 and FN fragments, we suggest that Hsp90 plays a direct role in FN matrix dynamics through interaction with FN and LRP-1. We suggest a dual interaction of Hsp90 with MMPs and in a complex with LRP-1 and the FN70 fragment as a possible regulator of FN matrix

dynamics. Further definition of the role of LRP-1 and FN70 in FN matrix assembly are required to confirm these hypotheses.

CHAPTER 5: REFERENCES

Aguirre, K.M., McCormick, R.J. & Schwarzbauer, J.E., 1994. Fibronectin self-association is mediated by complementary sites within the amino-terminal one-third of the molecule. *The Journal of biological chemistry*, 269(45), pp.27863–8. Available at: http://www.ncbi.nlm.nih.gov/pubmed/7961716.

Akiyama, S.K., Olden, K. & Yamada, K.M., 1995. Fibronectin and integrins in invasion and metastasis. *Cancer metastasis reviews*, 14(3), pp.173–89. Available at: http://www.ncbi.nlm.nih.gov/pubmed/8548867 [Accessed April 22, 2013].

Ali, J. a et al., 1993. The 43-kilodalton N-terminal fragment of the DNA gyrase B protein hydrolyzes ATP and binds coumarin drugs. *Biochemistry*, 32(10), pp.2717–2724. Available at: http://www.ncbi.nlm.nih.gov/pubmed/8383523.

Allan, R.K. et al., 2006. Modulation of chaperone function and cochaperone interaction by novobiocin in the C-terminal domain of Hsp90: evidence that coumarin antibiotics disrupt Hsp90 dimerization. *The Journal of Biological Chemistry*, 281(11), pp.7161–7171. Available at: http://www.ncbi.nlm.nih.gov/pubmed/16421106 [Accessed March 29, 2013].

Amolins, M. & Blagg, B.S.J., 2009. Natural Product Inhibitors of Hsp90: Potential Leads for Drug Discovery. *Mini Rev Med Chem*, 9(2), pp.140–152.

Anton, E.S. et al., 1994. Nerve growth factor and its low-affinity receptor promote Schwann cell migration. *Proceedings of the National Academy of Sciences of the United States of America*, 91(7), pp.2795–9. Available at: http://www.pubmedcentral.nih.gov/articlerender.fcgi?artid=43457&tool=pmcentrez&rendertype=abstract.

Bagatell, R. & Whitesell, L., 2004. Altered Hsp90 function in cancer : A unique therapeutic opportunity. *Mol Cancer Ther*, 3, pp.1021–1030.

Baron, M. et al., 1990. Structure of the fibronectin type 1 module. *Nature*, 345(6276), pp.642–6. Available at: http://www.ncbi.nlm.nih.gov/pubmed/2112232 [Accessed November 29, 2013].

Basu, S. et al., 2001. CD91 is a common receptor for heat shock proteins gp96, hsp90, hsp70, and calreticulin. *Immunity*, 14(3), pp.303–13. Available at: http://www.ncbi.nlm.nih.gov/pubmed/11290339.

Baugh, L. & Vogel, V., 2004. Structural changes of fibronectin adsorbed to model surfaces probed by fluorescence resonance energy transfer. *Journal of Biomedical Materials Research Part A*, 69(3), pp.525–534. Available at: http://www.ncbi.nlm.nih.gov/pubmed/15127399 [Accessed April 12, 2013].

Beaujouin, M. et al., 2010. Pro-cathepsin D interacts with the extracellular domain of the beta chain of LRP1 and promotes LRP1-dependent fibroblast outgrowth. *Journal of cell science*, 123(Pt 19), pp.3336–46. Available at: http://www.pubmedcentral.nih.gov/articlerender.fcgi?artid=2964349&tool=pmcentrez&rendertype=abstract [Accessed November 27, 2013].

Becker, B. et al., 2004. Induction of Hsp90 protein expression in malignant melanomas and melanoma metastases. *Experimental dermatology*, 13(1), pp.27–32. Available at: http://www.ncbi.nlm.nih.gov/pubmed/15009113.

Bendas, G. & Borsig, L., 2012. Cancer cell adhesion and metastasis: selectins, integrins, and the inhibitory potential of heparins. *International journal of cell biology*, 2012, p.676731. Available at: http://www.pubmedcentral.nih.gov/articlerender.fcgi?artid=3296185&tool=pmcentrez&rendertype=abstract [Accessed November 21, 2013].

Berry, H. et al., 1998. Proteolysis of Aggregated Fibronectin A Model for In Vivo Matrix Degradation. *Annals of the New York Academy of Sciences*, 864, pp.198–202.

Binder, R.J., Blachere, N.E. & Srivastava, P.K., 2001. Heat shock protein-chaperoned peptides but not free peptides introduced into the cytosol are presented efficiently by MHC I molecules. *The Journal of biological chemistry*, 276, pp.17163–17171.

Binder, R.J. & Srivastava, P.K., 2004. Essential role of CD91 in re-presentation of gp96-chaperoned peptides. *Proceedings of the National Academy of Sciences of the United States of America*, 101(16), pp.6128–33. Available at: http://www.pnas.org/content/101/16/6128.full [Accessed March 15, 2014].

Bonnefoy, A. & Legrand, C., 2000. Proteolysis of subendothelial adhesive glycoproteins (fibronectin, thrombospondin, and von Willebrand factor) by plasmin, leukocyte cathepsin G, and elastase. *Thrombosis research*, 98(4), pp.323–32. Available at: http://www.ncbi.nlm.nih.gov/pubmed/10822079 [Accessed November 23, 2013].

Bradford, M.M., 1976. A rapid and sensitive method for the quantitation of microgram quantities of protein utilizing the principle of protein-dye binding. *Analytical Biochemistry*, 72(1), pp.248–254. Available at: http://www.sciencedirect.com/science/article/pii/0003269776905273 [Accessed December 10, 2013].

Brenner, K.A., Corbett, S.A. & Schwarzbauer, J.E., 2000. Regulation of fibronectin matrix assembly by activated Ras in transformed cells. *Onco*, 19, pp.3156–3163.

Bretscher, M.S., 1992. Circulating integrins: alpha 5 beta 1, alpha 6 beta 4 and Mac-1, but not alpha 3 beta 1, alpha 4 beta 1 or LFA-1. *The EMBO journal*, 11(2), pp.405–10. Available at: http://www.pubmedcentral.nih.gov/articlerender.fcgi?artid=556468&tool=pmcentrez&rendertype=abstract [Accessed November 23, 2013].

Bretscher, M.S., 1989. Endocytosis and recycling of the fibronectin receptor in CHO cells. *The EMBO Journal*, 8(5), pp.1341–1348.

Caplan, A.J., Mandal, A.K. & Theodoraki, M. a, 2007. Molecular chaperones and protein kinase quality control. *Trends in cell biology*, 17(2), pp.87–92. Available at: http://www.ncbi.nlm.nih.gov/pubmed/17184992 [Accessed December 11, 2013].

Carraher, C.L. & Schwarzbauer, J.E., 2013. Regulation of matrix assembly through rigidity-dependent fibronectin conformational changes. *The Journal of biological chemistry*, 288(21), pp.14805–14. Available at: http://www.jbc.org/content/288/21/14805 [Accessed November 7, 2013].

Carrello, A., 1999. The Common Tetratricopeptide Repeat Acceptor Site for Steroid Receptor-associated Immunophilins and Hop Is Located in the Dimerization Domain of Hsp90. *Journal of Biological Chemistry*, 274(5), pp.2682–2689. Available at: http://www.jbc.org/content/274/5/2682.long [Accessed December 9, 2013].

Chadli, A., Felts, S.J. & Toft, D.O., 2008. GCUNC45 is the first Hsp90 co-chaperone to show alpha/beta isoform specificity. *The Journal of biological chemistry*, 283(15), pp.9509–12. Available at: http://www.pubmedcentral.nih.gov/articlerender.fcgi?artid=2442279&tool=pmcentrez&rendertype=abstract [Accessed November 21, 2013].

Chaturvedi, V. & Sreedhar, a S., 2010. Hsp90 inhibition induces destabilization of actin cytoskeleton in tumor cells: functional significance of Hsp90 interaction with F-actin. *Asian Pacific Journal of Tropical Medicine*, 3(9), pp.715–722. Available at: http://linkinghub.elsevier.com/retrieve/pii/S1995764510601721 [Accessed April 12, 2013].

Chaudhury, S., Welch, T.R. & Blagg, B.S.J., 2006. Hsp90 as a target for drug development. *ChemMedChem*, 1(12), pp.1331–40. Available at: http://www.ncbi.nlm.nih.gov/pubmed/17066389 [Accessed November 19, 2013].

Chen, C.Y. & Balch, W.E., 2006. The Hsp90 Chaperone Complex Regulates GDI-dependent Rab Recycling. *Molecular Biology of the cell*, 17(August), pp.3494–3507.

Chen, J.-S. et al., 2010. Secreted Heat Shock Protein 90α Induces Colorectal Cancer Cell Invasion through CD91/LRP-1 and NF-κB-mediated Integrin αV Expression. *The Journal of Biological Chemistry*, 285(33), pp.25458–25466. Available at: http://www.pubmedcentral.nih.gov/articlerender.fcgi?artid=2919109&tool=pmcentrez&rendertype=abstract [Accessed March 14, 2013].

Chen, S. et al., 1998. Differential interactions of p23 and the TPR-containing proteins Hop, Cyp40, FKBP52 and FKBP51 with Hsp90 mutants. *Cell stress & chaperones*, 3(2), pp.118–29. Available at: http://www.pubmedcentral.nih.gov/articlerender.fcgi?artid=312955&tool=pmcentrez&rendertype=abstract [Accessed December 9, 2013].

Chen, W.-S. et al., 2013. Secreted Heat Shock Protein 90α Induces NF-κB-Mediated TCF12 Expression to Down-Regulate E-Cadherin and Enhance Cell Migration and Invasion in Colorectal Cancer Cells. *The Journal of biological chemistry*, 288(13), pp.9001–9010. Available at: http://www.ncbi.nlm.nih.gov/pubmed/23386606 [Accessed March 10, 2013].

Cheng, C. et al., 2011. A fragment of secreted Hsp90 α carries properties that enable it to accelerate effectively both acute and diabetic wound healing in mice. *The Journal of Clinical Investigation*, 121(11), pp.4348–4361.

Cheng, C.-F. et al., 2008. Transforming Growth Factor (TGF)-Stimulated Secretion of HSP90 : Using the Receptor LRP-1/CD91 To Promote Human Skin Cell Migration against a TGF -Rich Environment during Wound Healing. *Molecular and Cellular Biology*, 28(10), pp.3344–3358. Available at: http://mcb.asm.org/cgi/doi/10.1128/MCB.01287-07 [Accessed November 12, 2013].

Cheng, C.-F. et al., 2008a. Transforming growth factor alpha (TGFalpha)-stimulated secretion of HSP90alpha: using the receptor LRP-1/CD91 to promote human skin cell migration against a TGFbeta-rich environment during wound healing. *Molecular and cellular biology*, 28(10), pp.3344–58. Available at: http://www.pubmedcentral.nih.gov/articlerender.fcgi?artid=2423165&tool=pmcentrez&rendertype=abstract [Accessed August 21, 2013].

Cheng, C.-F. et al., 2008b. Transforming Growth Factor α (TGFα)-Stimulated Secretion of HSP90α: Using the Receptor LRP-1/CD91 To Promote Human Skin Cell Migration against a TGFβ-Rich Environment during Wound Healing. *Molecular and Cellular Biology*, 28(10), pp.3344–3358. Available at: http://www.pubmedcentral.nih.gov/articlerender.fcgi?artid=2423165&tool=pmcentrez&rendertype=abstract [Accessed March 4, 2013].

Chiosis, G. et al., 2003. 17AAG : Low Target Binding Affinity and Potent Cell Activity −− Finding an Explanation 1 17AAG : Low Target Binding Affinity and Potent Cell Activity — Finding an Explanation 1. , pp.123–129.

Christensen, L., 1992. The distribution of fibronectin, laminin and tetranectin in human breast cancer with special attention to the extracellular matrix. *APMIS. Supplementum*, 26, pp.1–39. Available at: http://www.ncbi.nlm.nih.gov/pubmed/1576006 [Accessed November 25, 2013].

Chung, S.-W. et al., 2009. Extracellular heat shock protein 90 induces interleukin-8 in vascular smooth muscle cells. *Biochemical and biophysical research communications*, 378(3), pp.444–9. Available at: http://www.ncbi.nlm.nih.gov/pubmed/19028451 [Accessed December 5, 2013].

Cid, C. et al., 2004. Antibodies reactive to heat shock protein 90 induce oligodendrocyte precursor cell death in culture. Implications for demyelination in multiple sclerosis. *FASEB journal : official publication of the Federation of American Societies for Experimental Biology*, 18(2), pp.409–11. Available at: http://www.ncbi.nlm.nih.gov/pubmed/14688203.

Citri, A. et al., 2006. Hsp90 recognizes a common surface on client kinases. *The Journal of Biological Chemistry*, 281(20), pp.14361–14369. Available at: http://www.ncbi.nlm.nih.gov/pubmed/16551624 [Accessed April 12, 2013].

Conde, R. et al., 2009. Modulation of Hsf1 activity by novobiocin and geldanamycin. *Biochemistry and cell biology = Biochimie et biologie cellulaire*, 87(6), pp.845–51. Available at: http://www.ncbi.nlm.nih.gov/pubmed/19935870 [Accessed November 22, 2013].

Correia, A.L. et al., 2013. The hemopexin domain of MMP3 is responsible for mammary epithelial invasion and morphogenesis through extracellular interaction with HSP90 b. *Genes and Development*, 27, pp.805–817.

Crossman, D. & Nicchitta, C., 2007. Extracellular Functions for an Intracellular Protein: GRP94/GP96 Interactions with the Mammalian Immune System. In A. A. A. Asea & A. De Maio, eds. *Heat Shock Proteins: Potent Mediators of Inflammation and Immunity*. Heat Shock Proteins. Dordrecht: Springer Netherlands, pp. 147–158. Available at: http://www.springerlink.com/index/10.1007/978-1-4020-5585-0 [Accessed December 13, 2013].

Csermely, P. et al., 1998. The 90-kDa Molecular Chaperone Family : Structure , Function , and Clinical Applications . A Comprehensive Review. *Pharmacol. Ther.*, 79(2), pp.129–168.

Dallas, S.L. et al., 2005. Fibronectin regulates latent transforming growth factor-beta (TGF beta) by controlling matrix assembly of latent TGF beta-binding protein-1. *The Journal of biological chemistry*, 280(19), pp.18871–80. Available at: http://www.ncbi.nlm.nih.gov/pubmed/15677465 [Accessed November 18, 2013].

Dallas, S.L., Chen, Q. & Sivakumar, P., 2006. Dynamics of assembly and reorganization of extracellular matrix proteins. *Current topics in developmental biology*, 75, pp.1–24. Available at: http://www.ncbi.nlm.nih.gov/pubmed/16984808 [Accessed November 18, 2013].

Derocq, D. et al., 2012. Cathepsin D is partly endocytosed by the LRP1 receptor and inhibits LRP1-regulated intramembrane proteolysis. *Oncogene*, 31(26), pp.3202–12. Available at: http://www.pubmedcentral.nih.gov/articlerender.fcgi?artid=3579766&tool=pmcentrez&rendertype=abstract [Accessed December 12, 2013].

Dickinson, C.D. et al., 1994. Crystal structure of the tenth type III cell adhesion module of human fibronectin. *Journal of molecular biology*, 236(4), pp.1079–92. Available at: http://www.ncbi.nlm.nih.gov/pubmed/8120888 [Accessed November 29, 2013].

Didelot, C. et al., 2007. Anti-cancer therapeutic approaches based on intracellular and extracellular heat shock proteins. *Current medicinal chemistry*, 14(27), pp.2839–47. Available at: http://www.ncbi.nlm.nih.gov/pubmed/18045130 [Accessed November 28, 2013].

Didenko, T. et al., 2012. Hsp90 structure and function studied by NMR spectroscopy. *Biochimica et biophysica acta*, 1823(3), pp.636–47. Available at: http://www.ncbi.nlm.nih.gov/pubmed/22155720 [Accessed May 23, 2013].

Donnelly, A. & Blagg, B.S.J., 2009. Novobiocin and Additional Inhibitors of the Hsp90 C-Terminal Nucleotide-binding Pocket. *Current medicinal chemistry*, 15(26), pp.2702–2717. Available at: http://www.ncbi.nlm.nih.gov/pubmed/18554561.

Donnelly, A. & Blagg, B.S.J., 2008. Novobiocin and additional inhibitors of the Hsp90 C-terminal nucleotide-binding pocket. *Current medicinal chemistry*, 15(26), pp.2702–17. Available at: /pmc/articles/PMC2729083/?report=abstract [Accessed April 16, 2013].

Dustin, M.L. et al., 1997. Low affinity interaction of human or rat T cell adhesion molecule CD2 with its ligand aligns adhering membranes to achieve high physiological affinity. *The Journal of biological chemistry*, 272(49), pp.30889–98. Available at: http://www.ncbi.nlm.nih.gov/pubmed/9388235 [Accessed April 18, 2013].

Dutta, R. & Inouye, M., 2000. GHKL, an emergent ATPase/kinase superfamily. *Trends in biochemical sciences*, 25(1), pp.24–8. Available at: http://www.ncbi.nlm.nih.gov/pubmed/10637609 [Accessed November 28, 2013].

Echtenkamp, F.J. & Freeman, B.C., 2012. Expanding the cellular molecular chaperone network through the ubiquitous cochaperones. *Biochimica et biophysica acta*, 1823(3), pp.668–73. Available at: http://www.ncbi.nlm.nih.gov/pubmed/21889547 [Accessed December 11, 2013].

Ellis, I.R. et al., 2010. Migration Stimulating Factor (MSF) promotes fibroblast migration by inhibiting AKT. *Cellular signalling*, 22(11), pp.1655–9. Available at: http://www.ncbi.nlm.nih.gov/pubmed/20600851 [Accessed November 27, 2013].

Erickson, H.P., 2002. Stretching fibronectin. *Journal of muscle research and cell motility*, 23(5-6), pp.575–80. Available at: http://www.ncbi.nlm.nih.gov/pubmed/12785106.

Erickson, H.P., Carrell, N. & McDonagh, J., 1981. Fibronectin molecule visualized in electron microscopy: a long, thin, flexible strand. *The Journal of Cell Biology*, 91(3), pp.673–678. Available at: http://www.pubmedcentral.nih.gov/articlerender.fcgi?artid=2112785&tool=pmcentrez&rendertype=abstract.

Etique, N. et al., 2013. LRP-1: a checkpoint for the extracellular matrix proteolysis. *BioMed research international*, 2013, p.152163. Available at: http://www.pubmedcentral.nih.gov/articlerender.fcgi?artid=3723059&tool=pmcentrez&rendertype=abstract.

Eustace, B.K. et al., 2004. Functional proteomic screens reveal an essential extracellular role for hsp90 alpha in cancer cell invasiveness. *Nature Cell Biology*, 6(6), pp.507–514. Available at: http://www.ncbi.nlm.nih.gov/pubmed/15146192 [Accessed March 5, 2013].

Eustace, B.K. & Jay, D.G., 2004. Extracellular Roles for the Molecular Chaperone, hsp90. *Cell Cycle*, 3(9), pp.1098–1100. Available at: http://www.ncbi.nlm.nih.gov/pubmed/15190213.

Falzoni, S., Donvito, G. & Virgilio, F. Di, 2013. Detecting adenosine triphosphate in the pericellular space. *Interface Focus*, 3(April), pp.1–8.

Fernandez-Garcia, B. et al., 2013. Expression and prognostic significance of Fibronectin and Matrix Metalloproteases in breast cancer metastasis. *Histopathology*. Available at: http://www.ncbi.nlm.nih.gov/pubmed/24117661 [Accessed November 25, 2013].

Ferrarini, M. et al., 1992. Unusual expression and localization of heat-shock proteins in human tumor cells. *International journal of cancer. Journal international du cancer*, 51(4), pp.613–9. Available at: http://www.ncbi.nlm.nih.gov/pubmed/1601523 [Accessed November 18, 2013].

Frantz, C., Stewart, K.M. & Weaver, V.M., 2010. The extracellular matrix at a glance. *Journal of cell science*, 123(Pt 24), pp.4195–200. Available at: http://www.pubmedcentral.nih.gov/articlerender.fcgi?artid=2995612&tool=pmcentrez&rendertype=abstract [Accessed November 7, 2013].

Friedl, P., Zanker, K.S. & Brocker, E.-B., 1998. Cell Migration Strategies in 3-D Extracellular Matrix : Differences in Morphology , Cell Matrix Interactions , and Integrin Function. *Microscopy Research and Technique*, 378, pp.369–378.

Fulda, S. et al., 2010. Cellular stress responses: cell survival and cell death. *International journal of cell biology*, 2010, p.214074. Available at: http://www.pubmedcentral.nih.gov/articlerender.fcgi?artid=2825543&tool=pmcentrez&rendertype=abstract [Accessed November 20, 2013].

Garnier, C. et al., 2002. Binding of ATP to heat shock protein 90: evidence for an ATP-binding site in the C-terminal domain. *The Journal of Biological Chemistry*, 277(14), pp.12208–12214. Available at: http://www.ncbi.nlm.nih.gov/pubmed/11805114 [Accessed March 22, 2013].

Gaultier, A. et al., 2011. LRP1 regulates remodeling of the extracellular matrix by fibroblasts. *Matrix biology*, 29(1), pp.1–19.

Gee, E.P.S. et al., 2013. SLLISWD sequence in the 10FNIII domain initiates fibronectin fibrillogenesis. *The Journal of biological chemistry*, 288(29), pp.21329–40. Available at: http://www.ncbi.nlm.nih.gov/pubmed/23740248 [Accessed December 2, 2013].

Gold, L., Schwimmer & Quigley, J., 1989. Human plasma fibronectin as a substrate for human urokinase. *Biochemistry Journal*, 262, pp.529–534. Available at: http://www.biochemj.org/bj/262/bj2620529.htm [Accessed November 23, 2013].

Gopal, U. et al., 2011. A novel extracellular Hsp90 mediated co-receptor function for LRP1 regulates EphA2 dependent glioblastoma cell invasion. *PloS one*, 6(3), p.e17649. Available at: http://www.ncbi.nlm.nih.gov/pubmed/21408136 [Accessed November 26, 2013].

Grammatikakis, N. et al., 2002. The role of Hsp90N, a new member of the Hsp90 family, in signal transduction and neoplastic transformation. *The Journal of biological chemistry*, 277(10), pp.8312–20. Available at: http://www.ncbi.nlm.nih.gov/pubmed/11751906 [Accessed March 5, 2013].

Green, J.A. et al., 2009. beta1 integrin cytoplasmic domain residues selectively modulate fibronectin matrix assembly and cell spreading through talin and Akt-1. *The Journal of biological chemistry*, 284(12), pp.8148–59. Available at: http://www.pubmedcentral.nih.gov/articlerender.fcgi?artid=2658108&tool=pmcentrez&rendertype=abstract [Accessed December 12, 2013].

El Hamidieh, A., Grammatikakis, N. & Patsavoudi, E., 2012. Cell surface Cdc37 participates in extracellular HSP90 mediated cancer cell invasion. *PloS one*, 7(8), p.e42722. Available at: http://www.pubmedcentral.nih.gov/articlerender.fcgi?artid=3422348&tool=pmcentrez&rendertype=abstract [Accessed April 12, 2013].

Hance, M.W. et al., 2012. Secreted Hsp90 is a novel regulator of the epithelial to mesenchymal transition (EMT) in prostate cancer. *The Journal of biological chemistry*, 287(45), pp.37732–44. Available at: http://www.ncbi.nlm.nih.gov/pubmed/22989880 [Accessed March 20, 2013].

Hande, K.R., 1998. Clinical Oncology Update Etoposide : Four Decades of Development of a Topoisomerase II Inhibitor. , 34(10), pp.1514–1521.

Hartl, F.U. & Hayer-Hartl, M., 2002. Molecular chaperones in the cytosol: from nascent chain to folded protein. *Science (New York, N.Y.)*, 295(5561), pp.1852–8. Available at: http://www.ncbi.nlm.nih.gov/pubmed/11884745 [Accessed November 12, 2013].

Hegmans, J.P.J.J. et al., 2004. Proteomic analysis of exosomes secreted by human mesothelioma cells. *The American journal of pathology*, 164(5), pp.1807–15. Available at: http://www.pubmedcentral.nih.gov/articlerender.fcgi?artid=1615654&tool=pmcentrez&rendertype=abstract.

Hendrick, J.P. & Hartl, F.-U., 1995. The role of molecular chaperones in protein folding. *The FASEB Journal*, 9(December), pp.1559–1569.

Herz, J. et al., 1991. 39-kDa protein modulates binding of ligands to low density lipoprotein receptor-related protein/alpha 2-macroglobulin receptor. *The Journal of biological chemistry*, 266(31), pp.21232–8. Available at: http://www.ncbi.nlm.nih.gov/pubmed/1718973.

Holzbeierlein, J.M., Windsperger, A. & Vielhauer, G., 2010. Hsp90: a drug target? *Current Oncology Reports*, 12(2), pp.95–101. Available at: http://www.ncbi.nlm.nih.gov/pubmed/20425593 [Accessed March 20, 2013].

Hou, J. & Wang, L., 2012. FKBP5 as a selection biomarker for gemcitabine and Akt inhibitors in treatment of pancreatic cancer. *PloS one*, 7(5), p.e36252. Available at: http://www.pubmedcentral.nih.gov/articlerender.fcgi?artid=3348935&tool=pmcentrez&rendertype=abstract [Accessed September 2, 2013].

Hu, M. et al., 2004. EphA2 Induction of Fibronectin Creates a Permissive Microenvironment for Malignant Cells 1 1 MedImmune , Inc ., American Cancer Society , NIH / National

Cancer Institute Molecular Targeting and Drug Design Program , and U . S . Army Medical Research Acqui. *Molecular cancer research MCR*, 2, pp.533–540.

Humphries, M.J. et al., 1989. Role of Fibronectin in Adhesion, Migration, and Metastasis. *Cancer Investigation*, 7(4), pp.373–93. Available at: http://informahealthcare.com/doi/abs/10.3109/07357908909039866 [Accessed November 21, 2013].

Hunter, M.C., 2011. *Development of an assay for the identification of compounds that bind Hsp90*. Rhodes University.

Hynes, R.O., 1990. *Fibronectins*, Springer-Verlag. Available at: http://books.google.co.za/books/about/Fibronectins.html?id=Xu9qAAAAMAAJ&pgis=1 [Accessed November 27, 2013].

Hynes, R.O., 2009. The extracellular matrix: not just pretty fibrils. *Science (New York, N.Y.)*, 326(5957), pp.1216–9. Available at: http://www.pubmedcentral.nih.gov/articlerender.fcgi?artid=3536535&tool=pmcentrez&rendertype=abstract [Accessed November 7, 2013].

Jarvelainen, H. et al., 2009. Extracellular Matrix Molecules : Potential Targets in. *Pharmacological Reviews*, 61(2), pp.198–223.

Jia, D. et al., 2010. Development of a highly metastatic model that reveals a crucial role of fibronectin in lung cancer cell migration and invasion. *BMC Cancer*, 10(364), pp.1–12.

Johnson, B.D. et al., 2000. Hsp90 chaperone activity requires the full-length protein and interaction among its multiple domains. *The Journal of biological chemistry*, 275(42), pp.32499–507. Available at: http://www.jbc.org/content/275/42/32499.full [Accessed November 15, 2013].

Johnson, J.L., 2012. Evolution and function of diverse Hsp90 homologs and cochaperone proteins. *Biochimica et biophysica acta*, 1823(3), pp.607–13. Available at: http://www.ncbi.nlm.nih.gov/pubmed/22008467 [Accessed November 12, 2013].

Kamal, A. et al., 2003. A high-affinity conformation of Hsp90 confers tumour selectivity on Hsp90 inhibitors. *Nature*, 425(6956), pp.407–10. Available at: http://www.ncbi.nlm.nih.gov/pubmed/14508491 [Accessed November 20, 2013].

Kenny, H.A. et al., 2008. The initial steps of ovarian cancer cell metastasis are mediated by MMP-2 cleavage of vitronectin and fibronectin. *The Journal of Clinical Investigation*, 118(4), pp.1367–1379.

Khalil, A. a et al., 2011. Heat shock proteins in oncology: Diagnostic biomarkers or therapeutic targets? *Biochimica et Biophysica Acta*, 1816(2), pp.89–104. Available at: http://www.ncbi.nlm.nih.gov/pubmed/21605630 [Accessed March 12, 2013].

Kim, H. et al., 2012. BLT2 up-regulates interleukin-8 production and promotes the invasiveness of breast cancer cells. D. J. Templeton, ed. *PloS one*, 7(11), p.e49186.

Available at: http://dx.plos.org/10.1371/journal.pone.0049186 [Accessed December 5, 2013].

Kobayakawa, T. et al., 2008. Substitution of only two residues of human Hsp90alpha causes impeded dimerization of Hsp90beta. *Cell stress & chaperones*, 13(1), pp.97–104. Available at: http://www.pubmedcentral.nih.gov/articlerender.fcgi?artid=2666221&tool=pmcentrez&rendertype=abstract [Accessed December 4, 2013].

Koyasu, S. et al., 1986. Two mammalian heat shock proteins, HSP90 and HSP100, are actin-binding proteins. *Proceedings of the National Academy of Sciences of the United States of America*, 83(21), pp.8054–8. Available at: http://www.pubmedcentral.nih.gov/articlerender.fcgi?artid=386865&tool=pmcentrez&rendertype=abstract.

Kozaki, T. et al., 2003. Recombinant expression and characterization of a novel fibronectin isoform expressed in cartilaginous tissues. *The Journal of biological chemistry*, 278(50), pp.50546–53. Available at: http://www.ncbi.nlm.nih.gov/pubmed/14525997 [Accessed December 2, 2013].

Labat-Robert, J., 2012. Cell–Matrix interactions, the role of fibronectin and integrins. A survey. *Pathologie Biologie*, 60(1), pp.15–19. Available at: http://linkinghub.elsevier.com/retrieve/pii/S0369811411001416 [Accessed March 5, 2013].

Labat-Robert, J., 2002. Fibronectin in malignancy Effect of aging. *Cancer Biology*, 12(02), pp.187–195.

Laemmli, U.K., 1970. Cleavage of Structural Proteins during the Assembly of the Head of Bacteriophage T4. *Nature*, 227(5259), pp.680–685. Available at: http://www.nature.com/nature/journal/v227/n5259/pdf/227680a0.pdf [Accessed April 18, 2013].

Laurent-Matha, V. et al., 2012. Proteolysis of cystatin C by cathepsin D in the breast cancer microenvironment. *FASEB journal : official publication of the Federation of American Societies for Experimental Biology*, 26(12), pp.5172–81. Available at: http://www.ncbi.nlm.nih.gov/pubmed/22898924 [Accessed December 12, 2013].

Lee, C.-C. et al., 2011. The hexameric structures of human heat shock protein 90. *PloS one*, 6(5), p.e19961. Available at: http://www.pubmedcentral.nih.gov/articlerender.fcgi?artid=3102065&tool=pmcentrez&rendertype=abstract [Accessed March 26, 2013].

Lei, H., Romeo, G. & Kazlauskas, A., 2004. Heat shock protein 90alpha-dependent translocation of annexin II to the surface of endothelial cells modulates plasmin activity in the diabetic rat aorta. *Circulation research*, 94(7), pp.902–9. Available at: http://www.ncbi.nlm.nih.gov/pubmed/15001530 [Accessed December 4, 2013].

Li, J. & Buchner, J., 2013. Structure, function and regulation of the hsp90 machinery. *Biomedical journal*, 36(3), pp.106–17. Available at: http://www.ncbi.nlm.nih.gov/pubmed/23806880.

Li, S. et al., 2003. Vascular Smooth Muscle Cells Orchestrate the Assembly of Type I Collagen via ⎵ 2 ␑ 1 Integrin ,. *American Journal of Pathology*, 163(3), pp.1045–1056.

Li, W. et al., 2007. Extracellular heat shock protein-90alpha: linking hypoxia to skin cell motility and wound healing. *The EMBO journal*, 26(5), pp.1221–33. Available at: http://www.pubmedcentral.nih.gov/articlerender.fcgi?artid=1817627&tool=pmcentrez&rendertype=abstract [Accessed April 16, 2013].

Li, W., Sahu, D. & Tsen, F., 2011. Secreted heat shock protein-90 (Hsp90) in wound healing and cancer. *Biochimica et Biophysica Acta (BBA)*, 1823(3), pp.730–41. Available at: http://www.ncbi.nlm.nih.gov/entrez/query.fcgi?cmd=Retrieve&db=PubMed&dopt=Citation&list_uids=21982864 [Accessed March 6, 2013].

Li, W., Sahu, D. & Tsen, F., 2012. Secreted Heat Shock Protein-90 (Hsp90) in Wound Healing and Cancer. *Biochimica et Biophysica Acta*, 1823(3), pp.730–741.

Li, Z., Menoret, A. & Srivastava, P., 2002. Roles of heat-shock proteins in antigen presentation and cross-presentation. *Current Opinion in Immunology*, 14, pp.45–51.

Liao, D.F. et al., 2000. Purification and identification of secreted oxidative stress-induced factors from vascular smooth muscle cells. *The Journal of biological chemistry*, 275(1), pp.189–96. Available at: http://www.ncbi.nlm.nih.gov/pubmed/10617604.

Lin, T.-W. et al., 2007. Chicken heat shock protein 90 is a component of the putative cellular receptor complex of infectious bursal disease virus. *Journal of virology*, 81(16), pp.8730–41. Available at: http://www.pubmedcentral.nih.gov/articlerender.fcgi?artid=1951386&tool=pmcentrez&rendertype=abstract [Accessed November 27, 2013].

Liu, D. et al., 2010. Cell adhesion on nanopatterned fibronectin substrates. *Soft Matter*, 6(21), p.5408. Available at: http://xlink.rsc.org/?DOI=c0sm00201a [Accessed December 4, 2013].

Liu, X. et al., 2011. Cell surface heat shock protein 90 modulates prostate cancer cell adhesion and invasion through the integrin-β1/focal adhesion kinase/c-Src signaling pathway. *Oncology reports*, 25(5), pp.1343–51. Available at: http://www.ncbi.nlm.nih.gov/pubmed/21369706 [Accessed August 29, 2013].

Lohr, K.M. et al., 1990. The amino-terminal 29- and 72-Kd fragments of fibronectin mediate selective monocyte recruitment. *Blood*, 76(10), pp.2117–24. Available at: http://www.ncbi.nlm.nih.gov/pubmed/2242430.

López-Maderuelo, M.D. et al., 2001. Opposite effects of the Hsp90 inhibitor Geldanamycin: induction of apoptosis in PC12, and differentiation in N2A cells. *FEBS Letters*, 490(1), pp.23–27. Available at:

http://www.sciencedirect.com/science/article/pii/S0014579301021305 [Accessed November 22, 2013].

Loskutoff, D.J. et al., 1999. Regulation of cell adhesion by PAI-1. *APMIS : acta pathologica, microbiologica, et immunologica Scandinavica*, 107(1), pp.54–61. Available at: http://www.ncbi.nlm.nih.gov/pubmed/10190280 [Accessed April 18, 2013].

Lotz, G.P. et al., 2008. A novel HSP90 chaperone complex regulates intracellular vesicle transport. *Journal of cell science*, 121(Pt 5), pp.717–23. Available at: http://www.ncbi.nlm.nih.gov/pubmed/18270269 [Accessed November 26, 2013].

Lu, P., Weaver, V.M. & Werb, Z., 2012. The extracellular matrix: a dynamic niche in cancer progression. *The Journal of cell biology*, 196(4), pp.395–406. Available at: http://www.pubmedcentral.nih.gov/articlerender.fcgi?artid=3283993&tool=pmcentrez&rendertype=abstract [Accessed November 7, 2013].

Luo, B. et al., 2011. The endoplasmic reticulum chaperone protein GRP94 is required for maintaining hematopoietic stem cell interactions with the adult bone marrow niche. *PloS one*, 6(5), p.e20364. Available at: http://www.pubmedcentral.nih.gov/articlerender.fcgi?artid=3101259&tool=pmcentrez&rendertype=abstract [Accessed August 29, 2013].

Mao, Y. & Schwarzbauer, J.E., 2005. Fibronectin fibrillogenesis, a cell-mediated matrix assembly process. *Matrix biology*, 24, pp.389–399. Available at: http://www.ncbi.nlm.nih.gov/pubmed/16061370 [Accessed March 1, 2013].

Marcu, M.G., Schulte, T.W. & Neckers, L., 2000. Novobiocin and related coumarins and depletion of heat shock protein 90-dependent signaling proteins. *Journal of the National Cancer Institute*, 92(3), pp.242–8. Available at: http://www.ncbi.nlm.nih.gov/pubmed/10655441.

Maurizi, M.R. & Xia, D., 2004. Protein binding and disruption by Clp/Hsp100 chaperones. *Structure (London, England : 1993)*, 12(2), pp.175–83. Available at: http://www.ncbi.nlm.nih.gov/pubmed/14962378 [Accessed November 28, 2013].

Mayer, M.P. et al., 2000. Multistep mechanism of substrate binding determines chaperone activity of Hsp70. *Nature structural biology*, 7(7), pp.586–93. Available at: http://dx.doi.org/10.1038/76819 [Accessed December 12, 2013].

Mayer, M.P. & Bukau, B., 2005. Hsp70 chaperones: cellular functions and molecular mechanism. *Cellular and molecular life sciences : CMLS*, 62(6), pp.670–84. Available at: http://www.pubmedcentral.nih.gov/articlerender.fcgi?artid=2773841&tool=pmcentrez&rendertype=abstract [Accessed November 7, 2013].

McCready, J. et al., 2010. Secretion of extracellular hsp90α via exosomes increases cancer cell motility: a role for plasminogen activation. *BMC Cancer*, 10(1), p.294. Available at: http://www.pubmedcentral.nih.gov/articlerender.fcgi?artid=3087318&tool=pmcentrez&rendertype=abstract.

Mcdonald, J.A., Kelley, D.G. & Broekelmann, T.J., 1982. Role of Fibronectin in Collagen Deposition : Fab ' to the Gelatin-binding Domain of Fibronectin Inhibits Both Fibronectin and Collagen Organization in Fibroblast Extracellular Matrix Isolation of Procollagens and Collagen for Absorption of Antisera. *The Journal of cell biology*, 92(29), pp.485–492.

McKeown-Longo, P.J. & Mosher, D.F., 1985. Interaction of the 70,000-mol-wt amino-terminal fragment of fibronectin with the matrix-assembly receptor of fibroblasts. *The Journal of cell biology*, 100(2), pp.364–74. Available at: http://www.pubmedcentral.nih.gov/articlerender.fcgi?artid=2113439&tool=pmcentrez&rendertype=abstract.

McLaughlin, S.H. et al., 2006. The co-chaperone p23 arrests the Hsp90 ATPase cycle to trap client proteins. *Journal of molecular biology*, 356(3), pp.746–58. Available at: http://www.ncbi.nlm.nih.gov/pubmed/16403413 [Accessed March 4, 2013].

Montcourrier, P. et al., 1990. Cathepsin D in Breast Cancer Cells Can Digest Extracellular Matrix in Large Acidic Vesicles. *Cancer research*, 50(September), pp.6045–6054.

Morimoto, R., Sarge, K. & Abravayat, K., 1992. Transcriptional regulation of heat shock genes. A paradigm for inducible genomic responses. *Journal of Biological Chemistry*, 267, pp.21987–21990.

Mosher, D.F., 2012. *Fibronectin*, Elsevier. Available at: http://books.google.com/books?hl=en&lr=&id=leDMe4HSYv4C&pgis=1 [Accessed November 27, 2013].

Muratoglu, S.C. et al., 2010. Low density lipoprotein receptor-related protein 1 (LRP1) forms a signaling complex with platelet-derived growth factor receptor-beta in endosomes and regulates activation of the MAPK pathway. *The Journal of biological chemistry*, 285(19), pp.14308–17. Available at: http://www.pubmedcentral.nih.gov/articlerender.fcgi?artid=2863204&tool=pmcentrez&rendertype=abstract [Accessed August 21, 2013].

Neckers, L. & Lee, Y.-S., 2003. Cancer: the rules of attraction. *Nature*, 425(6956), pp.357–9. Available at: http://www.ncbi.nlm.nih.gov/pubmed/14508471 [Accessed December 10, 2013].

O'Hagan, K., 2012. *A Role for Heat Shock Protein 90 (Hsp90) in Fibronectin Matrix Dynamics*.

Ohashi, T. & Erickson, H.P., 2009. Revisitin the mystery of fibronectin multimers: the fibronectin matrix is composed of fibronectin dimers cross-linked by non-covalent bonds. *Matrix biology*, 22(5), p.4109. Available at: http://www.ncbi.nlm.nih.gov/pubmed/18554561.

Okiyoneda, T., Apaja, P. & Lukacs, G., 2012. Protein quality control at the plasma membrane. *Current Opinion in Cell Biology*, 23(4), pp.483–491.

Onuoha, S.C. et al., 2008. Structural studies on the co-chaperone Hop and its complexes with Hsp90. *Journal of molecular biology*, 379(4), pp.732–44. Available at: http://www.ncbi.nlm.nih.gov/pubmed/18485364 [Accessed November 15, 2013].

Orr, A.W. et al., 2006. Matrix-specific suppression of integrin activation in shear stress signaling. *Molecular biology of the cell*, 17(11), pp.4686–97. Available at: http://www.pubmedcentral.nih.gov/articlerender.fcgi?artid=1635406&tool=pmcentrez&rendertype=abstract [Accessed December 12, 2013].

Palecek, S.P., Horwitz, A.F. & Lauffenburger, D.A., 1999. Kinetic model for integrin-mediated adhesion release during cell migration. *Annals of biomedical engineering*, 27(2), pp.219–35. Available at: http://www.ncbi.nlm.nih.gov/pubmed/10199699 [Accessed April 18, 2013].

Palumbo, M., Nagel, J. & Petty, M.C., 2005. Surface Plasmon Resonance Detection of Metal Ions : Layer-by-Layer Assembly of Polyelectrolyte Sensing Layers on a Multichannel Chip. *IEEE Sensors Journal*, 5(6), pp.1159–1164.

Pankov, R., 2002. Fibronectin at a glance. *Journal of Cell Science*, 115(20), pp.3861–3863. Available at: http://jcs.biologists.org/cgi/doi/10.1242/jcs.00059 [Accessed November 7, 2013].

Pearl, L.H. & Prodromou, C., 2001. Structure, function and mechanism of the Hsp90 molecular chaperone. *Advance Protein Chemistry*, 59(null), pp.157–186. Available at: http://dx.doi.org/10.1016/S0065-3233(01)59005-1 [Accessed April 16, 2013].

Pereira, M. et al., 2002. The incorporation of fibrinogen into extracellular matrix is dependent on active assembly of a fibronectin matrix. *Journal of cell science*, 115(Pt 3), pp.609–17. Available at: http://www.ncbi.nlm.nih.gov/pubmed/11861767 [Accessed November 18, 2013].

Peterson, L.B. et al., 2013. The hERG channel is dependent upon the Hsp90alpha isoform for maturation and trafficking. *Molecular Pharmacology*, 9(6), pp.1841–1846.

Pick, E. et al., 2007. High HSP90 expression is associated with decreased survival in breast cancer. *Cancer research*, 67(7), pp.2932–7. Available at: http://www.ncbi.nlm.nih.gov/pubmed/17409397 [Accessed November 18, 2013].

Pickford, A.R. et al., 1997. Solution structure of a type 2 module from fibronectin: implications for the structure and function of the gelatin-binding domain. *Structure (London, England : 1993)*, 5(3), pp.359–70. Available at: http://www.ncbi.nlm.nih.gov/pubmed/9083105 [Accessed November 29, 2013].

Prince, T. & Matts, R.L., 2004. Definition of protein kinase sequence motifs that trigger high affinity binding of Hsp90 and Cdc37. *The Journal of biological chemistry*, 279(38), pp.39975–81. Available at: http://www.ncbi.nlm.nih.gov/pubmed/15258137 [Accessed December 11, 2013].

Prinsloo, E. et al., 2012. STAT3 interacts directly with Hsp90. *IUBMB Life*, 64(3), pp.266–273. Available at: http://www.ncbi.nlm.nih.gov/pubmed/22271514 [Accessed March 5, 2013].

Ratzke, C. et al., 2010. Dynamics of heat shock protein 90 C-terminal dimerization is an important part of its conformational cycle. *Proceedings of the National Academy of Sciences of the United States of America*, 107(37), pp.16101–16106. Available at: http://www.pubmedcentral.nih.gov/articlerender.fcgi?artid=2941327&tool=pmcentrez&rendertype=abstract [Accessed April 12, 2013].

Redlak, M.J. & Miller, T.A., 2011. Targeting PI3K/Akt/HSP90 signaling sensitizes gastric cancer cells to deoxycholate-induced apoptosis. *Digestive Diseases and Sciences*, 56(2), pp.323–329. Available at: http://www.ncbi.nlm.nih.gov/pubmed/20585984 [Accessed April 12, 2013].

Reitan, N.K. et al., 2012. Quantitative 3-D colocalization analysis as a tool to study the intracellular trafficking and dissociation of pDNA-chitosan polyplexes. *Journal of biomedical optics*, 17(2), p.026015. Available at: http://www.ncbi.nlm.nih.gov/pubmed/22463047 [Accessed April 18, 2013].

Retzlaff, M. et al., 2009. Hsp90 is regulated by a switch point in the C-terminal domain. *EMBO reports*, 10(10), pp.1147–53. Available at: http://dx.doi.org/10.1038/embor.2009.153 [Accessed November 22, 2013].

Reyes-Del Valle, J. et al., 2005. Heat shock protein 90 and heat shock protein 70 are components of dengue virus receptor complex in human cells. *Journal of virology*, 79(8), pp.4557–67. Available at: http://jvi.asm.org/content/79/8/4557 [Accessed November 27, 2013].

Ritossa, F., 1962. A New Puffing Pattern Induced by Temperature Shock and DNP in Drosophila. *Experientia*, 18(12), pp.571–573.

Robinson, E.E., Foty, R.A. & Corbett, S.A., 2004. Fibronectin Matrix Assembly Regulates α5β1-mediated Cell Cohesion. *Molecular Biology of the cell*, 15, pp.973–981.

Roman, J. & McDonald, J.A., 1993. Fibulin's organization into the extracellular matrix of fetal lung fibroblasts is dependent on fibronectin matrix assembly. *American journal of respiratory cell and molecular biology*, 8(5), pp.538–45. Available at: http://www.ncbi.nlm.nih.gov/pubmed/8481235 [Accessed November 18, 2013].

Ruoslahti, E., 1984. Fibronectin in cell adhesion and invasion. *Cancer metastasis reviews*, 3(1), pp.43–51. Available at: http://www.ncbi.nlm.nih.gov/pubmed/6324988.

Sabatier, L. et al., 2009. Fibrillin Assembly Requires Fibronectin. , 20, pp.846–858.

Sabeh, F., Shimizu-Hirota, R. & Weiss, S.J., 2009. Protease-dependent versus -independent cancer cell invasion programs: three-dimensional amoeboid movement revisited. *The Journal of cell biology*, 185(1), pp.11–9. Available at: http://jcb.rupress.org/content/185/1/11.full [Accessed November 12, 2013].

Sahu, D. et al., 2012. A potentially common peptide target in secreted heat shock protein-90α for hypoxia-inducible factor-1α-positive tumors. *Molecular biology of the cell*, 23(4), pp.602–13. Available at: http://www.pubmedcentral.nih.gov/articlerender.fcgi?artid=3279389&tool=pmcentrez&rendertype=abstract [Accessed November 23, 2013].

Salicioni, A.M. et al., 2004. Low density lipoprotein receptor-related protein-1 promotes beta1 integrin maturation and transport to the cell surface. *The Journal of biological chemistry*, 279(11), pp.10005–12. Available at: http://www.ncbi.nlm.nih.gov/pubmed/14699139 [Accessed December 2, 2013].

Salicioni, A.M. et al., 2002. The low density lipoprotein receptor-related protein mediates fibronectin catabolism and inhibits fibronectin accumulation on cell surfaces. *The Journal of biological chemistry*, 277(18), pp.16160–6. Available at: http://www.ncbi.nlm.nih.gov/pubmed/11867643 [Accessed September 12, 2013].

Saluta, M. & Bell, P.A., 1998. Troubleshooting GST fusion protein expression in E . coli. *Life Science News*, pp.1–3.

Sarto, C., Binz, P. a & Mocarelli, P., 2000. Heat shock proteins in human cancer. *Electrophoresis*, 21(6), pp.1218–26. Available at: http://www.ncbi.nlm.nih.gov/pubmed/10786894.

Schedin, P. et al., 2000. Fibronectin fragments induce MMP activity in mouse mammary epithelial cells: evidence for a role in mammary tissue remodeling. *Journal of cell science*, 113 (Pt 5, pp.795–806. Available at: http://www.ncbi.nlm.nih.gov/pubmed/10671369.

Scheibel, T. et al., 1997. ATP-binding Properties of Human Hsp90. *Journal of Biological Chemistry*, 272(30), pp.18608–18613. Available at: http://www.jbc.org/cgi/doi/10.1074/jbc.272.30.18608 [Accessed November 25, 2013].

Schmitt, E. et al., 2007. Intracellular and extracellular functions of heat shock proteins: repercussions in cancer therapy. *Journal of leukocyte biology*, 81(1), pp.15–27. Available at: http://www.ncbi.nlm.nih.gov/pubmed/16931602 [Accessed November 9, 2013].

Schwarzbauer, J.E., 1991. Identification of the fibronectin sequences required for assembly of a fibrillar matrix. *The Journal of cell biology*, 113(6), pp.1463–73. Available at: http://www.pubmedcentral.nih.gov/articlerender.fcgi?artid=2289042&tool=pmcentrez&rendertype=abstract.

Schwarzbauer, J.E. & Sechler, J.L., 1999. Fibronectin fibrillogenesis: a paradigm for extracellular matrix assembly. *Current Opinion in Cell Biology*, 11(5), pp.622–627. Available at: http://www.ncbi.nlm.nih.gov/pubmed/10508649.

Scilabra, S.D. et al., 2013. Differential regulation of extracellular tissue inhibitor of metalloproteinases-3 levels by cell membrane-bound and shed low density lipoprotein receptor-related protein 1. *The Journal of biological chemistry*, 288(1), pp.332–42.

Available at: http://www.jbc.org/content/288/1/332.long [Accessed November 20, 2013].

Sechler, J.L. et al., 2000. A novel RGD-independent fibronectin assembly pathway initiated by alpha4beta1 integrin binding to the alternatively spliced V region. *Journal of cell science*, 113 (Pt 8, pp.1491–8. Available at: http://www.ncbi.nlm.nih.gov/pubmed/10725231.

Shamovsky, I. & Nudler, E., 2008. New insights into the mechanism of heat shock response activation. *Cellular and molecular life sciences : CMLS*, 65(6), pp.855–61. Available at: http://www.ncbi.nlm.nih.gov/pubmed/18239856 [Accessed November 8, 2013].

Shi, F. & Sottile, J., 2009. Caveolin-1-dependent beta-1-integrin endocytosis is a critical regulator of fibronectin turnover. *Journal of cell science*, 121(Pt 14), pp.2360–2371.

Shi, F. & Sottile, J., 2011. MT1-MMP regulates the turnover and endocytosis of extracellular matrix fibronectin. *Journal of cell science*, 124(Pt 23), pp.4039–50. Available at: http://www.pubmedcentral.nih.gov/articlerender.fcgi?artid=3244985&tool=pmcentrez&rendertype=abstract [Accessed April 12, 2013].

Sidera, K. et al., 2008. A critical role for HSP90 in cancer cell invasion involves interaction with the extracellular domain of HER-2. *The Journal of biological chemistry*, 283(4), pp.2031–41. Available at: http://www.ncbi.nlm.nih.gov/pubmed/18056992 [Accessed April 16, 2013].

Sidera, K. et al., 2004. Involvement of cell surface HSP90 in cell migration reveals a novel role in the developing nervous system. *The Journal of biological chemistry*, 279(44), pp.45379–88. Available at: http://www.ncbi.nlm.nih.gov/pubmed/15302889 [Accessed March 5, 2013].

Siligardi, G. et al., 2002. Regulation of Hsp90 ATPase activity by the co-chaperone Cdc37p/p50cdc37. *The Journal of biological chemistry*, 277(23), pp.20151–9. Available at: http://www.ncbi.nlm.nih.gov/pubmed/11916974 [Accessed November 15, 2013].

Sims, J.D., McCready, J. & Jay, D.G., 2011. Extracellular Heat Shock Protein (Hsp)70 and Hsp90α Assist in Matrix Metalloproteinase-2 Activation and Breast Cancer Cell Migration and Invasion. *PloS one*, 6(4), p.e18848. Available at: http://www.pubmedcentral.nih.gov/articlerender.fcgi?artid=3077417&tool=pmcentrez&rendertype=abstract [Accessed March 5, 2013].

Singh, P., Carraher, C. & Schwarzbauer, J.E., 2010. Assembly of Fibronectin Extracellular Matrix. *Annu Rev Cell Dev Biol*, 26, pp.397–419.

Smith, D.F., 1998. Sequence motifs shared between chaperone components participating in the assembly of progesterone receptor complexes. *Biological chemistry*, 379(3), pp.283–8. Available at: http://www.ncbi.nlm.nih.gov/pubmed/9563823 [Accessed December 11, 2013].

Solier, S. et al., 2012. Heat shock protein 90α (HSP90α), a substrate and chaperone of DNA-PK necessary for the apoptotic response. *Proceedings of the National Academy of*

Sciences of the United States of America, 109(32), pp.12866–72. Available at: http://www.pubmedcentral.nih.gov/articlerender.fcgi?artid=3420188&tool=pmcentrez&rendertype=abstract [Accessed November 21, 2013].

Somanath, P. et al., 2007. Akt1 Signaling Regulates Integrin Activation, Matrix Recognition, and Fibronectin assembly. *Journal of Biological Chemistry*, 282(31), pp.22964–22976.

Song, X. et al., 2010. The regulatory mechanism of extracellular Hsp90{alpha} on matrix metalloproteinase-2 processing and tumor angiogenesis. *The Journal of biological chemistry*, 285(51), pp.40039–49. Available at: http://www.pubmedcentral.nih.gov/articlerender.fcgi?artid=3000986&tool=pmcentrez&rendertype=abstract [Accessed August 28, 2013].

Soti, C. et al., 2003. Comparative analysis of the ATP-binding sites of Hsp90 by nucleotide affinity cleavage: a distinct nucleotide specificity of the C-terminal ATP-binding site. *The Federation of European Biochemical Societies Journal*, 270(11), pp.2421–2428. Available at: http://doi.wiley.com/10.1046/j.1432-1033.2003.03610.x [Accessed April 12, 2013].

Sottile, J. & Chandler, J., 2005a. Fibronectin matrix turnover occurs through a caveolin-1-dependent process. *Molecular biology of the cell*, 16(2), pp.757–68. Available at: http://www.pubmedcentral.nih.gov/articlerender.fcgi?artid=545909&tool=pmcentrez&rendertype=abstract [Accessed August 25, 2013].

Sottile, J. & Chandler, J., 2005b. Fibronectin matrix turnover occurs through a caveolin-1-dependent process. *Molecular biology of the cell*, 16(2), pp.757–68. Available at: http://www.pubmedcentral.nih.gov/articlerender.fcgi?artid=545909&tool=pmcentrez&rendertype=abstract [Accessed March 4, 2013].

Sottile, J. & Hocking, D.C., 2002. Fibronectin Polymerization Regulates the Composition and Stability of Extracellular Matrix Fibrils and Cell-Matrix Adhesions. , 13(October), pp.3546–3559.

Sreedhar, A.S. et al., 2004. Hsp90 isoforms: functions, expression and clinical importance. *FEBS Letters*, 562(1-3), pp.11–15. Available at: http://linkinghub.elsevier.com/retrieve/pii/S0014579304002297 [Accessed November 15, 2013].

Stellas, D., El Hamidieh, A. & Patsavoudi, E., 2010. Monoclonal antibody 4C5 prevents activation of MMP2 and MMP9 by disrupting their interaction with extracellular HSP90 and inhibits formation of metastatic breast cancer cell deposits. *BMC Cell Biology*, 11, p.51. Available at: http://www.pubmedcentral.nih.gov/articlerender.fcgi?artid=2914660&tool=pmcentrez&rendertype=abstract.

Suto, R. & Srivastava, P.K., 1995. A mechanism for the specific immunogenicity of heat shock protein-chaperoned peptides. *Science (New York, N.Y.)*, 269(5230), pp.1585–8. Available at: http://www.ncbi.nlm.nih.gov/pubmed/7545313 [Accessed March 15, 2014].

Suzuki, S. & Kulkarni, A.B., 2010. Extracellular heat shock protein HSP90beta secreted by MG63 osteosarcoma cells inhibits activation of latent TGF-beta1. *Biochemical and Biophysical Research Communications*, 398(3), pp.525–531. Available at: http://www.pubmedcentral.nih.gov/articlerender.fcgi?artid=2922109&tool=pmcentrez&rendertype=abstract [Accessed April 12, 2013].

Taherian, A., Krone, P.H. & Ovsenek, N., 2008. A comparison of Hsp90alpha and Hsp90beta interactions with cochaperones and substrates. *Biochemistry and cell biology = Biochimie et biologie cellulaire*, 86(1), pp.37–45. Available at: http://www.nrcresearchpress.com/doi/abs/10.1139/O07-154#.Uo34YYn8Idk [Accessed November 21, 2013].

Taipale, M. et al., 2012. Quantitative analysis of HSP90-client interactions reveals principles of substrate recognition. *Cell*, 150(5), pp.987–1001. Available at: http://www.ncbi.nlm.nih.gov/pubmed/22939624 [Accessed February 28, 2013].

Taipale, M., Jarosz, D.F. & Lindquist, S., 2010. HSP90 at the hub of protein homeostasis: emerging mechanistic insights. *Nature reviews. Molecular cell biology*, 11(7), pp.515–28. Available at: http://dx.doi.org/10.1038/nrm2918 [Accessed December 11, 2013].

Theodoraki, M. & Caplam, A., 2013. Quality Control and Fate Determination of Hsp90 Client Proteins. *Biochimica et Biophysica Acta*, 1823(3), pp.683–688.

Thuringer, D. et al., 2011. Transactivation of the epidermal growth factor receptor by heat shock protein 90 via Toll-like receptor 4 contributes to the migration of glioblastoma cells. *The Journal of biological chemistry*, 286(5), pp.3418–28. Available at: http://www.pubmedcentral.nih.gov/articlerender.fcgi?artid=3030348&tool=pmcentrez&rendertype=abstract [Accessed December 5, 2013].

Tissières, A., Mitchell, H.K. & Tracy, U.M., 1974. Protein synthesis in salivary glands of Drosophila melanogaster: relation to chromosome puffs. *Journal of molecular biology*, 84(3), pp.389–98. Available at: http://www.ncbi.nlm.nih.gov/pubmed/4219221.

To, W.S. & Midwood, K.S., 2011. Plasma and cellular fibronectin: distinct and independent functions during tissue repair. *Fibrogenesis & tissue repair*, 4(1), p.21. Available at: http://www.pubmedcentral.nih.gov/articlerender.fcgi?artid=3182887&tool=pmcentrez&rendertype=abstract [Accessed April 22, 2013].

Towbin, H., Staehelin, T. & Gordon, J., 1979. Electrophoretic transfer of proteins from polyacrylamide gels to nitrocellulose sheets: procedure and some applications. *Proceedings of the National Academy of Sciences of the United States of America*, 76(9), pp.4350–4. Available at: http://www.pubmedcentral.nih.gov/articlerender.fcgi?artid=411572&tool=pmcentrez&rendertype=abstract [Accessed March 7, 2013].

Triantafilou, M. & Triantafilou, K., 2004. Heat-shock protein 70 and heat-shock protein 90 associate with Toll-like receptor 4 in response to bacterial lipopolysaccharide. *Biochemical Society transactions*, 32(Pt 4), pp.636–9. Available at: http://www.ncbi.nlm.nih.gov/pubmed/15270695 [Accessed March 5, 2013].

Tsutsumi, S., Scroggins, B., et al., 2009. A small molecule cell-impermeant Hsp90 antagonist inhibits tumor cell motility and invasion. *Oncogene*, 27(17), pp.2478–2487.

Tsutsumi, S., Beebe, K. & Neckers, L., 2009. Impact of heat-shock protein 90 on cancer metastasis. *Future Oncol.*, 5(5), pp.679–688.

Tsutsumi, S. & Neckers, L., 2007. Extracellular heat shock protein 90: a role for a molecular chaperone in cell motility and cancer metastasis. *Cancer Science*, 98(10), pp.1536–1539. Available at: http://www.ncbi.nlm.nih.gov/pubmed/17645779 [Accessed March 14, 2013].

Vabulas, R.M. et al., 2010. Protein Folding in the Cytoplasm and the Heat Shock Response. *Cold Spring Harbor Perspectives in Biology*, 2(12), pp.a004390–a004390. Available at: http://cshperspectives.cshlp.org/content/2/12/a004390.full [Accessed November 11, 2013].

Vakonakis, I. et al., 2007. Interdomain association in fibronectin: insight into cryptic sites and fibrillogenesis. *The EMBO journal*, 26(10), pp.2575–83. Available at: http://www.pubmedcentral.nih.gov/articlerender.fcgi?artid=1868906&tool=pmcentrez&rendertype=abstract [Accessed August 28, 2013].

Vérollet, C. et al., 2011. Extracellular proteolysis in macrophage migration: losing grip for a breakthrough. *European journal of immunology*, 41(10), pp.2805–13. Available at: http://www.ncbi.nlm.nih.gov/pubmed/21953638 [Accessed November 14, 2013].

Waalkes, S. et al., 2010. Fibronectin 1 mRNA expression correlates with advanced disease in renal cancer. *BMC cancer*, 10, p.503. Available at: http://www.pubmedcentral.nih.gov/articlerender.fcgi?artid=2949811&tool=pmcentrez&rendertype=abstract.

Wang, X. et al., 2009. The regulatory mechanism of Hsp90alpha secretion and its function in tumor malignancy. *Proceedings of the National Academy of Sciences of the United States of America*, 106(50), pp.21288–93. Available at: http://www.pubmedcentral.nih.gov/articlerender.fcgi?artid=2795546&tool=pmcentrez&rendertype=abstract.

Weder, H.G. et al., 1974. Determination of Binding Parameters from Scatchard Plots. *European Journal of Biochemistry*, 42, pp.475–481.

Whitesell, L. & Lindquist, S.L., 2005. HSP90 and the chaperoning of cancer. *Nature reviews. Cancer*, 5(10), pp.761–72. Available at: http://dx.doi.org/10.1038/nrc1716 [Accessed March 3, 2013].

Whitley, D., Goldberg, S.P. & Jordan, W.D., 1999. Heat shock proteins: a review of the molecular chaperones. *Journal of vascular surgery*, 29(4), pp.748–51. Available at: http://www.ncbi.nlm.nih.gov/pubmed/10194511.

Wierzbicka-Patynowski, I. & Schwarzbauer, J.E., 2003. The ins and outs of fibronectin matrix assembly. *Journal of cell science*, 116(Pt 16), pp.3269–76. Available at: http://www.ncbi.nlm.nih.gov/pubmed/12857786 [Accessed March 5, 2013].

Willnow, T.E. et al., 1995. Functional expression of low density lipoprotein receptor-related protein is controlled by receptor-associated protein in vivo. , 92(May), pp.4537–4541.

Wilson, S.H., 2003. Fibronectin Fragments Promote Human Retinal Endothelial Cell Adhesion and Proliferation and ERK Activation through alpha5beta1 Integrin and PI 3-Kinase. *Investigative Ophthalmology & Visual Science*, 44(4), pp.1704–1715. Available at: http://www.iovs.org/cgi/doi/10.1167/iovs.02-0773 [Accessed December 2, 2013].

Winters, B.S. et al., 2006. Three-dimensional Culture Regulates Raf-1 Expression to Modulate Fibronectin Matrix Assembly. *Molecular biology of the cell*, 17(August), pp.3386–3396.

Woodley, D.T. et al., 2009. Participation of the lipoprotein receptor LRP1 in hypoxia-HSP90alpha autocrine signaling to promote keratinocyte migration. *Journal of Cell Science*, 122(10), pp.1495–1498. Available at: http://www.ncbi.nlm.nih.gov/pubmed/19383717 [Accessed April 12, 2013].

Wright, L. et al., 2004. Structure-Activity Relationships in Purine-Based Inhibitor Binding to HSP90 Isoforms. *Chemistry & Biology*, 11, pp.775–785.

Wu, L. & Gonias, S.L., 2005. The low-density lipoprotein receptor-related protein-1 associates transiently with lipid rafts. *Journal of cellular biochemistry*, 96(5), pp.1021–33. Available at: http://www.ncbi.nlm.nih.gov/pubmed/16149055 [Accessed November 26, 2013].

Xu, J. & Mosher, D.F., 2011. *The Extracellular Matrix: an Overview* R. P. Mecham, ed., Berlin, Heidelberg: Springer Berlin Heidelberg. Available at: http://www.springerlink.com/index/10.1007/978-3-642-16555-9 [Accessed November 12, 2013].

Xu, W. et al., 2005. Surface charge and hydrophobicity determine ErbB2 binding to the Hsp90 chaperone complex. *Nature structural & molecular biology*, 12(2), pp.120–6. Available at: http://www.ncbi.nlm.nih.gov/pubmed/15643424 [Accessed December 11, 2013].

Xu, Y., Singer, M. a & Lindquist, S., 1999. Maturation of the tyrosine kinase c-src as a kinase and as a substrate depends on the molecular chaperone Hsp90. *Proceedings of the National Academy of Sciences of the United States of America*, 96(1), pp.109–14. Available at: http://www.pubmedcentral.nih.gov/articlerender.fcgi?artid=15101&tool=pmcentrez&rendertype=abstract.

Yao, C. et al., 2007. Interleukin-8 modulates growth and invasiveness of estrogen receptor-negative breast cancer cells. *International journal of cancer. Journal international du cancer*, 121(9), pp.1949–57. Available at: http://www.ncbi.nlm.nih.gov/pubmed/17621625 [Accessed December 5, 2013].

Young, J.C., Obermann, W.M. & Hartl, F.U., 1998. Specific binding of tetratricopeptide repeat proteins to the C-terminal 12-kDa domain of hsp90. *The Journal of biological*

chemistry, 273(29), pp.18007–10. Available at: http://www.ncbi.nlm.nih.gov/pubmed/9660753 [Accessed November 28, 2013].

Zagouri, F. et al., 2012. Heat Shock Protein 90 (Hsp90) Expression and Breast Cancer. *Pharmaceuticals*, 5(12), pp.1008–1020. Available at: http://www.mdpi.com/1424-8247/5/9/1008/ [Accessed November 18, 2013].

Zhang, X. et al., 2012. A Comparative Study of Fibronectin Cleavage by MMP-1, -3, -13, and -14. *Cartilage*, 3(3), pp.267–277. Available at: http://car.sagepub.com/cgi/doi/10.1177/1947603511435273 [Accessed November 23, 2013].

Zheng, Y. et al., 2007. Nicotine stimulates human lung cancer cell growth by inducing fibronectin expression. *American journal of respiratory cell and molecular biology*, 37(6), pp.681–90. Available at: http://www.ncbi.nlm.nih.gov/pubmed/17600315 [Accessed November 25, 2013].

Zuehlke, A. & Johnson, J.L., 2011. Hsp90 and co-chaperones twist the functions of diverse client proteins. *Biopolymers*, 93(3), pp.211–217.

Zurawska, A., Urbanski, J. & Bieganowski, P., 2008. Hsp90n - An accidental product of a fortuitous chromosomal translocation rather than a regular Hsp90 family member of human proteome. *Biochimica et Biophysica Acta*, 1784(11), pp.1844–1846. Available at: http://www.ncbi.nlm.nih.gov/pubmed/18638579 [Accessed March 20, 2013].